2011

Nuclear Reorganization and Gene Expression During Muscle Cell Differentiation

Amy L. Pitstick
Wright State University

NUCLEAR REORGANIZATION AND GENE EXPRESSION DURING MUSCLE CELL DIFFERENTIATION

A thesis submitted in partial fulfillment
of the requirements for the degree of
Master of Science

By

AMY LEE PITSTICK
B.S., University of Dayton, 2008

2011
Wright State University

Wright State University

SCHOOL OF GRADUATE STUDIES

November 17,2010

I HEREBY RECOMMEND THAT THE THESIS PREPARED UNDER MY SUPERVISION BY Amy Pitstick ENTITLED Nuclear reorganization and gene expression during muscle cell differentiation BE ACCEPTED IN PARTIAL FULFILLMENT OF THE REQUIREMENTS FOR THE DEGREE OF Master of Science.

Paula A. Bubulya, Ph.D.
Thesis Director

David Goldstein, Ph.D., Chair
Department of Biological Sciences
College of Science and Mathematics

Committee on
Final Examination

Mill Miller, Ph.D.

Scott Baird, Ph.D.

Andrew Hsu, Ph.D.
Dean, School of Graduate Studies

Abstract

Pitstick,A Lee. M.S., Department of Biological Sciences, Wright State University, 2011. Nuclear Reorganization and Gene Expression During Muscle Cell Differentiation.

Cellular differentiation is a process regulated by environmental, intracellular and intercellular factors. Myogenesis is a differentiation program in mammalian myotome cells in which Pax3 activates myogenic transcription factors to convert myotome cells to committed myoblasts. Myoblasts differentiate to become fully differentiated, multi-nucleated myotubes (Tajbakhsh et al., 1997). C2C12 cells are a model system for myogenesis. We noted that Bcl2-associated transcription factor (Btf) is upregulated during myogenesis. We observed that C2C12 nuclei reorganize during myogenesis. We observed that myoblast nuclei have approximately 5-10 small nucleoli, while nuclei in myotubes have fewer and larger nucleoli. Nucleolar reorganization occurs independently of multinucleation. Also, the reorganization is not a result of serum withdrawal, as other cell lines fail to show reorganization when grown in low serum conditions. Immunofluorescent data indicates nuclear speckles reorganize during myogenesis. Our results indicate that a large-scale reorganization of nucleoli and nuclear speckles occurs during myogenesis.

Table of Contents

Page

List of Figures

List of Tables

Table Page

Chapter One: Background and Significance

1.1 Nuclear Domains

The cell nucleus orchestrates numerous processes including DNA replication, DNA repair and recombination, ribosomal subunit assembly, nucleocytoplasmic and ribonucleoprotein trafficking, and pre-mRNA processing (Lamond and Earnshaw, 1998). These functions are often focused around distinct non-membrane bound organelles that include paraspeckles, nucleoli, perinucleolar compartments, Cajal bodies, Gems, promyelocytic leukemia (PML) bodies, and nuclear speckles (Spector, D.L., 2001; Lamond and Spector, 2003). The structural integrity and/or biogenesis of these organelles can often be attributed to sequence motifs found within the proteins that localize to these organelles (Taddei et al., 2004). These motifs mediate protein-protein and protein-nucleic acid interactions that result in self-assembly of these organelles (Taddei et al., 2004). For example, immunofluorescence studies using monoclonal antibodies localized the protein p120 to the nucleolus. These studies used site-directed mutagenesis to identify an arginine-rich domain that overlapped with the protein's nucleolar localization signal that was similar to that of other rRNA-binding proteins (Freeman et al., 1988; Gustafson et al., 1998). This data suggested that the nucleolus was capable of self-assembly and did not require an underlying scaffold structure (Gustafson et al., 1998). Nuclear speckles are also enriched with proteins whose sequence motifs are responsible for targeting them to nuclear speckles. Caceres and colleagues transiently overexpressed several cDNAs for epitope-tagged SR proteins coding for either the wild type protein or a deletion mutant construct and then studied the

cellular distribution of the tagged proteins (Caceres et al., 1997). This study revealed an arginine-serine rich (RS) domain within several SR pre-mRNA splicing factors that was necessary for targeting these proteins to nuclear speckles (Caceres et al., 1997). It is possible that additional mechanisms also support the organization of nuclear bodies. siRNA depletion of nuclear speckle protein Son showed a change in nuclear speckle morphology from a solid sphere to a “donut” shaped morphology suggesting Son may lend structural integrity to nuclear speckles and possibly serve as a protein scaffold for nuclear speckles (Sharma et al., 2010). In addition, a growing number of noncoding RNAs are involved in organization of nuclear bodies or their residential proteins. MALAT-1 is needed for proper distribution of splicing factors in nuclear speckles (Tripathy et al., 2010). Men ε and Men β are required for the integrity of nuclear paraspeckles (Sunwoo et al., 2008).

1.2 The Nucleolus

Organelles and other structures within interphase nuclei exhibit a non-random spatial organization in which each structure occupies a distinct and characteristic region or domain. The nucleolus is the most dominant function-based compartment within the nucleus. The nucleolus is the site of RNA polyermase I-mediated rDNA transcription and ribosomal subunit assembly (Taddei et al., 2004). The nucleolus is composed of three main sections, the innermost fibrillar center (FC), the dense fibrillar component (DFC), and the granular component (GC) (Taddei et al., 2004). Both the GC and DFC are embedded in the GC (Sirri et al., 2008). The FC has active and inactive rDNA genes and the DFC is where processing and assembly of rRNA takes place (Taddei et al., 2004). Finally, the later stages of ribosomal maturation and assembly take place in the GC

(Taddei et al., 2004). Nucleoli localize to tandem repeats of rDNA known as nucleolar organizing regions (NORs) (Taddei et al., 2004). Localization studies of NORs using immunofluorescence microscopy have showed that NORs associate with the nuclear envelope (Trumtel et al., 2000). This localization has been shown to be RNA polymerase I dependent because when rDNA is transcribed with RNA polymerase II the localization of nucleoli shifts away from the nuclear envelope (Trumtel et al., 2000). This model was tested by disrupting the formation of the RNA polymerase I complex and then using immunofluorescence to study localization of nucleolar protein ssb1. Localization of ssb1had shifted away from the periphery of the nuclear envelope to internal regions of the nucleus (Oakes, 1998).

The nucleolus forms around tandem repeats of rDNA referred to as nucleolar organizing regions (NOR's) (Schardin et al., 1985; Eils et al., 1996). The trans-association of rDNA and NORs begins in an asynchronous manner shortly after telophase of mitosis (Savino et al., 2008). Using cells stably transfected with green fluorescent protein (GFP) tagged fibrillarin and GFP-tagged Nop52, localization of nucleolar proteins was tracked using live microscopy (Savino et al., 2008). Results of this study revealed that in early telophase, fibrillarin was concentrated in both prenucleolar bodies (PNBs) and NORs; whereas, PNBs enriched with Nop52 did not appear until later (Savino et al., 2008). Furthermore, analysis of PNBs revealed that nucleolar proteins are most likely progressively delivered to nucleoli in the form of large complexes based on their appearance through electron microscopy (Savino et al., 2008). Using a combination of immunofluorescence, electron microscopy, and *in situ* hybridization to study localization of RNA polymerase I upstream binding factor (UBF), nucleolin, fibrillarin, and pre-rRNAs throughout mitosis and the beginning of interphase revealed the nucleolar assembly occurred independently of rDNA transcription and prior

to chromosome decondensation (Dousset et al., 2000). Other non-random aspects of nuclear organization have been seen with Cajal bodies. Cajal bodies are localized predominantly in the nucleoplasm at the periphery of nucleoli and to a lesser extent within nucleoli (Malatesta et al, 1994). Interestingly, Cajal bodies show dynamic organization within cell nuclei. Time-lapse confocal microscopy revealed that Cajal bodies are mobile structures that may actually pass through nucleoli (Boudonck et al., 1999). Nuclear body dynamics has also been observed for PML bodies, a subclass of which shows metabolic-energy-dependent movement through the nucleoplasm (Muratani et al., 2001).

1.3 Nuclear Speckles

Nuclear speckles were first reported by Hewson Swift in 1959 and termed interchromatic particles based on their appearance and localization as observed by electron microscopy (Swift, 1959). In 1961, the term “speckles” was introduced by J. Swanson Beck after he examined rat-liver sections which had been immunolabeled with the serum from patients suffering from autoimmune disorders (Beck, 1961). The connection between pre-mRNA splicing factors and speckles was first revealed when immunolabeling studies showed that nuclear speckles have small nuclear ribonucleoprotein (snRNP) splicing factors (Spector, et al., 1983). Nuclear speckles were later shown to be the equivalent of the interchromatin granule clusters (IGCs) (reviewed in Lamond and Spector, 2003.). IGCs vary in size and are irregularly shaped (Thiry, 1995). Nuclear speckles are located exclusively in the nucleus, contain little to no DNA and are distinct from other splicing factor-containing structures in the nucleus such as perichromatin fibrils, Cajal bodies, interchromatin granule-associated zones, and

paraspeckles (Huang and Spector, 1997; Thiry, 1995; Fox et al., 2002). *In situ* hybridization studies show that highly active genes and transcripts are associated with the periphery of nuclear speckles and BrUTP labeling in permeabilized mammalian cells showed that transcription also occurs within nuclear speckles (Wei et al., 1999; Xing et al., 1995).

Nuclear speckles contain pre-mRNA splicing factors including snRNPs and SR proteins (proteins with a region rich in arginine and serine residues) as observed by immunolabeling of these proteins (Fu, 1995). Additionally, proteomic analysis of nuclear speckles revealed that speckles contain the large subunit of RNA polymerase II (Saitoh et al., 2004). Studies revealing the dynamic behavior of nuclear speckles have shown a constant flux of splicing factors between nuclear speckles and the nucleoplasm, which suggested that nuclear speckles serve as storage sites for pre-mRNA processing machinery (Saitoh et al., 2004). Studies using live cell microscopy have documented the recruitment of splicing factors from nuclear speckles to sites of active transcription; furthermore, when pre-mRNA splicing is inhibited, speckles round up and become larger and more defined (Misteli, et al., 1997; O'Keefe, R.T., et al., 1994). Misteli et al. (1996) reported that phosphorylation of the RS domain of SR proteins mediates splicing factor recruitment to active transcription sites. Furthermore, the presence of a variety of kinases and phosphotases within nuclear speckles supports this hypothesis (Mintz et al., 1999). In addition to splicing factor phosphorylation, the carboxy terminus of the large subunit of RNA polyermase II is also phosphorylated and required for targeting splicing factors to sites of active transcription (Misteli and Spector, 1999). Removal of the carboxy-terminus from the large subunit of RNA polyermase II inhibits both splicing factor recruitment to the transcription site and pre-mRNA processing (Misteli and Spector, 1999).

1.4 Cell Cycle Dynamics of Nuclear Domain Organization

When cells enter mitosis, nuclear domains completely disassemble, then assemble in newly formed daughter nuclei, presumably using the above-described self-assembly mechanisms. Although direct comparisons have not previously been made, it seems reasonable that a similar assembly process to what has been observed for nucleoli in post-mitotic daughter cells could be involved in nucleolar reorganization in response to other biological cues. For part of my project, I wished to study nuclear reorganization during muscle cell differentiation. This situation is likely similar to mitotic exit, since differentiating muscle cells leave a proliferative state and become programmed toward a less proliferative, specific cell type. In order to properly describe subtle changes in nuclear organization as well as to put conclusions about my observations into context with what is already known about nucleolar organization, it was important to consider nuclear organization and dynamics of not only interphase cells but also cells undergoing mitotic division. In other words, an understanding of post-mitotic nuclear organization may lend insight to nuclear reorganization observed during muscle cell differentiation. During mitosis, nucleoli disassemble and are no longer visible during prophase when rDNA transcription is repressed (Sirri et al., 2008). Immunolabeling of rRNA processing machinery with autoimmune sera collected from patients showed that at the beginning of prophase, rRNA processing components do not stay associated with rDNA at the NORs but become distributed over the surface of chromosomes (Hernandez-Verdunt et al., 1993; Gautier et al., 1992). Kinetic studies of fluorescently tagged RNA polymerase I subunit RPA39 and nucleolar protein fibrillarin revealed that these components transiently dissociate from NORs during metaphase and return in anaphase (Leung et al., 2004). Live cell microscopy with green fluorescent protein (GFP) tagged nucleolar proteins fibrillarin and Nop52 revealed that components of the dense fibrillar center

(DFC) and granular component (GC) portions of the nucleolus relocate to the chromosome periphery and migrate with chromosomes during telophase (Savino et al., 2001). These proteins then assemble at pre-nucleolar bodies (PNBs) located at the chromosome surface followed by progressive delivery of nucleolar proteins to NORs (Savino et al., 2001).

Also as part of my project, I wanted to document changes in nuclear organization of nuclear bodies during muscle cell differentiation. Dynamics of nuclear bodies other than nucleoli has been documented during mitosis. For example, immunofluorescence microscopy using an anti-p80 coilin antibody revealed that Cajal bodies change in size and number during mitosis (Andrade et al., 1993). Serum starvation studies in 3T3 mouse fibroblasts, revealed that cells which are not actively cycling only posses 0-1 Cajal bodies (Andrade et al., 1993). The number of Cajal bodies per cells is highest in mid-to late G_1. As the cells progress through S phase and G_2, Cajal bodies decrease in number and in size and eventually disappear in mitosis (Andrade et al., 1993; Andrade et al., 1991). Paraspeckles remain intact throughout mitosis until the cell enters telophase (Fox et al., 2002). Paraspeckles are RNA polyermase II transcription-dependent bodies found adjacent to nuclear speckles during interphase. In early telophase, when RNA polyermase II transcription is absent, paraspeckle proteins redistribute and form a crescent shaped perinucleolar cap within the nucleolus (Fox et al., 2002). As the cells exit mitosis and RNA polymerase II transcription resumes, paraspeckles reform in the interchromatin space in close proximity to nuclear speckles (Fox et al., 2002). Interestingly, the *multiple endocrine neoplasia (Men1)* locus shows upregulation of two noncoding RNAs, Men ε and Men β, during differentiation of mouse muscle cells (Sunwoo et al., 2008). Changes in nuclear organization of paraspeckles correlate with upregulated expression of these noncoding RNAs, as foci containing these

RNAs are enlarged and more numerous in differentiated myotubes than in myoblasts (Sunwoo et al., 2008).

Nuclear speckles, just like paraspeckles, undergo reorganization during mitosis at the onset of nuclear envelope break down (NEBD). At this time, proteins associated with nuclear speckles become diffusely distributed throughout the cytoplasm (Ferreira et al., 1994; Spector et al., 1986). When the cells progress to metaphase, proteins from nuclear speckles predominantly remain diffusely distributed in the cytoplasm. During metaphase, these proteins start to accumulate in one to three small structures called mitotic interchromatin granules (MIGs) that increase in size and number through anaphase and early telophase (Ferreira et al., 1994; Leser et al., 1989; Prasanth et al., 2003; Spector and Lammond, 2010). After mid-to late telophase, following reformation of the nuclear envelope and nuclear lamina, localization of pre-mRNA splicing factors to MIGs decreases as they enter newly formed daughter nuclei (Prasanth et al., 2003).

1.5 Myogenesis

Myogenesis is the progression of undifferentiated somite cells to fully differentiated, multi-nucleated myotubes. All skeletal muscle arises from mesodermal precursor cells in the somite (Molkentin and Olson, 1996). Somite cells themselves are created from the segmentation of paraxial mesoderm; furthermore, the somite becomes compartmentalized into separate cellular regions in response to signals from the notochord and neural tube during embryogenesis (Christ and Ordahl, 1995). Once the signals are received, the dorsal portion of the somite, also referred to as the dermamyotome, will give rise to the dermis and skeletal muscle (Molkentin and Oson, 1996). Specifically, induction of myogenesis comes from the notochord and ventral half

of the neural tube. The myogenic signal consisting of Wnt and Shh signaling proteins is soluble, it is essential for expression of basic helix-loop-helix (bHLH) myogenic regulatory factors (MRFs) and it does not require cell-to-cell contact (Buffinger and Stockdale, 1995). MRFs posses a conserved basic helix loop helix (bHLH) tertiary structure and they all bind to similar sequences of DNA to activate muscle-specific genes (Weintraub et al., 1991). The mode of action for MRFs entails heterodimerization with E2A gene products followed by binding to the consensus sequence of the E Box near the promoter region of muscle-specific genes (Molkentin and Olson, 1996). The E box is a DNA sequence typically found upstream of the promoter of genes that is recognized for binding of bHLH structural motif of MRFs in order to enhance transcription (Chaudhary et al., 1999). In addition to promoting transcription of muscle-specific genes, MRFs can physically interact with myocyte enhancer factors (MEFs) to activate muscle-specific genes (Molkentin et al., 1995). MRFs have a very potent regulatory effect capable of converting many non-muscle cell types into muscle *in vitro* (Choi et al, 1990, Davis et al., 1987, Molkentin and Olsen, 1996).

Munsterberg and colleagues showed that Wnt 1, Wnt 3, and Wnt 4 cooperate with Sonic Hedge Hog (Shh) to induce myogenesis in somites isolated *in vitro* (Munsterberg et al., 1995; Molkentin and Olson, 1996). Wnt signaling is mediated by a β-catenin-TCF/LEF-dependent canonical pathway which directly interacts with MyoD to enhance MyoD binding to the E box in the promoters of muscle specific genes (Kim et al., 2008). Within the lateral somite, these signals originate from the neural tube and notochord and induce the Pax3 transcription factor that in turn activates expression of MRF family members MyoD and Myf5 (Muntsberg and Lassar 1995; Weintraub et al., 1991). A schematic representation of muscle cell differentiation induction can be found in Figure 1.1.

Figure 1.1. Induction of muscle cell differentiation via Wnt and Shh. Signalling proteins Wnt and Sonic hedge hog (Shh) originate from the ventral neural tube and notochord, respectively, and induce differentiation through activation of MRF family members Myf5 and MyoD (Stern et al., 1995). Adapted from Molkentin and Onson, 1998.

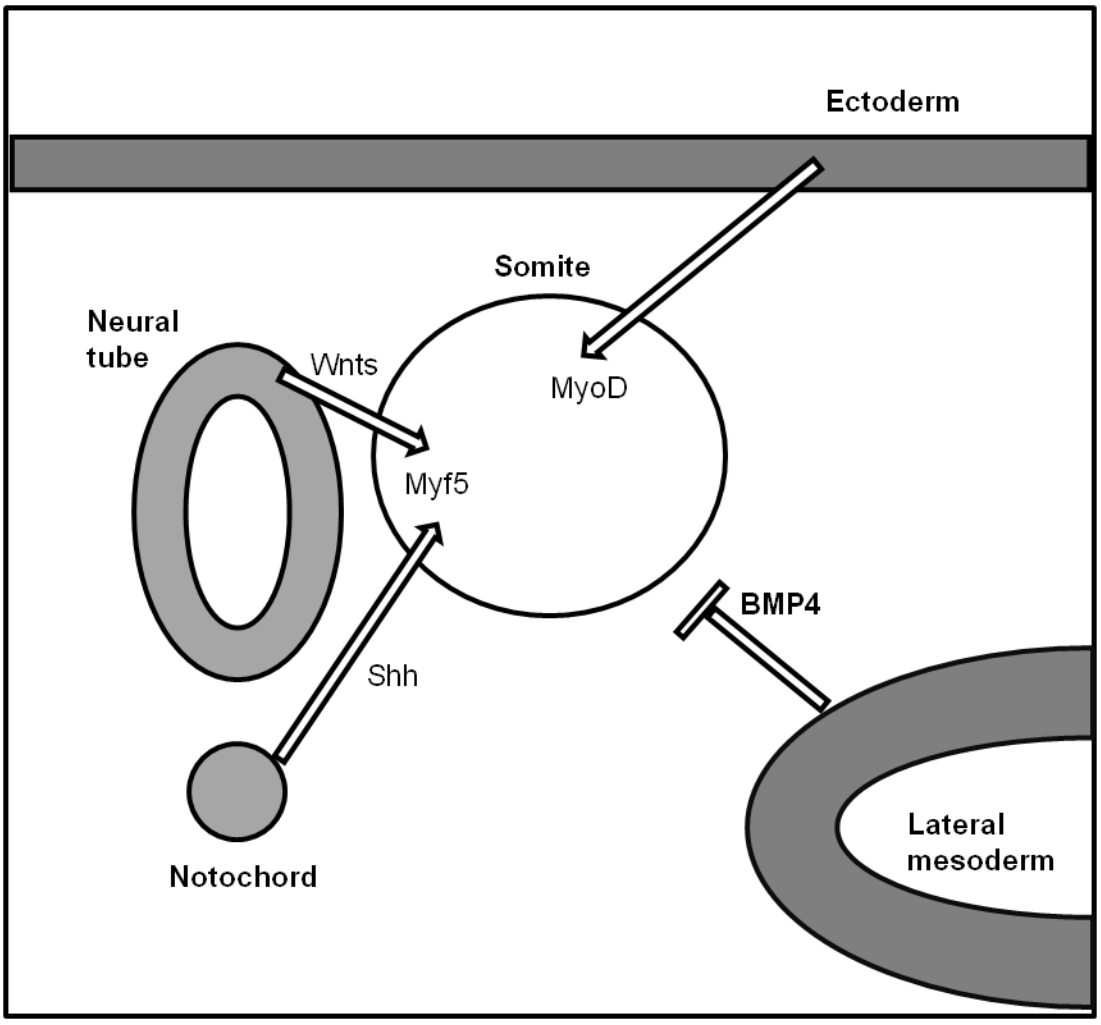

Adapted fromMolkentin and Olson, 1996

After Pax3 induces expression of MyoD in muscle precursor cells, MyoD-driven activation of additional MRFs needed for differentiation is sequestered in proliferating myoblasts through direct transcriptional repression and by blocking signaling pathways. Within proliferating myoblasts, several proteins and cellular signaling pathways work to suppress transcriptional activity of MRFs and myocyte enhancer factors (MEFs). The Inhibitor of Differentiation (Id) protein negatively regulates MRFs to inhibit myogenesis; specifically, Id will bind and sequester either MRFs or E2A proteins to prevent MRFs from binding to the consensus sequence within the E box in the promoter region of muscle specific genes (Benezra et al., 1990). Myostatin is another protein involved in negatively regulating transcription of MRFs. Specifically, myostatin inhibits the synthesis and activity of MyoD (McPherron et al., 1997; Amthor et al., 2004; Guttridge 2004). Myostatin is a member of the transforming growth factor-β family and is unique in that it negatively regulates both myogenesis and muscle cell proliferation in order to maintain muscle homeostasis within an organism. Organisms null for myostatin show increased muscle mass due to hypertrophy (McPherron et al., 1997).

Multiple other signaling pathways are involved in negatively regulating myogenesis within proliferating myoblasts. The Janus kinase signal transducer and activator of transcription (JAK-STAT) pathway is a very well characterized pathway that is both required for myoblast proliferation and an important checkpoint to prevent premature differentiation of myoblasts; furthermore, knockdown of the JAK1-STAT1-STAT3 pathway induced premature differentiation of myoblasts through induction of MyoD and MEF2 and downregulation of Id1 (Luguo et al., 2007; O'Shea et al., 2002). The Stau1 pathway is also involved in negative regulation of myogenesis (Yamaguchi et al., 2008), as knockdown of Stau1 enhanced myogenesis. Cells depleted of Stau1showed an increase in myogenin promoter activity, indicating that Stau1 may work

to inhibit an event directly prior to activation of the myogenin promoter (Yamahuchi et al., 2008). Stau1 also inhibits myogenesis through association with the UPF-1 protein, which is a component of mRNA decay machinery that attacks MyoD mRNA (Yamaguchi et al., 2008). Another signaling pathway, the notch pathway, inhibits myogenesis through repression of MyoD (Buas and Kadesch 2010; Kopan et al., 1994). Ectopic expression of notch inhibits differentiation of C2 myoblasts upon serum deprivation and stops the conversion of 3T3 cells transfected with expression vectors driving Myf5 or MyoD expression. Furthermore, evidence indicates that notch expression does not stop the binding of E proteins to the E box-binding site within MyoD, but rather targets the bHLH region of MyoD following heterodimerization (Kopan et al., 1994).

In order for myoblasts to differentiate, they must withdraw from the cell cycle (Molkentin and Olson, 1996). Withdrawal from the cell cycle and subsequent transcription of muscle-specific genes requires the removal or depletion of fibroblast growth factors (FGFs) in the surrounding environment (Menko and Boettiger, 1987). After FGFs are absent from the environment, several proteins associated with the cell cycle and cell cycle progression is modified in terms of structure and/or expression levels to promote cell cycle withdrawal and differentiation. For example, the retinoblastoma (Rb) protein is phosphorylated in proliferating cells to sequester it and its growth-inhibiting activity; however, when FGFs are depleted, the Rb protein is dephosphorylated and becomes active (Molkentin and Olson, 1996; Weinberg, 1995). Rb then sequesters the E2F family of transcription factors that directly activate the expression of several genes required for cell proliferation (Weinberg 1995). MRFs are suppressed in proliferating myoblasts, and forced expression of these proteins inhibits cell cycle progression, suggesting that MRFs and proteins associated with cell cycle progression modify each other's activities (Molkentin and Olson, 1996) as exemplified by

the relationship between cyclin D1, Rb, Cdk inhibitor 21, and MRF proteins. In proliferating myoblasts, cyclin D1 suppresses Rb and allows for progression of the cell cycle, specifically at the G_1-S transition. Furthermore, cyclin D1 inhibits MyoD-mediated transcriptional activation of MRFs (Skapek et al., 1995; Molkentin and Olson, 1996). After myoblasts receive the signal to differentiate, Cdk inhibitor p21 is upregulated and suppresses cyclin D1 (Skapek et al., 1995). When cyclin D1 is inhibited, Rb and MyoD are no longer sequestered and can inhibit cell cycle progression and allow activation of MRFs respectively (Skapek et al., 1995; Guo et al., 1995). Figure 1.2 summarizes these interactions.

When differentiation is induced and cell cycle progression is halted, expression of muscle-specific genes is upregulated, further directing myoblasts along the differentiation program. In addition to MyoD and Myf5, the MRF family of proteins consists of Myogenin and Myf4, which also play crucial roles in ensuring terminal differentiation of myoblasts (Weintraub et al., 1991). Following activation of the MRFs myogenin and Myf4, myogenin is likely to cooperate with MyoD and Myf5 to activate muscle contractile genes such as myosin heavy chain (MHC) (Lassar et al., 1991). During differentiation, expression and activity of MRFs is positively regulated through a number of proteins and pathways. For example, the half-lives of MyoD, myogenin, and p21 mRNAs are extended during myogenesis (Myer et al., 1997; Kao et al., 1994). Proteins HuR and NF90 both work to bind to the Au-rich element of the 3' untranslated region (3' UTR) of muscle-specific transcripts to protect against degradation (Myer et al., 1997; Kao et al., 1994). A protein called titin-cap (TCAP) positively regulates myogenesis through interaction with myostatin. When TCAP is knocked down via RNA interference, the expression of MyoD and myogenenin also decreases (Nicholas et al., 2002). Another protein, numb, works to promote myogenesis through inhibition of the

Figure 1.2. Interaction between MRFs and cell cycle progression-related proteins. MRFs and proteins involved with cell cycle progression modify each other's activities. In proliferating myoblasts cyclin D1 supresses Rb and MyoD-mediated transcriptional activation of MRFs. In differentiating myoblasts, Cdk inhibitor p21 inhibits cyclin D1 and Rb and MyoD-mediated transcription become active. Adapted from Molkentin and Olson, 1998.

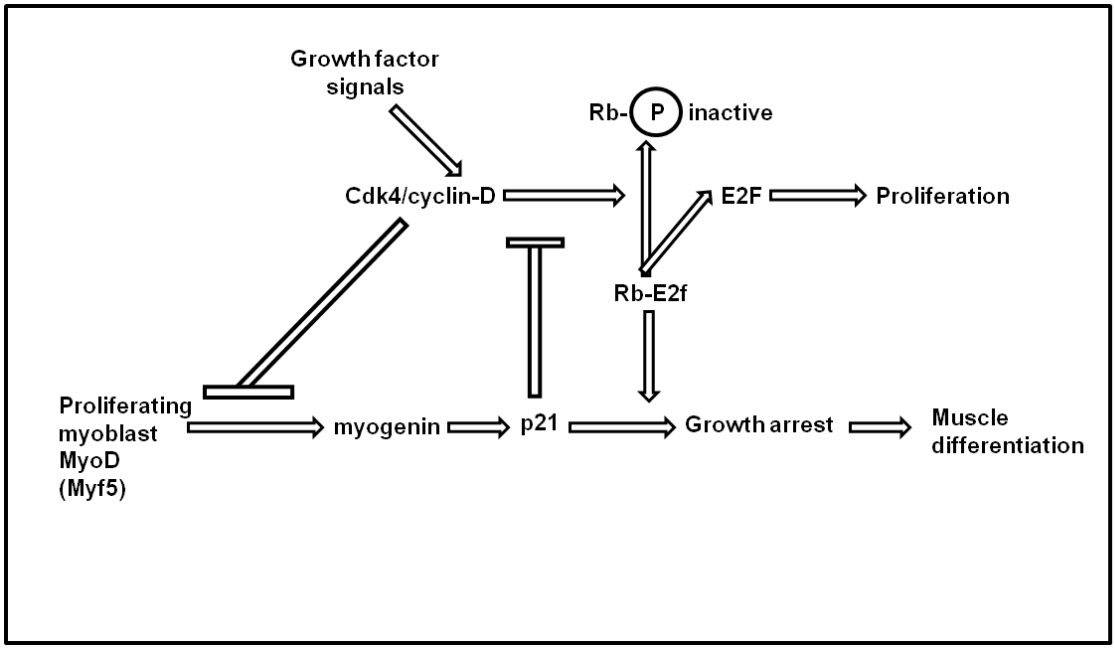

Adapted from Molkentin and Olson, 1996

notch signaling pathway (Buas and Kadesch 2010). During endocytic trafficking, notch can be sent to the early endosome for recycling in the cell or sent to the late endosome for degredation. Overexpression of numb followed by surface biotinylation and trafficking assays revealed that in the presence of numb, notch is preferentially sent to the late endosome for degredation indicating that numb inhibits the notch signaling pathway through endocytosis (McGill et al., 2009).

After myoblasts receive the signal to terminally differentiate, myoblasts will align into a chain-like formation in preparation of fusion to become the multi-nucleated myotube (Knudsen, 1985). Cellular fusion within myogenesis is actually divided into two stages; the first consisits of myoblasts fusing with other myoblasts, and the second involves myoblasts fusing to existing myotubes (Rochlin et al., 2010). The alignment process is mediated by cellular membrane glycoproteins including several cadherins and cell adhesion molecules (CAMs). Furthermore, this process requires that neighboring cells participating in the fusion event are all myoblasts (Knudsen et al., 1990). In order for myoblasts to become aligned, they must first migrate towards one another. The actin cytoskeleton is crucial in facilitating migration of myoblasts. Myoblasts treated with latrunculin A or cytochalasin D (that interfere with F-actin) exhibit hindered myoblast migration (Coue et al., 1987; Dhawan and Helfman, 2004; Nowak et al., 2009; Constantin et al., 1995; Sanger and Holtzer, 1972). Once myoblasts are aligned, cellular membranes are dissolved and multiple myoblasts join together to form one multinucleated myotube (Konigsberg, 1963; Mintz and Baker, 1967). Different proteins are involved in myoblast-to-myoblast fusion than are involved in myoblast-to-myotube fusion (Rochlin et al., 2010). Proteins including β1-integrin, VLA-4, VCAM, and caveolin-3 are involved in myoblast-to-myoblast fusion (Schwander et al., 2003; Rosen et al., 1992; Galbiati et al., 1999). The NAFTC2 pathway activated by calcium, calmodulin, and

IL-4 cytokine is involved in regulating myoblast-to-myotube fusion (Rochlin et al., 2010).

In summary, there is a relatively clearly defined molecular pathway for muscle cell differentiation and for regulation of gene expression during myogenesis. The proteins involved in the molecular pathways leading to muscle cell differentiation provide an excellent roadmap of cellular markers that can be used to understand how proteins that have not previously been assigned any functions in muscle cells might participate in muscle cell differentiation. Within this study, we used key proteins and morphological states (namlely myogenin, myosin heavy chain (MHC), and mulitinucleation) to study how Bcl-2- associated transcription factor (Btf) functions might possibly participate muscle cell differentiation. Using a combination of immunofluorescence labeling of Btf as well as myogenin and MHC and western blot analysis, we have studied the labeling and relative expression levels of Btf throughout the differentiation time course using a C2C12 mouse myoblast cell line.

1.6 Nuclear Organization and Muscle Cell Differentiation

Cellular differentiation requires a vast shift in gene expression. Given that nuclear structure is functionally related to gene expression, it stands to reason that a shift in gene expression would lead to a shift in nuclear structure. Recent studies indicate that genome architecture is dynamic and varies with the cell cycle and physiological state of the cell (Ferguson and Ward, 1992; Vourch'h et al., 1993; Nagase et al., 1996; Brero, et al., 2005). During cellular differentiation, genes that have been previously silenced through repressive conformations imposed by nucleosomes must be made accessible to transcription factors (Cairns, 2009). Nucleosome-enforced repression can be overcome by a combination of tissue-specific transcription factors and multi-subunit machineries that remodel nucleosomes (Berkes and Tapscott, 2005). In the case of myogenesis, MyoD and Myf5 must be able to bind the E box within the promoter regions of muscle-

specific bHLH genes such as myogenin and Myf4 (Berkes and Tapscott, 2005). A combination of physical and functional interactions between bHLH proteins and SWI/SNF chromatin remodeling complexes allow for the rearrangement of nucleosomes to remodel the chromatin in way that favors transcriptional access of MyoD and Myf5 to muscle-specific bHLH and MEF2 factors (de la Serna et al., 2001; Simone et al., 2004). The SWItch/Sucrose NonFermentable (SWI/SNF) is an ATP-dependent chromatin remodeling unit which consists several proteins that are products of the SNF and SWI genes as well as two main catalytic subunits, Brg1 and Brm (de la Serna et al., 2001; Simone et al., 2004; de la Serna et al., 2006). In addition to catalytic subunits, different combinations of noncatalytic subunits including Brg1/Brm-associated factors (BAFs) provide the SWI/SNF complex with molecular variability allowing the complex to selectively interact with different tissue-specific transcription factors and other chromatin-remodelling enzymes (Wu et al., 2009). The mechanism by which the SWI/SNF complex remodels chromatin involves altering the position of nucleosomes along the DNA through ATPase activity that works to destabilize DNA-histone interactions; however, the exact change in structure is unknown (Pazin et al., 1997; Whitehouse et al., 1999). In addition to general chromatin remodeling, Chaly and Munro studied localization of centromeres during myogenesis *in vitro* using a L6E9 rat myoblast cell line (Chaly and Munro, 1996). During myogenesis, centromeres relocated to the nuclear periphery; furthermore, condensed chromatin was more prevalent at the myotube nuclear envelope as observed by electron microscopy (Chaly and Munro, 1996). Regions of heterochromatin also display a spatial clustering that is reliant on histone deacetylase (HDAC) activity (Terranova et al., 2005). However, characterization of nuclear organization of other nuclear domains during muscle differentiation is limited, and our project aimed to observe changes in nucleoli and nuclear speckles relative to the differentiation timeline in C2C12 cells.

1.7 Bcl-2 Associated Transcription Factor

Several nuclear speckle proteins have recently gained attention due to unique domain structure and/or suggested functions. One of the non-classical SR proteins identified in a proteomic analysis of purified mouse nuclear speckles was Bcl-2 associated transcription factor (Btf) (Saitoh et al., 2004). Btf showed some colocalization with splicing factors in nuclear speckles, and it has an RS domain; however, the RS domain in Btf is located at the N-terminus rather than the C-terminus where it is typically found in classical SR proteins (Saitoh et al., 2004; Mintz et al., 1999). Btf is a transcription repressor that, when overexpressed, induces apoptosis through inhibition of the anti-apoptotic Bcl-2 protein family (Kasof et al., 1999; Haraguchi et al., 2004). Interestingly, Btf is expressed at high levels in skeletal muscle (Haraguchi et al., 2004; Nagase et al., 1996). Previous evidence suggests that Btf may associate with emerin, (Haraguchi et al., 2004; L. Ford and P. Bubulya, unpublished data), a 34kDa, 254-amino acid, serine-rich inner nuclear envelope protein (Haraguchi et al., 2004; Fairley et al., 1999).

Emerin is thought to possibly regulate mechanosensitive and stress-induced genes, contributing to overall muscle maintenance and integrity (Fairley et al., 1999; Ostlund et al., 1999). In addition to Btf, emerin binds to lamins A and C, lending structural integrity to the cell according to the Structural Hypothesis (Salpingidou et al., 2007). The Structural Hypothesis proposes that the network of emerin and lamins serve as the load-bearing center of the nuclear envelope, and that bridging complexes span the nuclear envelope connecting the inner nuclear membrane with the actin cytoskeleton (Hutchinson et al., 2002; Crisp et al., 2006). Muscle cells null for emerin undergo cell death and eventual muscle wasting; furthermore, a number of emerin mutations have been associated with Emery-Dreifuss Muscular Dystrophy (Broers et al., 2004,

Salpinidou et al., 2007). Select mutations in emerin that have been associated with EDMD occur within the region of emerin that associates with Btf (Salpinidou et al., 2007). Although emerin with such naturally occurring mutations (for example, a serine to phenylalanine substitution at residue 54 (S54F), a proline to histidine substitution at residue 183 and a proline to threonine substitution at residue 183) demonstrated normal levels and localization (Haraguchi et al., 2004), One might predict disrupted Btf-emerin association, that could lead to altered function in muscle cells. Based on the supposed interaction of Btf and emerin and Btf's putative role in EDMD, we wish to investigate a possible role for Btf in muscle cells. However, because the behavior of nuclear speckles and constituent proteins is poorly characterized during muscle cell differentiation, we set out to build a timeline of these events in C2C12 mouse myoblasts.

Chapter 2: Hypothesis and Experimental Amis

Emery-Dreifuss muscular dystrophy (EDMD) is an X-linked recessive disorder causing progressive muscle wasting, cardiomyopathy, and a deformation of muscular tissue in the elbows, Achilles tendon, ankles, and spine (Emery 1989). Sudden death resulting from cardiac defects can be averted with early diagnosis and pacemaker placement; however, there is no treatment for the accompanying muscle wasting (Ellis *et al.* 1999). Most EDMD patients are null for the nuclear protein emerin resulting from nonsense mediated decay (Haraguchi et al., 2004). Emerin is a 34kDa, 254 amino acid, and serine rich, nuclear envelope protein; furthermore, emerin is predicted to be a type II membrane protein possessing a transmembrane region (Haraguchi et al., 2004; Fairley et al., 1999). Emerin is thought to possibly regulate mechanosensitive and stress-induced genes, contributing to overall muscle maintenance and integrity (Fairley et al., 1999; Ostlund et al., 1999). A subset of EDMD patients demonstrate normal amounts and localization of emerin at the inner nuclear membrane in contrast to most EDMD patients whom produce no detectable emerin as observed by immunoblotting and immunohistochemistry; furthermore, all of these mutations that produce seemingly "normal" emerin occur within regions of emerin which associate with Btf (Haraguchi et al., 2004; Fairley et al., 1999). This set of mutations includes a serine to phenylalanine substitution at residue 54 (S54F), a proline to histidine substitution at residue 183 and a proline to threonine substitution at residue 183 (Haraguchi et al., 2004).

Based on the supposed interaction of Btf and emerin as well as Btf's putative role in EDMD, we investigated a possible role for Btf in muscle cells using a C2C12 mouse

myoblast cell line. C2C12 differentiation in our hands reflected timing and gross morphological changes seen previously (Konigsburg, 1963; Mintz and Baker, 1967; Lassar et al., 1989). This is important because it allowed likewise comparison of our data and data of other labs which have done work on muscle cell differentiation in C2C12 cells. Preliminary experiments revealed that Btf was upregulated during differentiation as observed by immunoflourescence microscopy and immunoblotting (Figure 2.1) (Theadore Hufford, Alok Sharma and Paula Bubulya, unpublished data). I performed differentiation time course experiments in which I immunolabled Btf and muscle specific proteins which validated observations made by an undergraduate honors student who had only done the experiment once. I therefore hypothesized that increased expression of Btf may be important for muscle cell differentiation. In order to test this hypothesis, I designed experiments in which Btf was overexpressed and experiments in which Btf was depleted. Given that Btf is upregulated during differentiation, I overexpressed Btf in undifferentiated C2C12 cells to determine if overexpression of Btf could induce differentiation or possibly expedite the differentiation time course as compared to C2C12 cells undergoing a normal differentiation time course induced by serum deprivation. Controls were included to assert that transfection alone was not altering differentiation, that transfected cells could indeed differentiate, and that timing of differentiation in transfected samples which were either induced or not induced to differentiate matched the timing of untransfected samples maintained in the same conditions. Given that Btf is upregulated during differentiation, I also designed experiments to deplete Btf in C2C12 cells and induce differentiation to determine if C2C12 cells depleted of Btf could undergo normal differentiation. siRNA was utilized for Btf depletion and differentiation via serum deprivation was induced 24 hours following siRNA treatment. Cells treated with siRNA buffer alone, siRNA oligs targeted against luciferase, as well as untransfected cells were used as controls.

Figure 2.1. Western blot analysis to detect expression of nuclear and muscle specific proteins during differentiation of C2C12 myoblasts. WCNE was prepared on each day of the differentiation time course. Equal total protein in each sample was loaded onto SDS-PAGE and transferred to a nitrocellulose membrane for immunoblotting. Upon stimulus to differentiate, expression of muscle-specific gene myogenin was increased at Day 1 and MHC expression was increased at Day 2. Btf expression is detectable at Day 1 and increases through Day 4 of the differentiation time course. Nuclear speckle protein SF2/ASF also show increased in expression between Day 0 and Day 1. Actin was used as an equal loading control. Western Blot was performed by Alok Sharma.

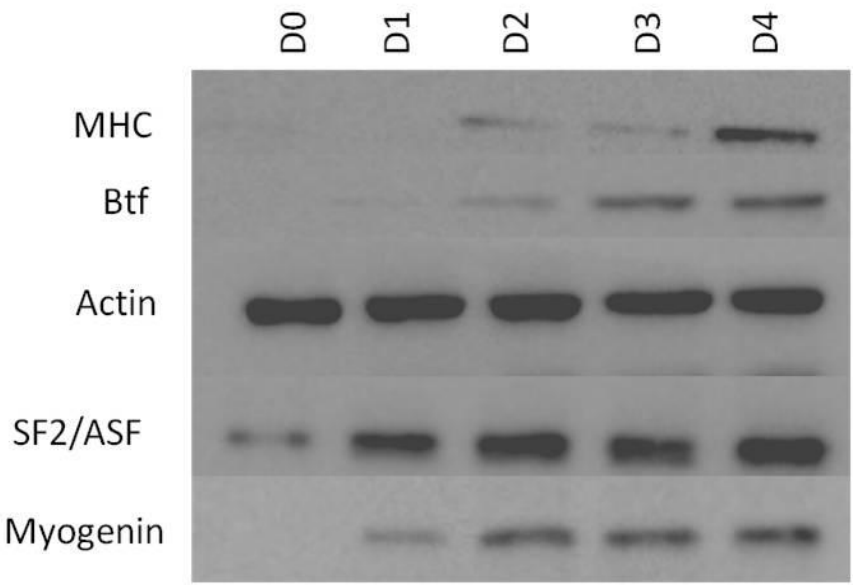
D0
D1
D2
D3
D4
MHC
Btf
Actin
SF2/ASF
Myogenin

In addition to Btf upregulation during C2C12 differentiation, preliminary experiments showed surprising nuclear reorganization. To investigate this further, I did differentiation time course experiments in which I observed nuclear domains. My results substantiated observations made by an undergraduate honors student who had only done the experiment once. I therefore proposed that muscle cell differentiation as observed in C2C12 cells resulted in reorganization of nuclear domains. To test this hypothesis, I designed experiments to investigate nuclear speckle and nucleolar organization throughout the differentiation process as well as experiments to assert that the observed nuclear reorganization was not a result of serum starvation. To observe nuclear speckles and nucleoli during the differentiation process, I performed differentiation time course experiments in which I immunolabeled for nuclear speckle protein Son or nucleolar protein fibrillarin as well as muscle specific proteins myogenin and MHC. I also performed serum starvation experiments with HeLa and MEF cells to confirm that the nuclear reorganization observed in differentiating C2C12 cells was not a result of serum starvation or a muscle specific phenomenon. Throughout differentiation, both nuclear speckles and nucleoli change in morphology from diffuse and less enriched bodies to more punctuate and enriched bodies; therefore, I hypothesized that nuclear domains most likely reorganize in one and/or two ways. One proposed method is that nuclear domains fuse during differentiation and the other possibility is that some nuclear domains recede while others enlarge (Figure 2.2). To test this hypothesis, I designed experiments to image nucleoli in differentiating C2C12 cells live. I performed experiments to optimize transfection of CFP-fibrillarin plasmid DNA via electroporation and experiments to determine the optimal time for imaging to capture the change in nucleolar morphology.

Figure 2.2. Proposed model for nuclear reorganziation as observed in differentation of C2C12 myoblasts. Two modes of action were proposed to describe the change in nuclear organization. The first model suggests that multiple domains fuse together over time, while the second models suggests that certain nuclear domains become larger while others recede over time.

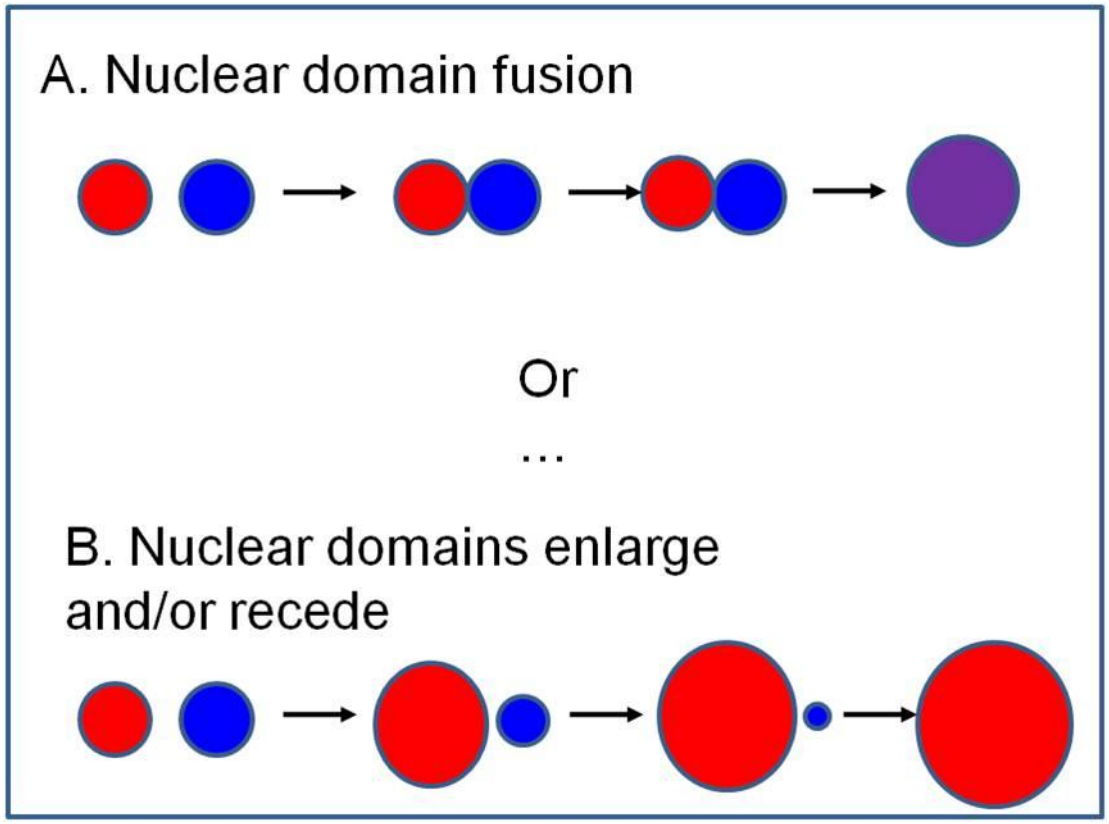
A. Nuclear domain fusion
Or
…
B. Nuclear domains enlarge
and/or recede

I hypothesized that Btf is important for muscle cell differentiation and muscle cell differentiation results in nuclear reorganization. My specific experimental aims were as follows:

Aim I.

Investigate effects of Btf overexpression and depletion on C2C12 differentiation.

Aim II.

Characterize the nuclear reorganization events that occur during muscle differentiation and image nucleolar reorganization events in live cells.

Chapter Three: Materials and Experimental Methods

3.1 Cell Culture

C2C12 cells (ATCC) were passaged for three days to expand the culture. Frozen stocks of equal passage number (passage 4) were stored at -80°C for all experiments. C2C12 and mouse embryonic fibroblast (MEF) cells were maintained in growth medium (GM) which consisted of Dulbecco's Modified Eagles Medium (DMEM) supplemented with 15% Fetal Bovine Serum and 1% penicillin/streptomycin (50:100 units penicillin, 50:100 µg streptomycin; Invitrogen) (Growth Medium, GM). HeLa cells were maintained in DMEM supplemented with 10% FBS and 1% penicillin/streptomycin. All cells were kept in a humidified 37°C incubator injected with 5% carbon dioxide. For each experiment, a fresh vial of C2C12 cells was thawed, plated in a 100mm x 20mm culture dish and grown for approximately 36 hours until the cells reached 60-70% confluency. MEF and HeLa cells were grown in 100mm x 20mm culture dishes and were passaged when the cells obtained 70-80% confluency. To passage MEF and HeLa, cells were first briefly washed three times with phosphate buffered saline (PBS; 137 mM NaCl; 2.7 mM KCl; 4.3 mM Na2HPO4; 1.47 mM KH2PO4, pH 7.4). Following washing, the cells were incubated with trypsin-EDTA (Invitrogen; 0.25% trypsin solution) for 3 minutes at 37°C with minimal agitation. Approximately 5 mL of DMEM + 15% FBS was added to inactivate the trypsin, and the suspension was transferred to a 15 mL conical tube and centrifuged at 1500 rpm for 2 minutes. The supernatant was removed by aspiration and the pellet was resuspended with 5 mL of DMEM + 15% FBS. The cells were then either plated into fresh 100 mm x 20 mm culture dishes or counted and plated into well dishes

for experiments.

3.2 Plating Cells

To plate cells for differentiation time courses, siRNA depletion experiments, YFP-fusion protein overexpression experiments and all other experiments, the cells were first collected from the 100 mm x 20 mm culture dishes, centrifuged, and resupsended as previously described. Ten microliters of the cell suspension was loaded onto each side of a Bright-Line Hemocytometer and the cells were counted and averaged to determine cell concentration. Cells were diluted to the appropriate concentration with DMEM+ 15% (for C2C12)or 10% FBS (for HeLa or MEF) and plated in wells with coverslips for processing for immunofluorescence and live cell imaging, or without coverslips for protein and RNA extraction. For all differentiation time course studies, $2x10^5$ C2C12 cells were plated in 35mm dishes. For all MEF and HeLa immunofluorescence experiments, $1x10^5$ cells were plated in 35mm dishes. For siRNA experiments, $1x10^5$ C2C12, MEF, and HeLa cells were plated in each well of 24-well dishes. For live cell imaging optimization experiments, $2.5x10^5$ C2C12 cells were plated onto each well of a 6-well dish. For live imaging, $5x10^5$ C2C12 cells were plated into each 60 mm x 15 mm dish.

3.3 Coverslip Preparation

All coverslips were cleaned thoroughly by washing in one part nitric acid and two parts hydrochloric acid for approximately 2 hours with occasional stirring; continuous rinsing in distilled water was done until the pH returned to approximately 7.0. The coverslips were then stored in 70% ethanol and flamed prior to use. Coverslips to be used with C2C12 cells were treated with 0.001% Poly-L-lysine (Sigma) for five minutes

at room temperature. The mixture was removed by aspiration, the coverslips were dried for 30 minutes at room temperature, and washed three times for 5 minutes each with PBS at room temperature. The coverslips were either used immediately or stored at 4°C.

3.4 Induction of C2C12 Differentiation

C2C12 differentiation was induced via serum deprivation or self-induction through cell-to-cell contact (Yaffe and Saxel, 1977). For induction of differentiation using serum deprivation, the cells were plated one day prior to inducing differentiation (Day -1) in GM. Differentiation was induced on Day 0 of the time course by removing GM and washing briefly three times with PBS to remove any remaining GM. Differentiation was then induced with the addition of differentiation medium (DM) consisting of DMEM supplemented with 2% Horse Serum and antibiotics streptomycin and penicillin. For self-induction of C2C12 differentiation, cells were plated at $3.5x10^5$ C2C12 in 35mm dishes. Cells were maintained in GM throughout the entire differentiation time course and GM was replenished every 48 hours. Cells were monitored daily for the formation of myotubes as an indication that differentiation was proceeding normally.

3.5 Immunofluorescence

C2C12 cells were washed briefly three times with PBS and fixed with 2% formaldehyde (2 grams paraformaldehyde dissolved into 100 mL PBS) for 15 minutes at room temperature. Cells were washed 3 x 5 minutes with PBS. Cells were permeabilized with 0.2% Triton X-100 in PBS for 10 minutes and washed 3 x 5 minutes in PBS + 0.5% normal goat serum (NGS; Gibco) at room temperature. Cells were incubated with primary antibodies WU10 (anti-Btf, 1:1000), WU13 (anti-Son, 1:1000), human anti-nucleolar antibody (anti-fibrillarin , 1:500; Sigma Aldrich, St. Louis, MO), monoclonal F5D (anti-myogenin,1:500; University of Iowa Developmental Studies Hybridoma Bank, Iowa

City, IA), monocolonal MF20 (anti-MHC, 1:1000; University of Iowa Developmental Studies Hybridoma Bank, Iowa City, IA), monocolonal anti-fibrillarin (1:500; Abcam, Cambridge, MA), and anti-Asym 25 (1:100, provided by Jocelyn Cote, University of Ottowa, Ottowa, Ontario) for 1 h at room temperature in a humidified chamber. Cells were washed 3 x 5 minutes with PBS + 0.5% NGS and incubated with either FITC-, Texas Red-, or Cy5-conjugated secondary antibodies (1:2000; Jackson Immunoresearch Laboratory) for 1 h at room temperature in a dark, humidified chamber. Cells were washed once in PBS + 0.5% NGS, then with PBS + DAPI (10µg/ml) in PBS in the second wash. Coverslips were mounted using 12 µl of mounting medium containing anti-fade (polyphenylinediamine), sealed with nail polish, and stored at -80°C. HeLa cells were processed the same as C2C12 cells with the exception that permeabilization was performed for 5 minutes. MEFs were also processed the same as C2C12 cells but fixation was done with 4% formaldehyde.

3.6 Microscopy

The cells were imaged used a DeltaVision RT real time restoration system (Applied Precision) with PLAN-APO oil, 1.4 N.A. objectives (Olympus). C2C12 cells were imaged with a 40x objective lens and MEF and HeLa cells were imaged with a 60x objective lens. Images were obtained with a cool snap CCD camera and SoftWorx Explorer Suite was used for visualization and processing. Z-stacks consisting of 0.2 µm increments through the z-plane of the cells were displayed as a volume projection to include all images from the z-stack of interest. For live imaging, z-stacks were collected at 30 minute intervals in 0.30 µm increments throughout the entire depth of all C2C12 nuclei within a region of interest.

3.7 Whole Cell Nuclear Extract Preparation

C2C12 cells for immunoprecipitation experiments were extracted using the whole cell nuclear extract (WCNE) protocol established by Wysocka et al. (2003). The cells were removed from the plate by applying PBS to the cells and scraping using a rubber policeman. The cells were then placed in an eppendorf tube and centrifuged for 5 minutes at 1200 rpm. Lysis buffer [300mM NaCl, 100mM Tris (pH 8.0), 0.2mM EDTA (pH 8.0), 0.1% NP40, 10% glycerol and protease inhibitor cocktail (Pierce, 1 tablet per 10 ml of lysis buffer added freshly prior to cell extraction] was added to the pellet and incubated at 4°C on a tube rotator. After incubation with lysis buffer, the extract was centrifuged for 10 minutes at 14,000 rpm at 4°C and the supernatant was collected and stored at -80ºC.

3.8 Protein Extraction, Bradford Assays, and SDS-PAGE

Cells were washed with PBS and scraped from the dish using 1ml of PBS and a rubber policeman. The wells were then washed with additional PBS, the samples were collected, centrifuged at 4°C for 5 minutes in a clinical centrifuge at 1200 rpm, the supernatant was removed, the pellet washed with additional PBS, and the samples centrifuged again for 1 minute. The supernatant was removed, the pellet was resuspended with 50-100 µl of RNase-free water, an equal volume of 2x Laemmli buffer (4% SDS, 20% glycerol, 1.4M β-mercaptoethanol, 0.125 M Tris HCl, and bromophenol blue) was added, and the samples were stored at -80°C. Before Bradford Assays were performed, the protein samples were boiled for 5 minutes to denature the proteins. For the Bradford Assays, standards of 1µg, 2µg, 5µg, 10µg, and 20µg of BSA were prepared in distilled water in a total volume of 4µl. 2µl of cell extract was mixed with distilled water for a total volume of 4µl. 496µl of water and 500µl of Thermo Scientific Coomassie Plus

Protein Assay Reagent were then added for a final volume of 1mL. Samples were loaded into 1 mL cuvettes and absorbance was measured at λ495 on a Milton Roy Spectronic 1001 Plus. A graph of OD versus µg protein was plotted with the standard samples and a best fit line was applied. Once protein concentrations of experimental samples were determined using absorbance readings and the standard curve, 40ug of each sample was loaded into the wells of a 10% or 15% poly-acrylamide gel [resolving gel: 10% or 15% Degassed acrylamide/bis, 0.125 M Tris HCl (pH 8.8), 0.1% SDS; stacking gel: 10% Degassed acrylamide/bis, 0.125 M Tris HCl (pH 6.8), 0.1% SDS], and gel electrophoresis was performed in Running Buffer [30 mM Tris HCL, 144 mM glycine, 0.01% SDS] at 150 V for approximately one hour. Precision Plus protein ladder purchased from BioRad served as the molecular mass marker. The proteins were then transferred from the polyacrylamide running gel to a nitrocellulose membrane at 200 mA for 90 minutes using chilled Transfer Buffer (Running Buffer containing 20% methanol). Ponceau (0.5% Ponceau S, 1% acetic acid) staining was used to confirm successful transfer and to mark well lanes and marker. The nitrocellulose membrane was blocked to avoid non-specific binding of antibodies using PBST [0.22 M sodium phosphate monobasic, 1.2 M sodium phosphate dibasic anhydrous, 137 mM sodium chloride, and 1.0% Tween] and 5% non-fat dry milk. The membrane was then cut horizontally to separate the region of the membrane with the protein of interest and the protein used as equal loading control to allow for dual probing. Primary antibodies were diluted in 5% non-fat dry milk in PBST, applied to the membrane, and incubated for 1 hour at room temperature. The membrane was washed 3 x 5 minutes with PBST on a shaker, and species-specific antibodies conjugated with horseradish peroxidase (HRP) diluted in PBST + 5% nonfat dry milk were applied to the membrane and incubated for 1 hour at room temperature on a shaker. The membrane was washed 3 x 5 minutes with PBST the membrane was developed using Thermo Scientific Pierce ECL Western Blotting

Substrate. The blot was then imaged on Fuji LAS- 4000 Luminescent Image Analyzer (Fujifilm Life Science USA, Stamford, CT).

3.9 RNA Extraction

Cells to be harvested for RNA extraction were plated as described above. All RNA extractions were performed using Qiagen RNeasy reagents and supplied protocols. DMEM was removed from cells and collected in 15 ml conical tubes. The cells were washed briefly with PBS, incubated with trypsin, collected using 1 mL DMEM, and centrifuged for 2 minutes in a conical centrifuge at 1500 rpm. The supernatant was removed, the pellet was washed with PBS, the samples were centrifuged again for 2 minutes in a conical centrifuge at 1500 rpm, and supernatant was removed. Pellets were resuspended with 350ul of Qiagen RNeasy RLT buffer and vortexed for 1 minute. 350µl of 70% ethanol was added and 700 µl of the sample was loaded into a RNeasy spin column and centrifuged for 15 seconds at 1600 rpm. 700 µl of Qiagen RNeasy RW1 buffer was added to the column and centrifuged as before. 500ul of Qiagen RNeasy RPE buffer was added to the column, centrifuged as before, and an additional 500ul of RPE buffer was added to the column and centrifuged for 2 minutes at 1600 rpm. To elute the RNA, 30µl of RNase-free water was applied directly to the spin column membrane and centrifuged for 1 minute. This step was repeated and the eluted RNA was stored at -80°C.

3.10 Midi Prep and Restriction Digest of Plasmid DNA Preparation

All plasmid preparations were done with Promega's Wizard's® *Plus* Midipreps DNA Purification System. Plasmid DNA for transfection was isolated from glycerol stocks of E. coli cultures containing respective plasmids that were prepared by previous lab members. E. coli from glycerol stocks was added to 3 mL cultures of sterile LB Broth

supplemented with 1 µl/mL of either ampicillin or kanamycin as appropriate for each plasmid and incubated overnight in an orbital shaker at 37°C. 2mL of the 3mL overnight suspension was added to 100 mL of sterile LB Broth and incubated as before. The 100 mL culture was transferred to a sterile 250 mL centrifuge tube and centrifuged at 10,000 RCF's for 10 minutes at 4°C and the supernatant was removed. The pellet was resupsended in 3 mL of Promega Resuspension Buffer, followed by 3 mL of Promega Lysis Buffer and finally 3 mL of Promega Neutralization Buffer. The suspension was centrifuged again at 14,000 RCF's for 15 minutes and the supernatant was decanted through filter paper into a fresh 50mL Falcon tube. 10mL of Promega Purification Resin was added to the supernatant, then the mixture was transferred into a Promega Midi-prep column and a vacuum source was applied. The DNA-bound resin was washed twice with 15 mL of Promega Wash Buffer. DNA was eluted with 300 µl of 65-70°C RNase-free water. The DNA was then precipitated out by adding 30 µl of 3.0mM sodium acetate and 900µl of 95% ethanol and incubated at -20°C for at least four hours. The DNA was then centrifuged at 1600 rpm for five minutes, the supernatant was removed, and the pellet was washed with 95% ethanol, and centrifuged again as described above. The supernatant was removed and the pellet was allowed to dry, 200 µl TE was added to dissolve the DNA. DNA was then quantified using ND-1000 Spectrophotometer NanoDrop. Plasmid identity was confirmed by digesting DNA with appropriate restriction enzymes at 37ºC for two hours. 6x loading dye was added to each digested plasmid sample and loaded onto an 1% agarose gel containing ethidium bromide and run at 70V for 1 hour. Gels were then imaged using a Fotodyne camera with an ethidium bromide filter and Foto/UV 26 gel box. Gel images were processed using PC Image software.

3.11 Transfection of DNA by Electroporation

C2C12 cells were cultured, collected, and counted as previously described. Cells were resuspended in electroporation buffer [EB; 1x HBS, 5uM CaCl] at a concentration of $5x10^5$ cells per 250 µl of EB. Appropriate concentrations of plasmid DNA and salmon sperm DNA (see chart below) were added to each 4 mm gap cuvette and incubated for one minute and then 250 µl of cells in EB were added to each cuvette.

Plasmid	µg of Plasmid DNA	µg of Salmon Sperm DNA
CFP-Fibrillarin	4	80
YFP-Btf	4	80
YFP-SF2	4	60

C2C12 cells were electroporated using a BioRad GenePulser XCell [220V, 950µF, and 0Ω]. Cells were incubated on ice for 10 minutes post-electroporation, resuspended in 1 mL of DMEM per cuvette, and plated.

3.12 RNA Interference

Cells were plated as previously described in antibiotic-free DMEM supplemented with 10% FBS. siRNA transfection was done 24 hours after cells were plated. HeLa and C2C12 cells were transfected using Gibco 1x Opti-MEM, Invitrogen Oligofectamine Reagent, Dharmacon 1x siRNA buffer, 20µM Luciferase oligo [Dharmacon], and 20 µM human siRNA oligo 2 (hsi-2) [Dharmacon] as follows:

Condition	Tube 1	Tube 2
Mock	15µl Oligofectamine	250µl Opti-MEM
	60µl Opti-MEM	15µl siRNA Buffer
Control	15µl Oligofectamine	250µl Opti-MEM
	60µl Opti-MEM	15µl 20µM Luciferase oligo
Mouse si-1siRNA duplex	15µl Oligofectamine	250µl Opti-MEM
	60µl Opti-MEM	15µl 20µM msi-1
Human si-2 siRNA duplex	15µl Oligofectamine	250µl Opti-MEM
	60µl Opti-MEM	15µl 20µM hsi-2

Contents were added to each tube and incubated for 5 minutes at room temperature. Contents of Tube 2 were added to Tube 1 and incubated for 20 minutes at room temperature. 340 µl of each mixture was added to appropriate wells. HeLa and C2C12 cells were incubated for 24 hours and then processed. For C2C12 differentiation time course studies, differentiation was induced via serum deprivation (in DM) 24 hours post-transfection. Mock, control, msi-1, and hsi-2 samples were processed at Day 0, Day 2, and Day 4 of the differentiation time course for immunofluorescence, protein extraction, and RNA extraction.

3.13 Live Cell Microscopy

C2C12 were cultured, plated, and electroporated as described above. Differentiation was induced in DM 12 hours post-transfection and imaging began ~30 hours into the differentiation time course. The coverslip was removed from GM and loaded onto the live cell chamber apparatus and perfused with Leibovitz's L-15 Medium (Invitrogen)

supplemented with 2% HS. Cells were imaged with the DeltaVision RT system using point visiting every 30 minutes for 8 hours using CFP and YFP channels. Images were displayed as time-lapse videos.

3.14 Nucleoli and Mitotic Counts

Nucleoli counts were performed on fixed cells processed by immunofluorescence for visualization of fibrillarin. For C2C12 cells, 50 myoblast nuclei and 50 myotube nuclei were randomly selected by blindly selecting areas of the coverslip for image capture. Each nucleus selected was then scored for the number of nucleoli present as indicated by fibrillarin staining. MHC or myogenin-negative cells were scored as undifferentiated cells. Cells positive for MHC or myogenin were scored as differentiating cells. These counts were done for each day of the differentiation time course. These counts were done for three separate time courses, the counts were averaged, and standard deviation was determined. For HeLa and MEF counts, 50 nuclei from both “high serum” (10% FBS) and ‘low serum” (0.5% FBS) were scored for number of nucleoli for each day of the 4 day time course. Counts from C2C12, HeLa and MEF cells were plotted on a graph of # Nuclei versus # Nucleoli. Mitotic counts were performed by randomly selecting 50 nuclei as described above and determining the number of mitotic cells present out of the 50 nuclei selected. Percentage of mitotic cells present was determined for C2C12, HeLa, and MEF cells, and displayed in charts.

Chapter 4: Examining Btf's Role in Myogenesis

4.1 Btf Expression Increases During Myogenesis in C2C12 Cells

To begin to understand if Btf has a role in myogenesis, I examined Btf in differentiating C2C12 cells. C2C12 cells were plated, allowed to attach for 24 hours, and induced to differentiate by switching from growth medium (GM) to differentiation medium (DM). C2C12 cells were processed for immunofluorescence on Day 0 at the time on induction through Day 4 of the differentiation time course to immunolabel Btf as well as muscle specific proteins myogenin and MHC. Myogenin and MHC served as markers to indicate myoblasts undergoing differentiation. Cells that were positive for expression of myogenin exhibited increased nuclear labeling of Btf as compared to neighboring undifferentiated myoblasts (Figure 4.1). Increased nuclear labeling of Btf was detected in some cells that were not MHC positive but all cells which were positive for myogenin showed increased nuclear labeling of Btf (Figure 4.1 and 4.2). Increased nuclear labeling of Btf was also observed in myoblasts that had not yet fused into multinucleated myotubes (Figure 4.1 and 4.2). Immunofluorescence data taken together with immunoblot data collected by Alok Sharma (Figure 2.1) suggests that increased expression of Btf is an early event in the differentiation process. While the immunoblot shows globally that Btf expression increases, IF data indicates that the increase is seen in the myoblasts undergoing differentiation (myoblasts which stain positive for muscle-specific proteins that serve as differentiation markers). Increased expression of Btf persisted through Day 4 of the

Figure 4.1. Expression of Btf and Myogenin in differentiating C2C12 cells. After differentiation was induced, myoblasts began to show nuclear expression of muscle-specific protein myogenin. Expression of myogenin appeared as early as Day 0 in spontaneously differentiating cells (Panels A-D, arrows, red signal indicates immunolabeling of myogenin with F5D anti-myogenin antibody). As early as Day 0, cells positive for myogenin exhibited a higher level of Btf labeling (Panels A-D, arrows, green signal indicates immunolabeling of Btf with WU10 antibody) as compared to neighboring undifferentiating cells (Panels A-D, arrowheads). Increased labeling of Btf in differentiating myoblasts persisted through Days 3 and 4 in nuclei of myotubes (Panels M-P, arrows) and Day 4 (Panels Q-T, arrows). DNA was stained with DAPI. Boxed regions are enlarged in the lower set of panels shown at each time point. Bar = 5μm.

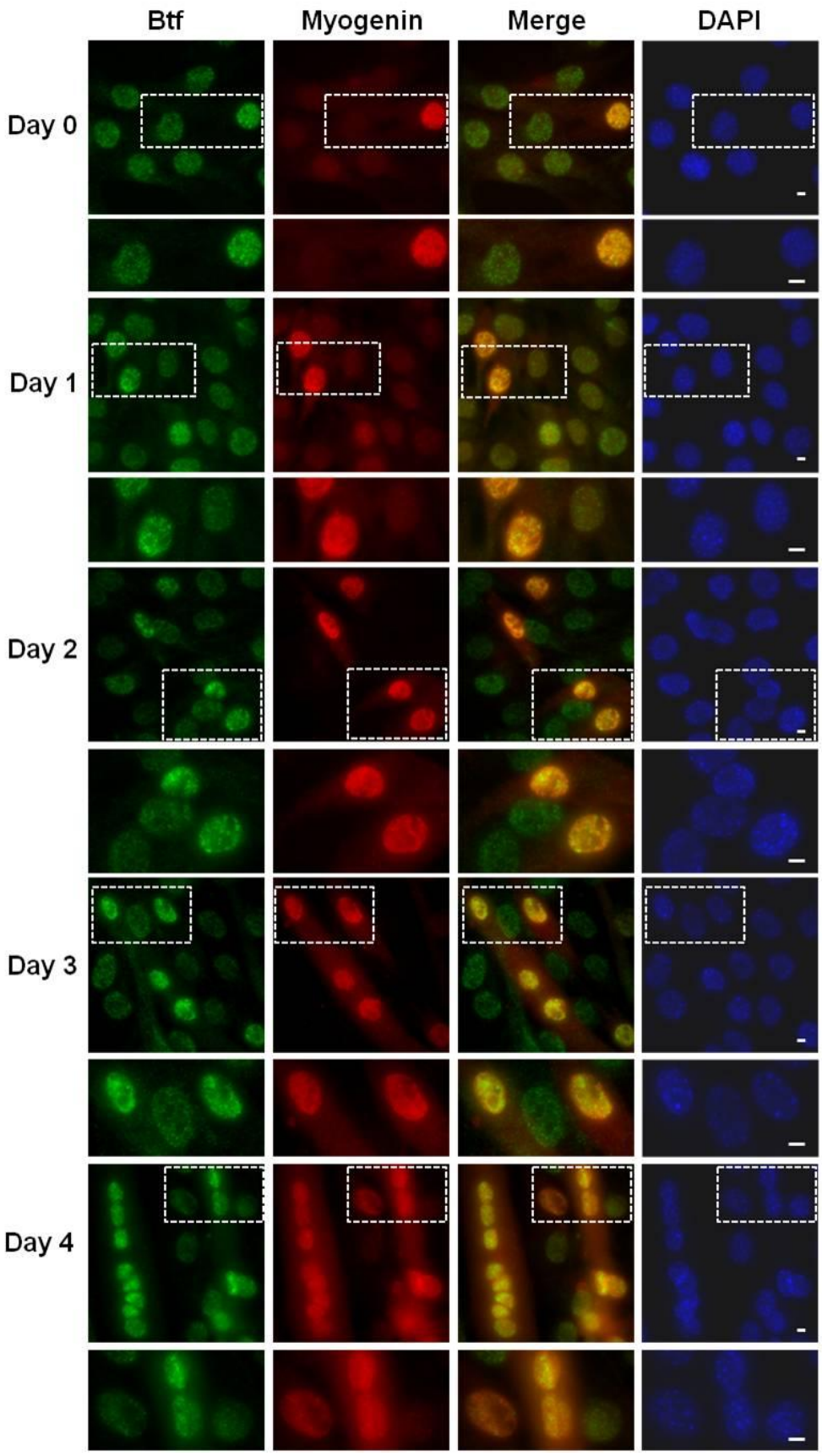
Btf
Myogenin
Merge
DAPI
Day 0
Day 1
Day 2
Day 3
Day 4

Figure 4.2. Expression of Btf and MHC in differentiating C2C12 cells. After differentiation was induced, myoblasts began to show cytoplasmic expression of muscle-specific protein myosin heavy chain (MHC). Expression of MHC appeared as early as Day 1 and marked myoblasts undergoing differentiation (Panels E-H, arrows, red signal indicates immunolabeling of MHC with MF20 antibody). By Day 2, differentiating myoblasts (Panels I-L, arrows) exhibited higher levels of nuclear Btf as compared to neighboring MHC-negative myoblasts (Panels I-L, arrow heads, green signal indicates immunolabeling of Btf with WU10 antibody). By Day 4, MHC positive cells were more prevalent and fused into multinucleated myofibrils. DNA was stained with DAPI. Bar = 5µm

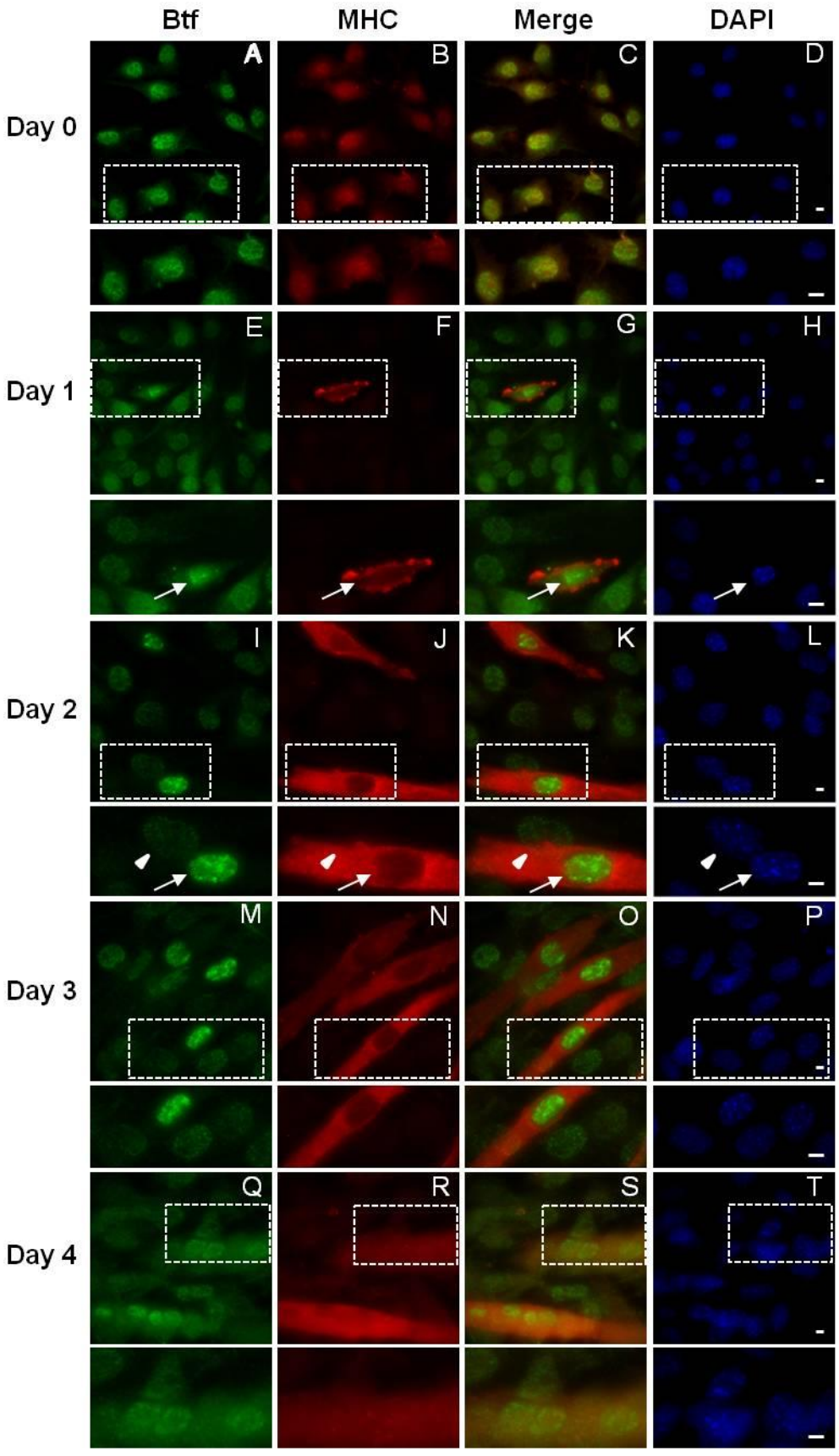
Btf
MHC
Merge
DAPI
Day 0
Day 1
Day 2
Day 3
Day 4
A
B
C
D
E
F
G
H
I
J
K
L
M
N
O
P
Q
R
S
T

differentiation time course (Figure 4.1 and Figure 4.2). All cells throughout the entire differentiation time course which were positive for muscle specific proteins myogenin or MHC exhibited increased nuclear labeling of Btf.

4.2 Overexpression of Btf Alone does Not Induce Differentiation of C2C12 Cells

Because Btf expression increases early in C2C12 differentiation, we wanted to test whether increased expression of Btf alone might alternatively shift the timing of differentiation events in C2C12 cells maintained in GM. C2C12 cells were transfected with empty YFP plasmid DNA or YFP-Btf plasmid DNA via electroporation. C2C12 cells transfected with empty YFP plasmid DNA were maintained in GM for the entire time course as a control to assert that transfection alone did not alter the uninduced differentiation time course. Cells transfected with YFP-Btf were divided into two groups, one that was maintained in GM and another that was induced to differentiate by switching to DM. C2C12 cells transfected with empty YFP plasmid DNA served as a control to assert that any changes seen in samples transfected with YFP-Btf were not simply a result of the transfection process or YFP expression, but indeed a result of Btf overexpression. C2C12 cells that were transfected with YFP-Btf and induced to differentiate were used to verify that transfected cells could undergo differentiation and to compare the time course of transfected cells to that of a normal time course in terms of muscle specific protein expression and gross morphological changes. In addition to transfected samples, untransfected C2C12 cells were either maintained in GM or induced to differentiate on Day 0 of the time course by switching to DM. Untransfected cells were induced to differentiate in parallel and served as a normal differentiation time course comparison. Untransfected cells maintained in GM were used to determine the frequency of spontaneous differentiation of transfected cells that were not induced. By including all of these conditions, it was possible to compare the differentiation time

courses of cells overexpressing Btf (uninduced and induced) to normally differentiating untransfected cells (induced or uninduced), and note any changes in differentiation timing, cellular phenotypes, or expression of marker proteins of interest.

A summary of the overall experimental design for Btf overexpression can be found in Figure 4.3. Cells from all groups were processed for immunolabeling on Day 0, Day 2, and Day 4 of the time course. Transfected C2C12 cells were processed for immunoflourescence labeling of muscle specific proteins myogenin and MHC. Transfected cells were observed for expression of myogenin and MHC as well as exogenous Btf. Untransfected cells were processed for immunofluorescence labeling of both endogenous Btf as well as muscle specific proteins myogenin and MHC. Cells that were transfected with empty YFP plasmid DNA and cells that were transfected with YFP-Btf and maintained in GM showed no expression of muscle specific proteins myogenin or MHC until Day 4 of the time course (Figure 4.4 – Figure 4.9), indicating that spontaneous differentiation was infrequent in this experiment. Progression of the differentiation time course in cells that were not induced to differentiate appeared delayed in comparison to normal differentiation time courses in which myogenin expression occurs at Day 1 and MHC expression occurs at Day 2. Untransfected C2C12 cells maintained in GM also showed no expression of muscle specific proteins myogenin or MHC until Day 4 of the time course which indicates that delayed differentiation observed in transfected cells maintained in GM was not a result of transfection or overexpression of Btf (Figure 4.6 and Figure 4.9). It is worth noting that all C2C12 cells that were maintained in GM failed to form multinucleated myotubes by Day 4 (Figure 4.6 and Figure 4.9). Cells that were transfected with YFP-Btf and were induced to differentiate showed expression of both myogenin and MHC at Day 2 of the time course (Figure 4.5 and Figure 4.8) and increased through Day 4 (Figure 4.6 and Figure 4.9)

Figure 4.3. Overexpression of Btf experimental design. C2C12 myoblasts were divided into five groups. A portion of C2C12 myoblasts were transfected with the parental plasmid containing only the YFP protein sequence and were maintained in growth medium (DMEM + 15% FBS, GM) for the entire experiment. C2C12 cells were also transfected with the YFP-Btf plasmid and half of the samples were induced to differentiate via serum deprivation and the other half was maintained in GM for the entire experiment. Untransfected C2C12 cells were divided into two groups and one group was induced to differentiate via serum deprivation for a normal time course and one group was maintained in GM for the entire experiment. Abbreviations for experimental conditions are provided in parentheses.

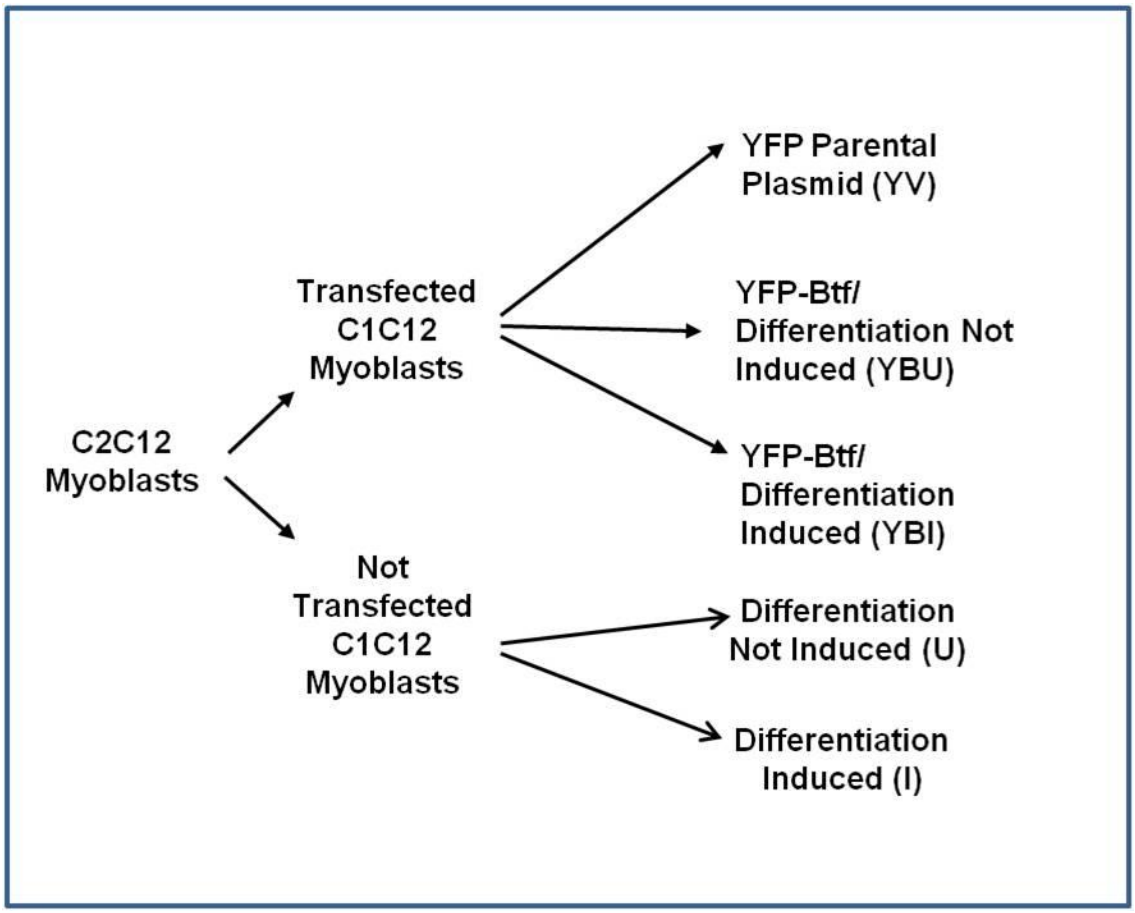
C2C12
Myoblasts
Transfected
C1C12
Myoblasts
Not
Transfected
C1C12
Myoblasts
YFP Parental
Plasmid (YV)
YFP-Btf/
Differentiation Not
Induced (YBU)
YFP-Btf/
Differentiation
Induced (YBI)
Differentiation
Not Induced (U)
Differentiation
Induced (I)

Figure 4.4. Overexpression of Btf and expression of myogenin at Day 0 of the differentiation time course. At Day 0 of the time course, none of the experimental conditions showed nuclear expression of muscle specific protein myogenin (red signal indicates immunolabeling of myogenin with F5D antibody). Both untransfected cells maintained in GM (Panels M-P, arrows) and untransfected cells induced to differentiate (Panels Q-T, arrows) contain mitotic cells indicating the cells are still in a proliferative state. DNA was stained with DAPI. Bar = 5μm.

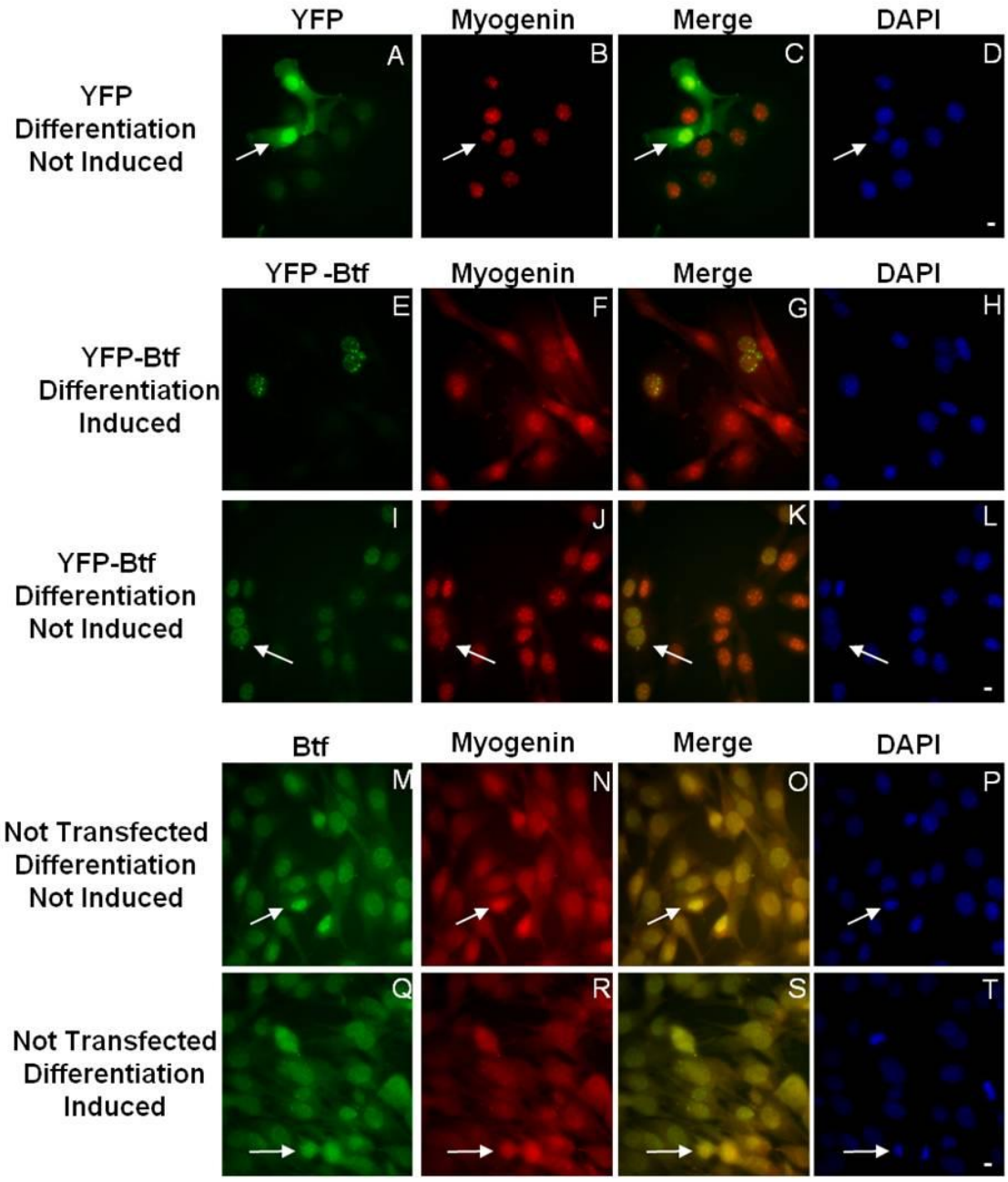
YFP
Myogenin
Merge
DAPI
A
B
C
D
YFP
Differentiation
Not Induced
YFP -Btf
Myogenin
Merge
DAPI
E
F
G
H
YFP-Btf
Differentiation
Induced
I
J
K
L
YFP-Btf
Differentiation
Not Induced
Btf
Myogenin
Merge
DAPI
M
N
O
P
Not Transfected
Differentiation
Not Induced
Q
R
S
T
Not Transfected
Differentiation
Induced

Figure 4.5. Overexpression of Btf and expression of myogenin at Day 2 of the differentiation time course. At Day 2 of the differentiation time course, all cells which were maintained in GM still did not exhibit expression of muscle specific protein myogenin. Cells transfected with YFP-Btf and induced to differentiate (Panels E-H, arrows, red signal indicates immunolabeling of myogenin with F5D antibody) and untransfected cells which were induced to differentiate (Panels Q-T, arrows) contain cells positive for myogenin as expected of cells after 48 hours of serum deprivation indicating a normal differentiation time course. DNA was stained with DAPI. Bar = 5μm.

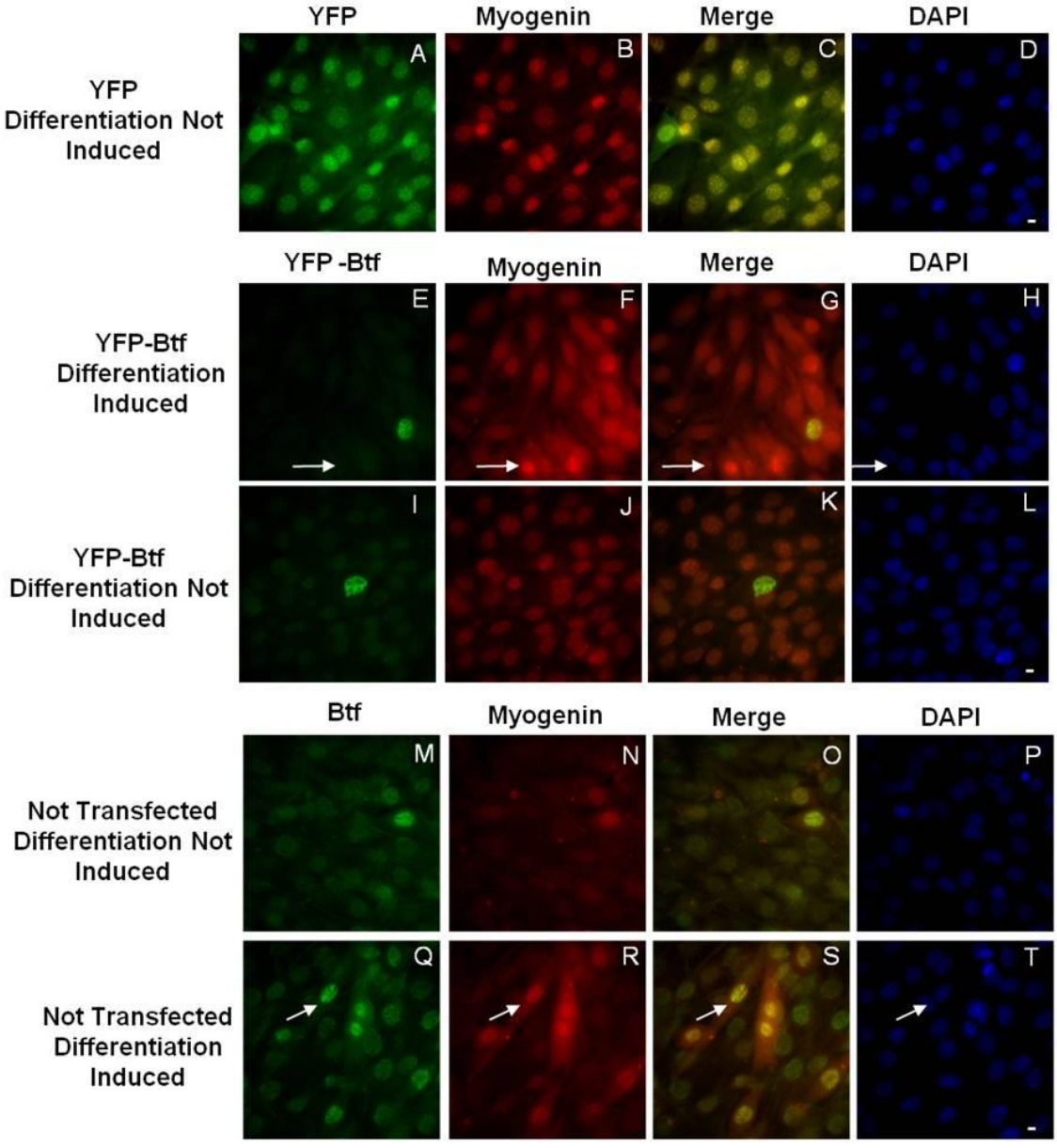
YFP
Myogenin
Merge
DAPI
YFP Differentiation Not Induced
A
B
C
D
YFP -Btf
Myogenin
Merge
DAPI
YFP-Btf Differentiation Induced
E
F
G
H
YFP-Btf Differentiation Not Induced
I
J
K
L
Btf
Myogenin
Merge
DAPI
Not Transfected Differentiation Not Induced
M
N
O
P
Not Transfected Differentiation Induced
Q
R
S
T

Figure 4.6. Overexpression of Btf and expression of myogenin at Day 4 of the differentiation time course. Four days after the time course was started, all samples contain myoblasts positive for muscle specific protein myogenin. Cells transfected with empty YFP and maintained in GM were positive for myogenin at Day 4 (Panels A-D, arrows, green signal indicates expression of exogenous YFP) as were surrounding cells which were not successfully transfected (Panels A-D, arrowheads) indicating that transfection of YFP did not hinder the myoblast's ability to differentiate. Cells transfected with YFP-Btf and induced to differentiate (Panels E-H) showed multiple myogenin positive myoblasts which had fused into myotubes. Cells transfected with YFP-Btf and maintained in GM (Panels I-L, arrows, green signal indicates expression of YFP-Btf) exhibited expression levels of myogenin (red signal indicates immunolabeling of myogenin with F5D antibody) similar to untransfected cells maintained in GM. Untransfected cells that were induced to differentiate showed a normal progression of the differentiation time course (Panels Q-T). DNA was stained with DAPI. Bar = 5μm.

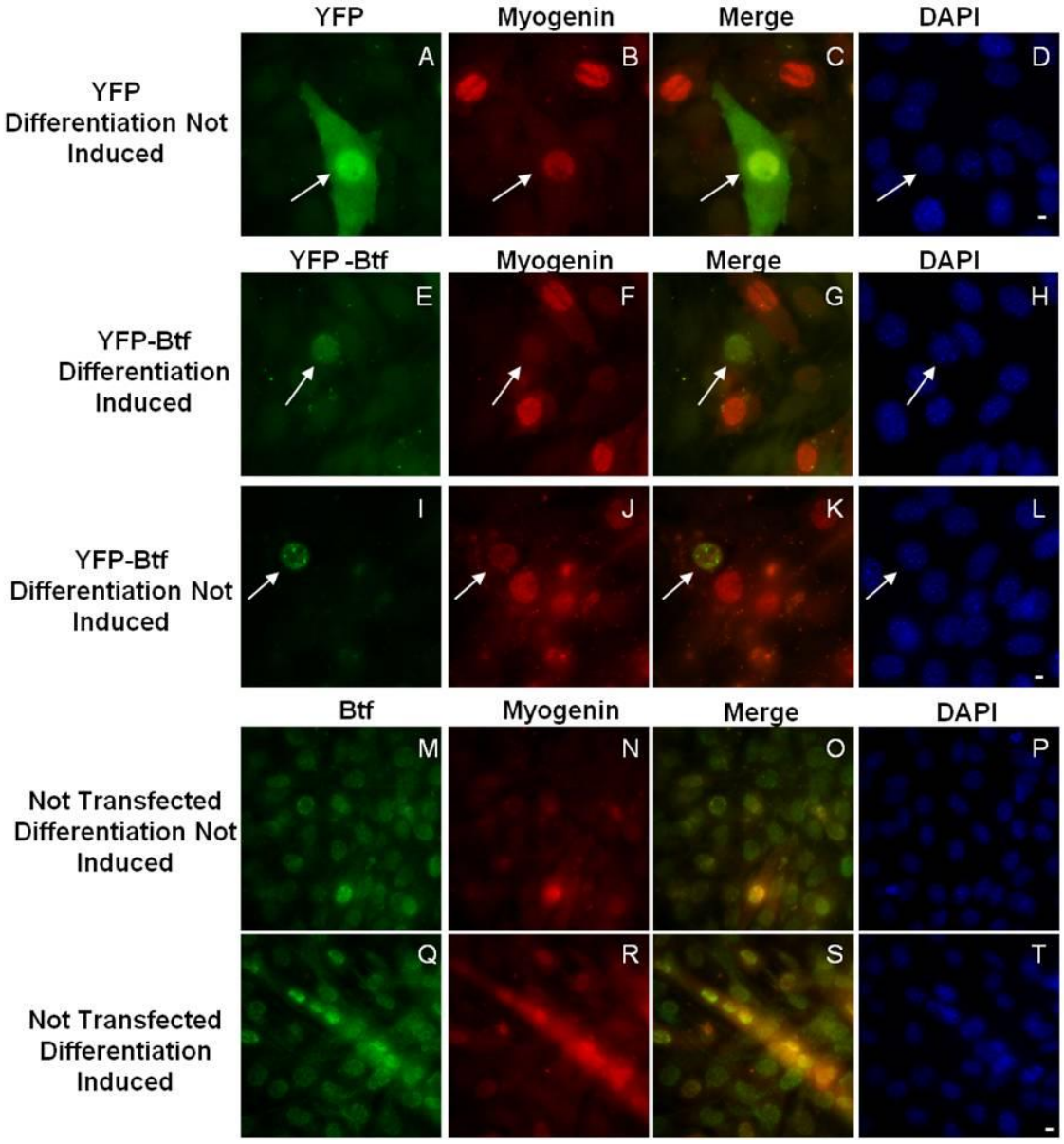
YFP
Myogenin
Merge
DAPI
A
B
C
D
YFP
Differentiation Not
Induced
YFP -Btf
Myogenin
Merge
DAPI
E
F
G
H
YFP-Btf
Differentiation
Induced
I
J
K
L
YFP-Btf
Differentiation Not
Induced
Btf
Myogenin
Merge
DAPI
M
N
O
P
Not Transfected
Differentiation Not
Induced
Q
R
S
T
Not Transfected
Differentiation
Induced

Figure 4.7. Overexpression of Btf and expression of MHC at Day 0 of the differentiation time course. Cells transfected with empty YFP and maintained in GM (Panels A-D, green signal indicates expression of exogenous YFP) and cells transfected with YFP-Btf and maintained in GM (Panels I-L, green signal indicates expression of YFP-Btf) were negative for cytoplasmic expression of MHC (red signal indicates immunolabeling of MHC with MF20 antibody) as were untransfected cells maintained in GM (Panels M-P, green signal indicates immunolabeling of endogenous Btf with WU10 antibody). Cells transfected with YFP-Btf that were induced to differentiate (Panels E-H) as well as cells that were not transfected and induced to differentiatecells (Panels Q-T) showed no expression of MHC as expected at Day 0 of the differentiation time course. The presence of mitotic cells in untransfected cells that were induced to differentiate (Panels Q-T, arrows) indicate that differentiation had not been activated. DNA was stained with DAPI. Bar = 5μm.

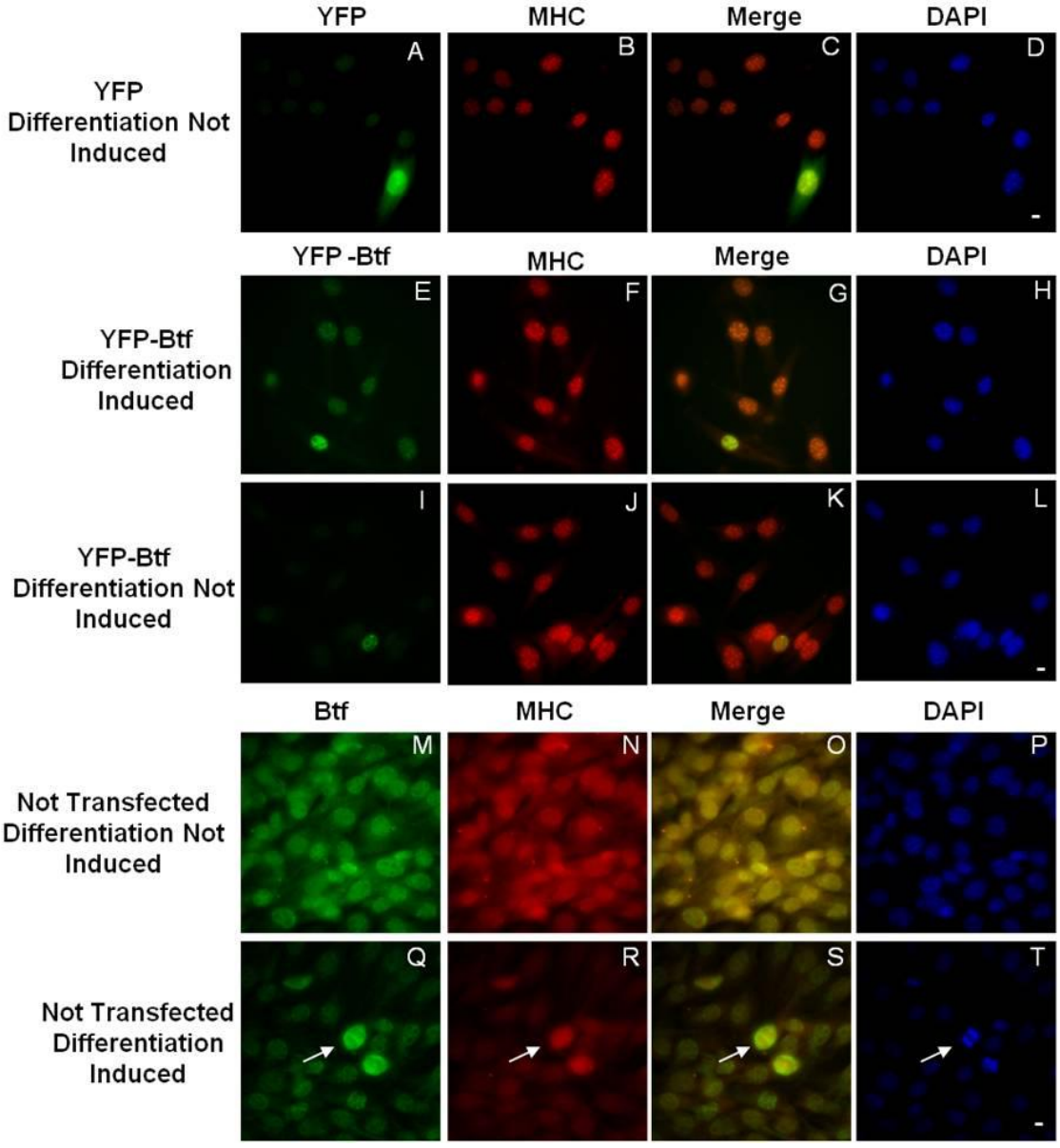
YFP
MHC
Merge
DAPI
A
B
C
D
YFP
Differentiation Not
Induced
YFP -Btf
MHC
Merge
DAPI
E
F
G
H
YFP-Btf
Differentiation
Induced
I
J
K
L
YFP-Btf
Differentiation Not
Induced
Btf
MHC
Merge
DAPI
M
N
O
P
Not Transfected
Differentiation Not
Induced
Q
R
S
T
Not Transfected
Differentiation
Induced

Figure 4.8. Overexpression of Btf and expression of MHC at Day 2 of the differentiation time course. Cells transfected with empty YFP plasmid and maintained in GM (Panels A-D) and cells transfected with YFP-Btf and maintained in GM (Panels I-L) were negative for MHC expression at Day 2. Cells transfected with YFP-Btf and induced to differentiate (Panels E-H, green signal indicates expression of YFP-Btf) and untransfected cells induced to differentiate (Panels Q-T, green signal indicates immunolabeling of endogenous Btf with WU10 antibody) showed the greatest number of MHC positive cells as expected. One myoblast in the untransfected cells maintained in GM was positive for MHC indicating that some spontaneous differentiation was occurring in this experiment (Panels M-P, arrows, red signal indicates immunolabeling of MHC with MF20 antibody). DNA was stained with DAPI. Bar = 5μm.

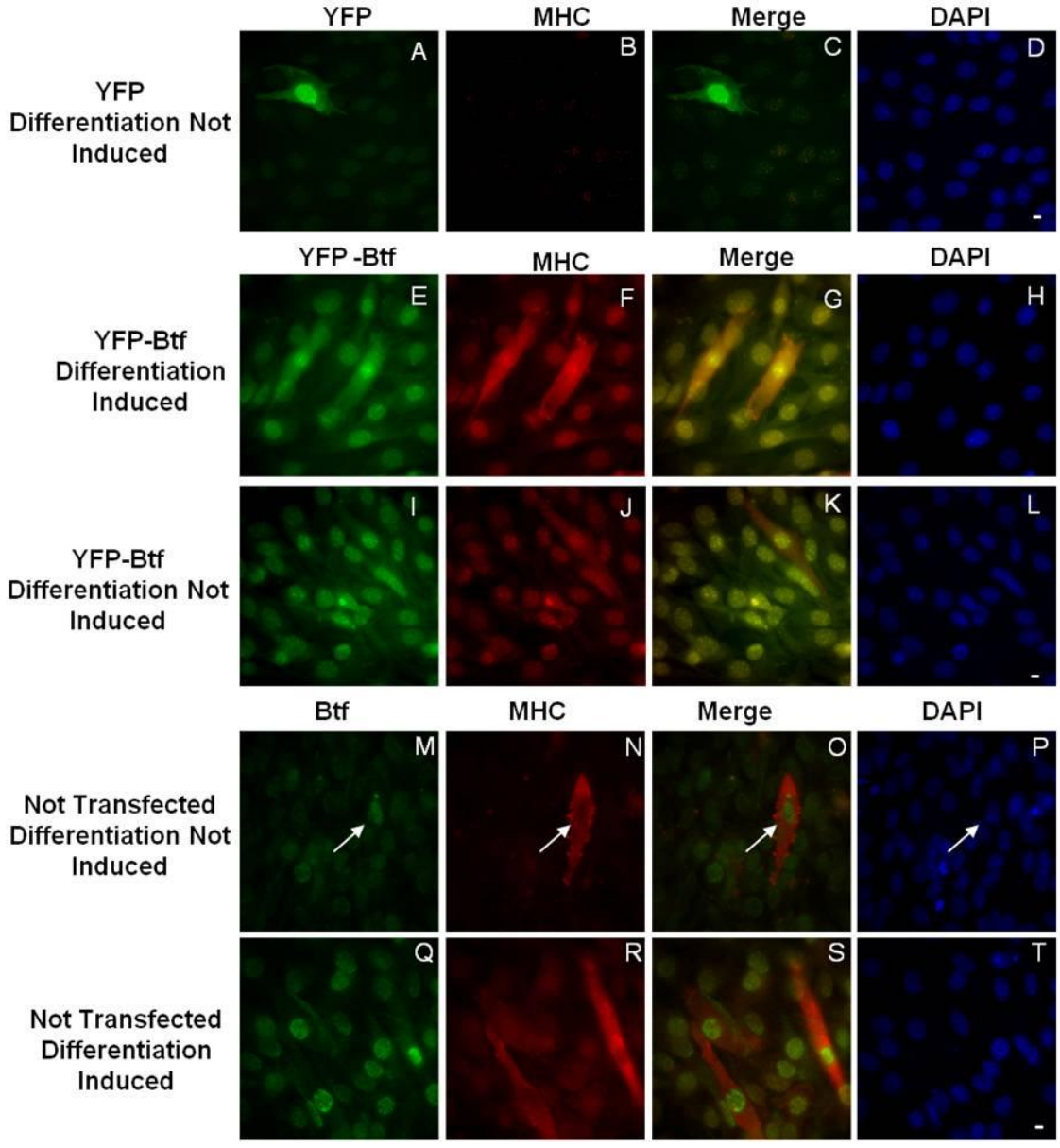
YFP
MHC
Merge
DAPI
A
B
C
D
YFP
Differentiation Not
Induced
YFP -Btf
MHC
Merge
DAPI
E
F
G
H
YFP-Btf
Differentiation
Induced
I
J
K
L
YFP-Btf
Differentiation Not
Induced
Btf
MHC
Merge
DAPI
M
N
O
P
Not Transfected
Differentiation Not
Induced
Q
R
S
T
Not Transfected
Differentiation
Induced

Figure 4.9. Overexpression of Btf and expression of MHC at Day 4 of the differentiation time course. By Day 4 of the time course, all experimental groups contained myoblasts positive for MHC expression (all Panels, red signal indicates immunolabeling of MHC with MF20 antibody). Cells in all groups that were induced to differentiate formed multi-nucleated myotubes, whereas cells in all groups maintained in GM did not form multi-nucleated myotubes. DNA was stained with DAPI. Bar = 5μm.

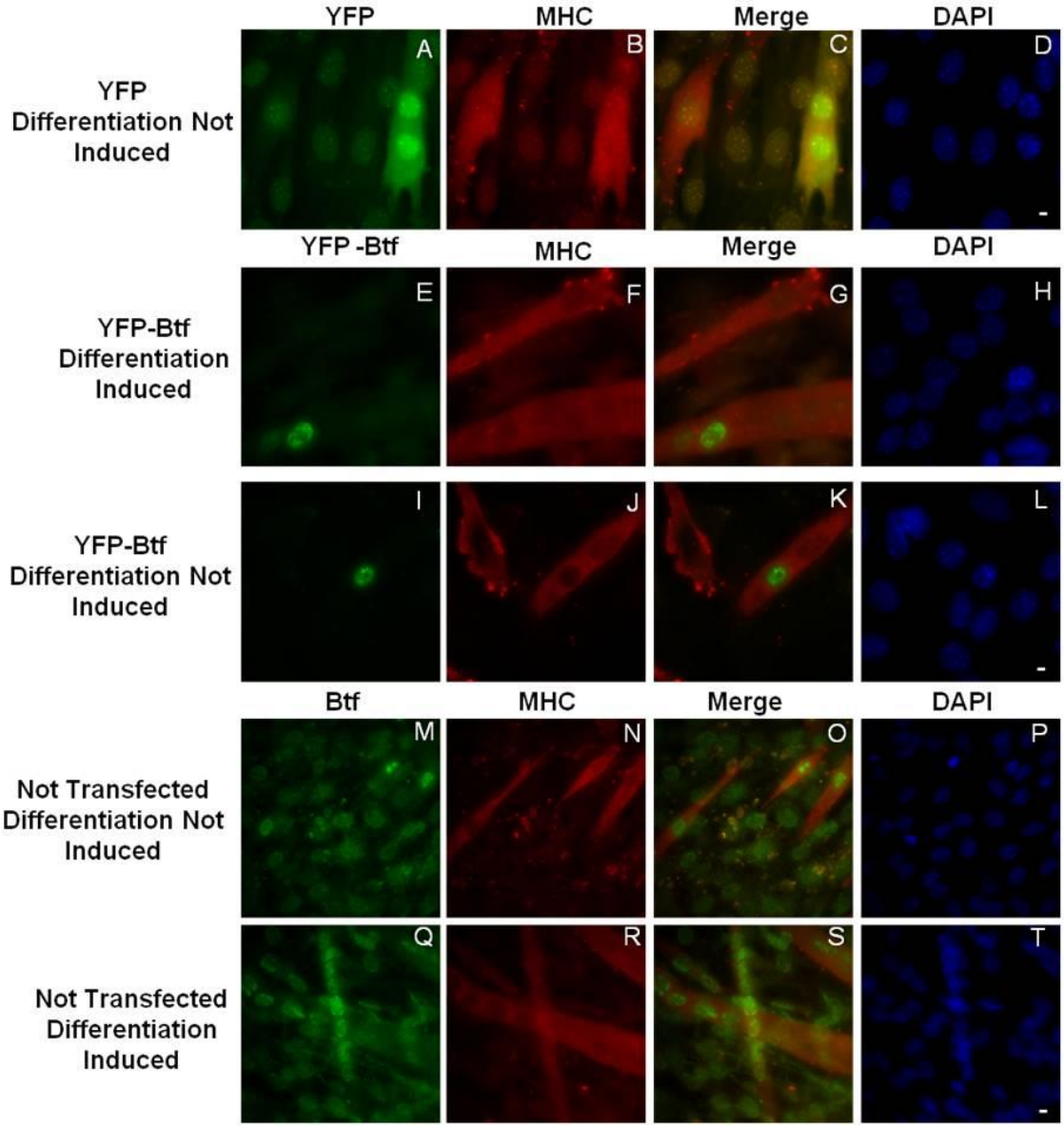
YFP
MHC
Merge
DAPI
A
B
C
D
YFP
Differentiation Not
Induced
YFP -Btf
MHC
Merge
DAPI
E
F
G
H
YFP-Btf
Differentiation
Induced
I
J
K
L
YFP-Btf
Differentiation Not
Induced
Btf
MHC
Merge
DAPI
M
N
O
P
Not Transfected
Differentiation Not
Induced
Q
R
S
T
Not Transfected
Differentiation
Induced

which reflected normal timing of the differentiation time course. Untransfected C2C12 cells that were induced to differentiate exhibited expression of myogenin and MHC at Day 2 and increased through Day 4 of the time course confirming the cells were undergoing normal differentiation (Figure 4.5 and Figure 4.6). All C2C12 cells that were induced to differentiate formed multinucleated myotubes by Day 4 of the time course as expected (Figure 4.6 and Figure 4.9). It is also worth noting that by Day 4, both induced and uninduced cells overexpressing YFP-Btf exhibit myotubes containing nuclei both positive for overexpression and negative for overexpression of YFP-Btf (Figure 4.9, Panels E-L). Endogenous Btf expression levels for all induced samples and all uninduced samples were similar as observed by immunoblot data (Figure 4.10). This suggests that all induced or uninduced time courses proceeded with similar timing regardless of overexpression of YFP or YFP-Btf and that overexpression of YFP-Btf produced no observable changes in endogenous Btf levels throughout the differentiation time course. Immunoblotting using an anti-GFP antibody which recognizes the YFP tag confirmed that YFP-Btf was overexpressed in the C2C12 cells.

In addition to expression of muscle specific proteins and changes in gross morphology, all experimental samples were observed for presence of mitotic cells to determine if the cells were cycling or had exited the cell cycle. In order to differentiate, cells must first exit the cell cycle; therefore, observing the number of mitotic cells in a population served as an indicator of differentiation. All cells that were maintained in GM for the duration of the experiment exhibited a higher number of mitotic cells as compared to cells that were induced to differentiate (Table 4.1). A lower number of mitotic cells was expected for cells induced to differentiate because in order to differentiate the cells must first exit the cell cycle. A higher proportion of mitotic cells in cells that were transfected with YFP-Btf maintained in GM suggests that overexpression of Btf alone was not

Figure 4.10. Western blot analysis to detect expression of endogenous Btf throughout time course testing the effect of Btf overexpression on differentiation. WCNE was prepared on Day 0, Day 2, and Day 4 of the differentiation time course. Equal total protein in each sample was loaded onto SDS-PAGE and transferred to a nitrocellulose membrane for immunoblotting. At Day 0 of the time course, Btf signal is undetectable in all samples as expected. By Day 2 of the time course Btf is detectable in cells which were transfected with YFP-Btf and induced to differentiate and untransfected cells which were induced to differentiate. A detectible signal for Btf is still absent at Day 2 for all other samples which were maintained in GM throughout the entire time course. By Day 4 of the time course Btf is detectable in all samples.

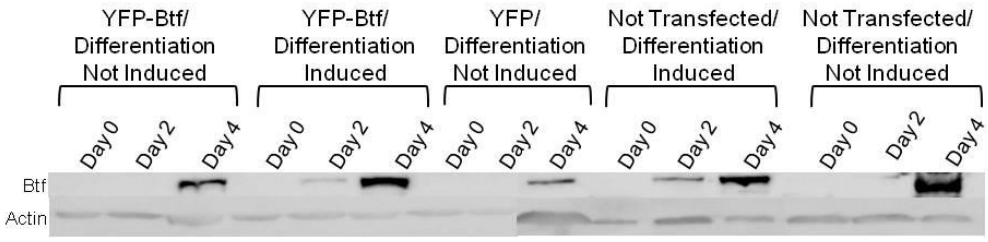
YFP-Btf/
Differentiation
Not Induced
YFP-Btf/
Differentiation
Induced
YFP/
Differentiation
Not Induced
Not Transfected/
Differentiation
Induced
Not Transfected/
Differentiation
Not Induced
Day 0
Day 2
Day 4
Btf
Actin

Table 4.1. Mitotic counts for all experimental conditions in Btf overexpression time course. One hundred cells were randomly selected for image capture and mitotic cells were counted for each experimental condition in the Btf overexpression time course. This process was repeated for cells co-labeled with myogenin and MHC. C2C12 cells which were transfected with the YFP plasmid and maintained in growth medium (DMEM + 15% FBS, GM) showed an overall decrease in mitotic cells but still possessed more mitotic cells at Day 4 than any of the experimental groups in which differentiation was induced. C2C12 cells which were transfected with YFP-Btf and induced to differentiate decreased greatly in their mitotic population from Day 0 to Day 4. C2C12 cells which were transfected with YFP-Btf and grown in GM maintained approximately the same number of mitotic cells during the time course. C2C12 cells that were not transfected but were induced to differentiate showed an almost complete absense of mitotic cells at day 2 and Day 4. C2C12 cells which were neither transfected nor induced to differentiate maintained an approximately consistent mitotic population.

	Day 0		Day 2		Day 4	
	#Mitotic Cells/100 Cells		#Mitotic Cells/100 Cells		#Mitotic Cells/100 Cells	
Experimental Condition	Myogenin	MHC	Myogenin	MHC	Myogenin	MHC
YFP/ Differentiation Not Induced	14	15	20	14	6	7
YFP-Btf/ Differentiation Induced	11	12	5	5	3	2
YFP-Btf/ Differentiation Not Induced	10	11	15	16	8	12
Not Transfected/ Differentiation Induced	18	12	2	1	1	0
Not Transfected/ Differentiation Not Induced	14	15	11	13	12	11

capable of inducing the cells to exit the cell cycle and progress along the differentiation pathway.

4.3 Ineffective Knockdown of Btf Using siRNA

Because Btf protein expression increases early during C2C12 differentiation, we wondered if Btf depletion might hinder differentiation. Undifferentiated C2C12 cells have a very low baseline level of Btf; therefore, determining whether Btf siRNA duplexes could effectively knock down Btf in undifferentiated cells would be difficult. In order to optimize depletion of Btf, preliminary experiments were done using HeLa and mouse embryonic fibroblasts (MEFs). HeLa cells were used as a control to confirm that I could produce a successful depletion because other lab members have optimized effective depletion of Btf in HeLa cells. MEFs were used because they are a mouse cell line with higher baseline levels of Btf in which to test oligos targeted against mouse Btf mRNA. Upon examination of the mouse Btf sequence, it was discovered that an oligo targeted against human Btf, hsi-2, matched a sequence within mouse Btf and was used along with four oligos targeted towards mouse Btf (msi-1-4). Preliminary experiments showed that in MEF cells, hsi-2 showed nearly complete depletion of Btf and msi-1 showed partial depletion of Btf (Figure 4.12). In addition to immunoblot data, immunoflourescence data confirmed that in MEF cells, hsi-2 was the most effective at knocking down Btf, and msi-1 was also partially effective. Once the most effective oligos were chosen, we designed an experiment to deplete Btf and induce differentiation in C2C12 cells, as shown in the experimental design summary in Figure 4.11. C2C12 cells were transfected with siRNA buffer (mock), siRNA oligos targeted against luciferase (control), and siRNA oligos targeted against Btf (hsi-2) and incubated for 24 hours. Mock-treated cells served as a

Figure 4.11. Btf depletion via siRNA interference experimental design. C2C12 myoblasts were transfected with either siRNA buffer (mock), siRNA oligos targeted against luciferase (control), or siRNA oligos targeted against Btf (hsi-2) and allowed to incubate for 24 hours. 24 hours after siRNA transfection (Day 0), C2C12 myoblasts were induced to differentitate and processed for immunolabeling of Btf and muscle specific proteins myogenin and MHC as well as protein extraction for immunoblotting. Cells were processed as described above again at Day 2 and Day 4 of the differentiation time course.

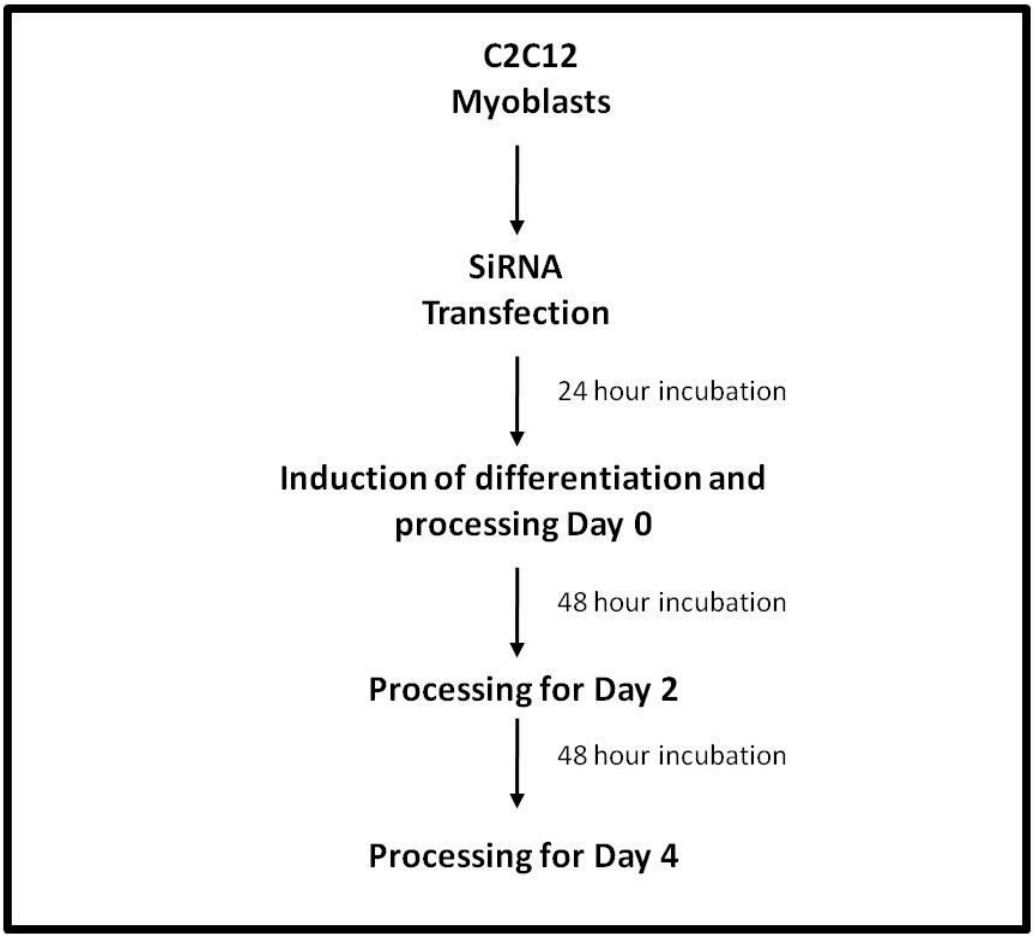
C2C12
Myoblasts
SiRNA
Transfection
24 hour incubation
Induction of differentiation and
processing Day 0
48 hour incubation
Processing for Day 2
48 hour incubation
Processing for Day 4

Figure 4.12 Depletion of Btf via siRNA in mouse embryonic fibroblasts (MEFs). MEF cells were transfected with siRNA buffer (mock), siRNA oligos targeted against luciferase (control), and mouse Btf (msi-1 – msi-4) and human Btf (hsi-2) and extracted for SDS-PAGE 48 hours after transfection. Btf was detected at ~150 kDa in mock and control cells. Btf. Cells treated with siRNA oligo 1 targeted against mouse Btf (msi-1) showed a slight depletion of Btf. Cells treated with siRNA oligo 2 targeted against human Btf (his-2) showed nearly complete depletion of Btf. Actin was used as a loading control.

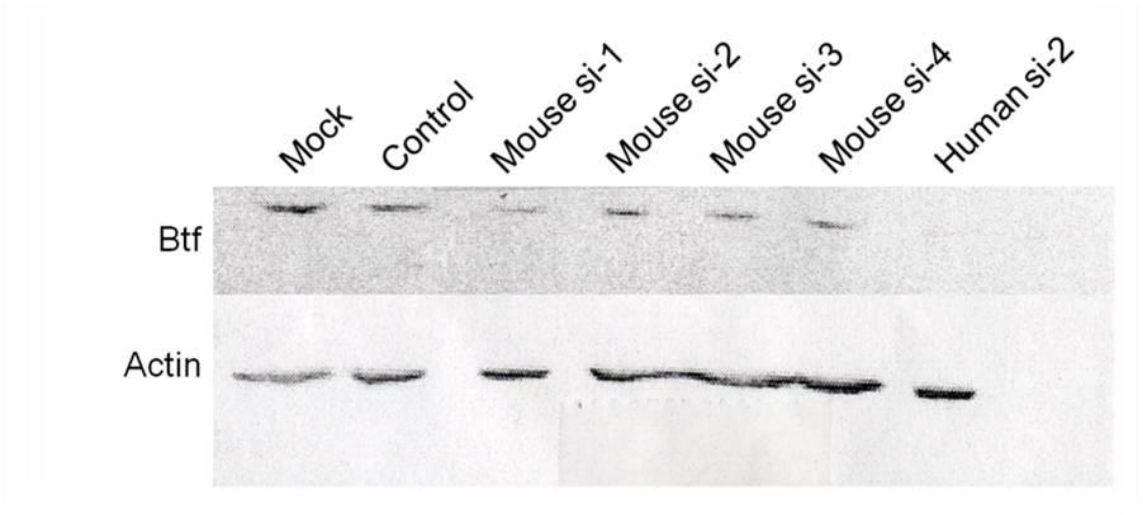
Mock
Control
Mouse si-1
Mouse si-2
Mouse si-3
Mouse si-4
Human si-2
Btf
Actin

control to assert that vehicle alone did not hinder differentiation. siRNA oligos targeting luciferase were used to control for any general off-target effects of the siRNA transfection. C2C12 cells were then processed for immunofluorescence labeling of Btf and muscle specific protein MHC on Day 0, Day 2 and Day 4 of the differentiation time course (Figure 4.11). Muscle specific protein MHC served as a marker to indicate cells undergoing differentiation. All C2C12 cells showed no expression of MHC on Day 0 of the differentiation time course as expected (Figure 4.13). By Day 2 of the differentiation time course, all experimental conditions showed myoblasts positive for MHC and an increased level of Btf expression (Figure 4.13). By Day 4 of the differentiation time course, all experimental conditions showed multinucleated myotubes (Figure 4.13). For all days of the differentiation time course myoblasts that were treated with siRNA oligos targeted against Btf did not show depletion of Btf (Figure 4.13). Different concentrations of siRNA reagents and post-transfection incubation periods in multiple experiments all yielded the same results; however, siRNA depletion of Btf was successful in MEF and HeLa cells. Undifferentiated C2C12 cells have very low basal levels of Btf; therefore, detecting depletion of Btf in undifferentiated C2C12 cells is very difficult and the cells were allowed to differentiate in order to determine if depletion had occured. For future attempts of this project I might recommend attempting siRNA transfection via electroporation given that ineffective depletion of Btf might have been a result of poor transfection efficiency, as C2C12 cells are notoriously hard to transfect, and electroporation conditions have been optimized which yield high transfection efficiency in C2C12 cells.

Figure 4.13. Btf depletion with siRNA duplex was ineffective in C2C12. C2C12 cells were transfected with siRNA buffer (mock), siRNA oligos targeted against luciferase (control), and Btf (hsi-2) and processed 48 hours later for Day 0. At Day 0, cells treated with hsi-2 oligos targeted against Btf showed no apparent depletion of Btf (panels Aa, Ae, and Ai, green signal indicates immunolabeling of Btf with WU10 antibody and red signal indicates immunolabeling of MHC with MF20 antibody). At Day 2 and Day 4, Btf still does not appear to be depleted (Panels Ba, Be, Bi, Ca, Ce, and Ci), as the fluorescence labeling of Btf is similar among controls and his-2-treated cells. DNA was stained with DAPI. Bar = 5μm.

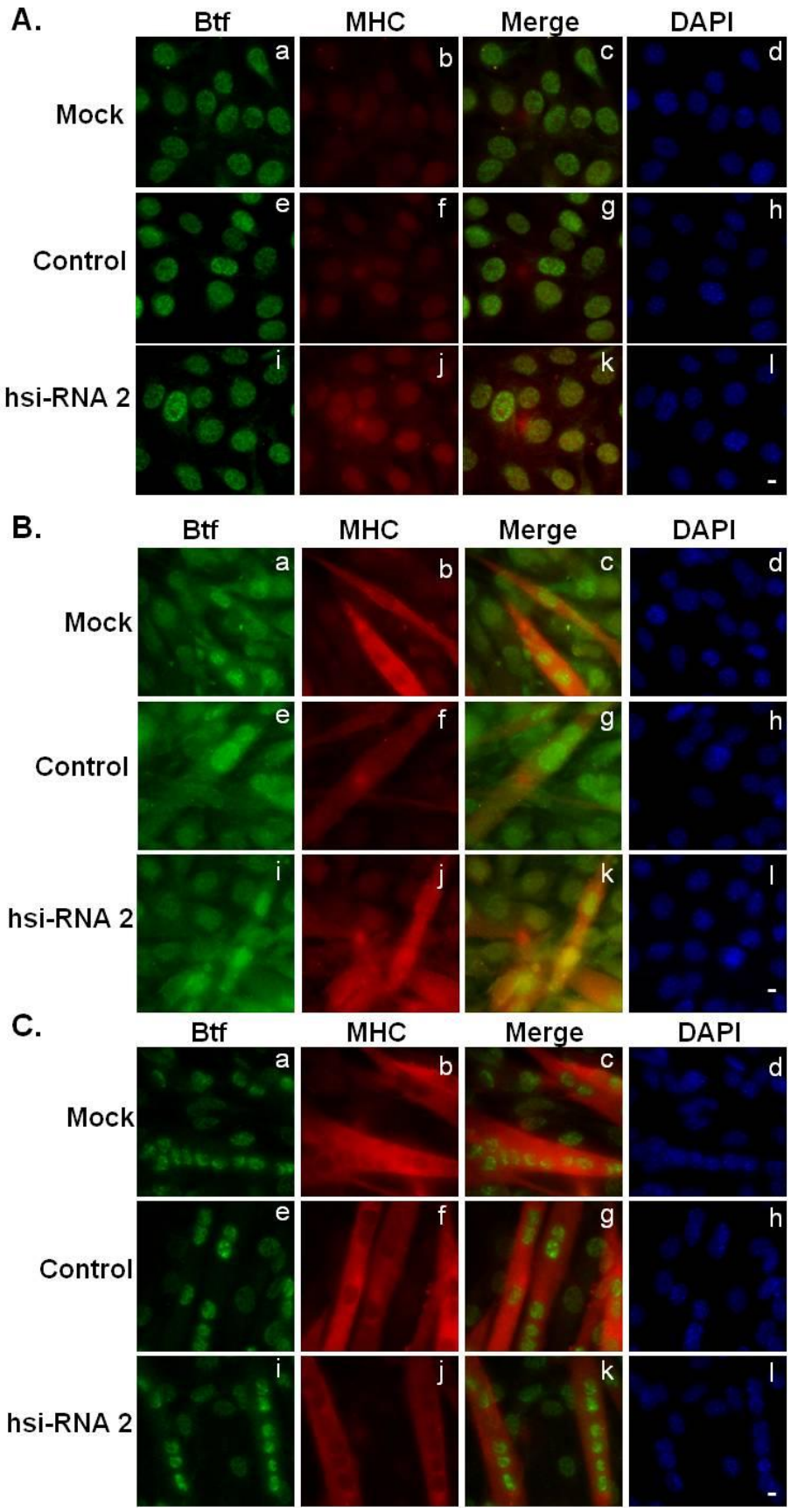
A.
Btf
MHC
Merge
DAPI
Mock
Control
hsi-RNA 2
a
b
c
d
e
f
g
h
i
j
k
l
B.
Btf
MHC
Merge
DAPI
Mock
Control
hsi-RNA 2
a
b
c
d
e
f
g
h
i
j
k
l
C.
Btf
MHC
Merge
DAPI
Mock
Control
hsi-RNA 2
a
b
c
d
e
f
g
h
i
j
k
l

Chapter 5: Investigating Nuclear Reorganization in C2C12 Cells

5.1 Nuclear Speckles Reorganize During Myogenesis in C2C12 Cells.

A preliminary experiment performed by an undergraduate honors student revealed reorganization of nuclear speckles during C2C12 differentiation (Theadore Hufford and Paula Bubulya, unpublished data). To confirm observations seen in the preliminary experiment and further investigate nuclear reorganization during differentiation of C2C12 myoblasts, I performed differentiation time course experiments to study organization of nuclear speckles throughout differentiation. C2C12 myoblasts were plated, allowed to attach for 24 hours, and induced to differentiate on Day 0 by switching from growth medium (GM) to differentiation medium (DM). C2C12 cells were processed Day 0 through Day 4 for immunofluorescence labeling of nuclear speckle protein Son as well as muscle specific proteins myogenin and MHC. Muscle specific proteins myogenin and MHC served as markers to indicate differentiating myoblasts. As early as Day 0, myoblasts positive for myogenin exhibited more defined, larger, and brighter nuclear speckles in comparison to neighboring undifferentiated myoblasts that showed punctuate nuclear speckle labeling (Figure 5.1). Some MHC negative cells exhibited reorganized nuclear speckles (Figure 5.2). This data taken together with the fact that reorganized nuclear speckles were observed in myoblasts which had not yet fused into multinucleated myotubes suggests that nuclear speckle reorganization occurs is early in the differentiation time course.

Figure 5.1. Reorganization of nuclear speckles in differentiating myoblasts expressing myogenin. After induction of differentiation, myoblasts begin to exhibit nuclear expression of muscle specific protein myogenin. By Day 2 of the differentiation time course, cells positive for myogenin (Panels I-L, arrows, red signal indicates immunolabeling of muscle specific protein myogenin with F5D anti-myogenin antibody) exhibit a more defined speckle phenotype (green signal indicates immunolabling of nuclear speckle protein Son with polyclonal WU13 antibody) as compared to neighboring undifferentiated myoblasts (Panels I-L, arrowheads). DNA was stained with DAPI. Bar = 5µm.

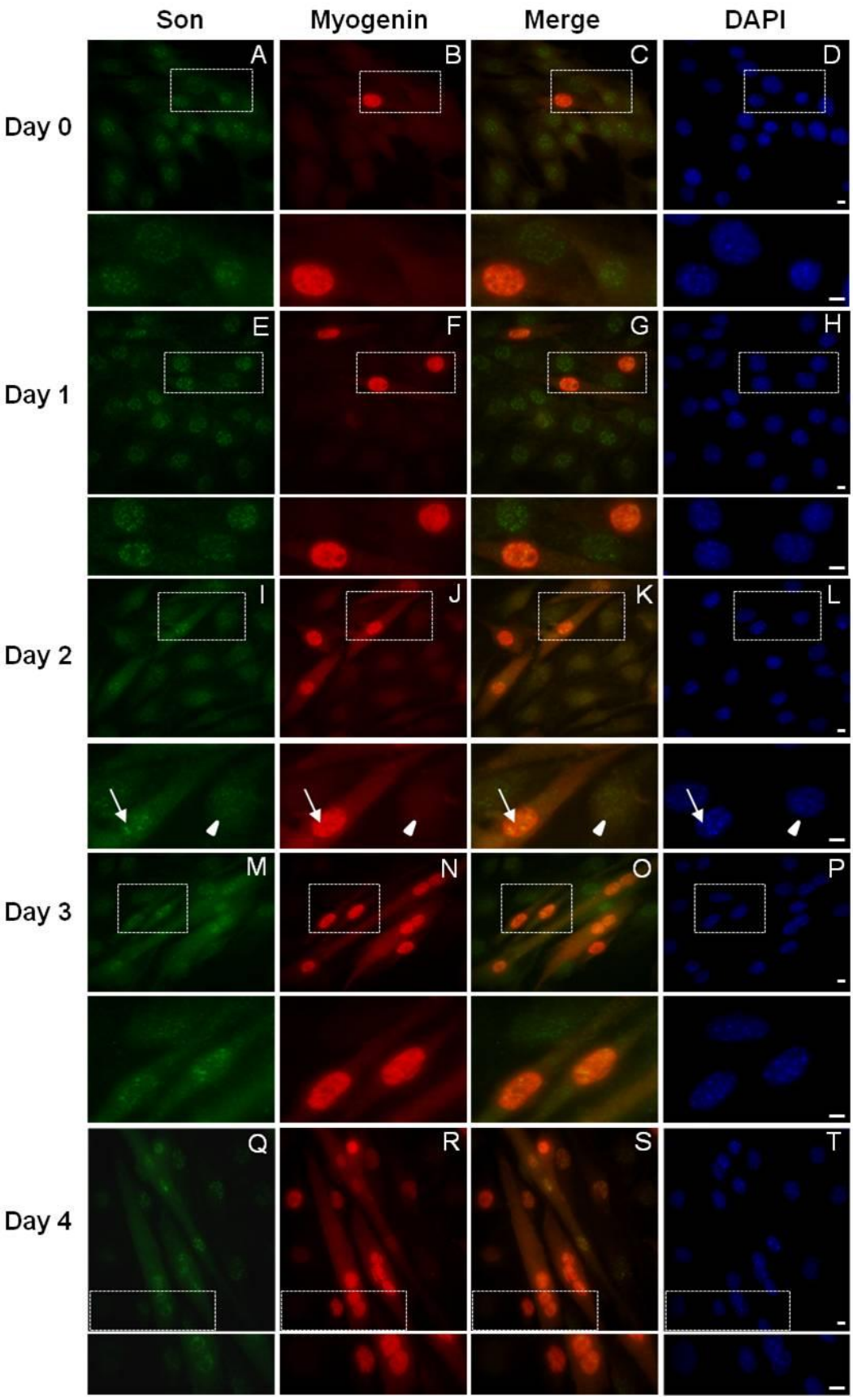
Son
Myogenin
Merge
DAPI
Day 0
Day 1
Day 2
Day 3
Day 4
A
B
C
D
E
F
G
H
I
J
K
L
M
N
O
P
Q
R
S
T

Figure 5.2. Reorganization of nuclear speckles in differentiating myoblasts expressing MHC. Approximately 48 hours after induction of differentiation, myoblasts begin to exhibit cytoplasmic expression of the muscle-specific protein MHC. Myoblasts positive for MHC (Panels I-L, arrows, red signal indicates immunlabeling of MHC with MF20 anti-MHC antibody) exhibit a more defined speckle phenotype (green signal indicates immunolabling of nuclear speckle protein Son with polyclonal WU13 antibody) as compared to neighboring undifferentiated myoblasts (Panels I-L, arrowheads). DNA was stained with DAPI. Bar = 5µm.

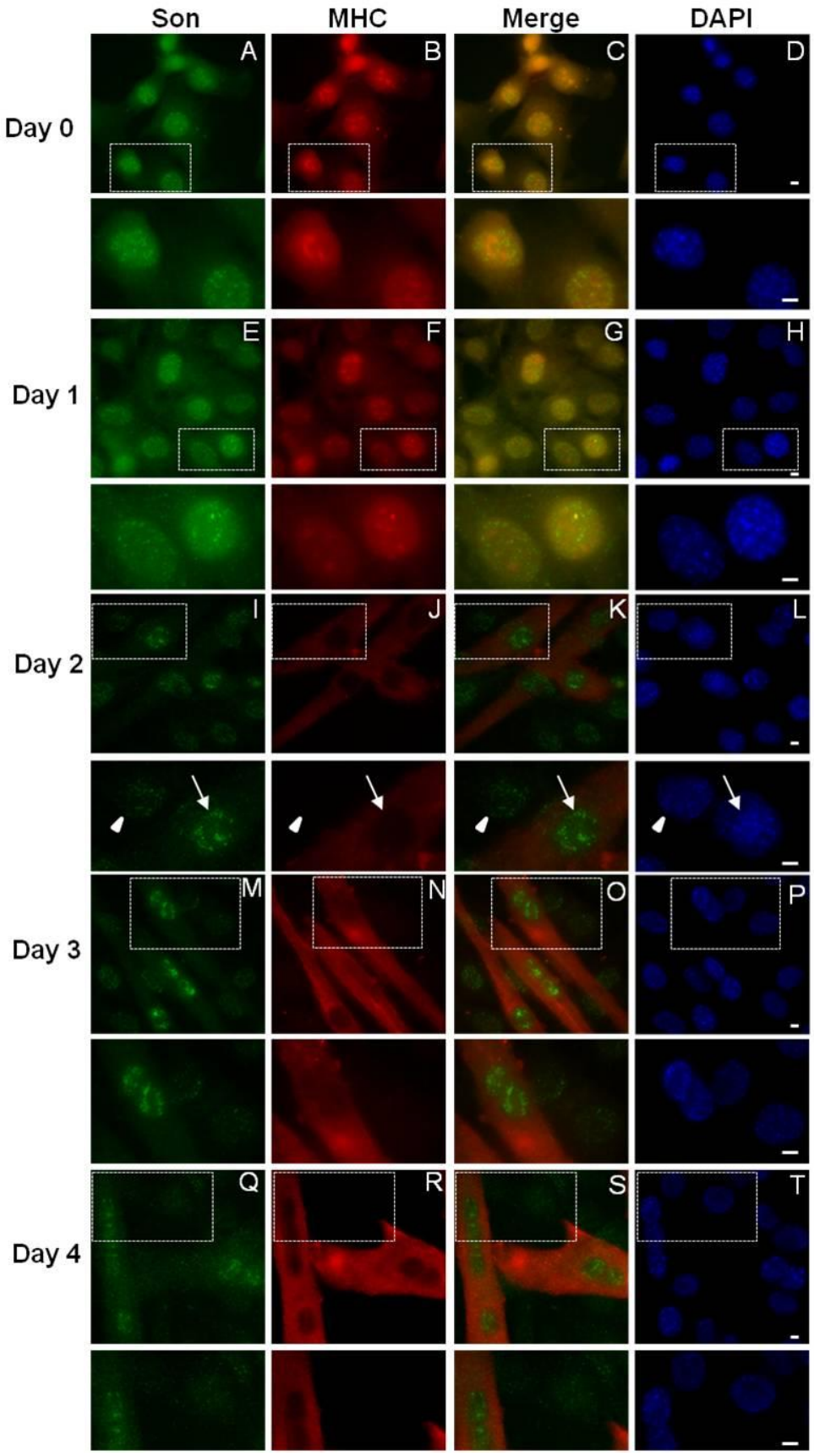
Son
MHC
Merge
DAPI
Day 0
Day 1
Day 2
Day 3
Day 4
A
B
C
D
E
F
G
H
I
J
K
L
M
N
O
P
Q
R
S
T

5.2 Nucleoli Reorganize During Myogenesis in C2C12 Cells.

In addition to nuclear speckles, preliminary data showed that nucleoli in differentiating C2C12 cells reorganize (Theadore Hufford and Paula Bubulya, unpublished data). In order to confirm this data and further characterize nucleolar reorganization, I performed differentiation time course experiments in which I monitored nuclear expression and compartmentalization of rRNA processing factor fibrillarin. C2C12 myoblasts were plated, allowed to attach for 24 hours, and induced to differentiate on Day 0 by switching from GM to DM. C2C12 cells were processed on Day 0 through Day 4 for immunofluorescence labeling of fibrillarin as well as for muscle specific proteins myogenin and MHC. Myogenin and MHC served as markers to indicate differentiating myoblasts. Myogenin positive cells were present at Day 0 and Day 1; however, myogenin positive cells on Day 0 and Day 1 did not show a reorganization of nucleoli (Figure 5.3). By Day 2 of the differentiation time course, myogenin positive myoblasts showed a reorganization of nucleoli from approximately 5-10 small punctate bodies to approximately 1-5 more prominent bodies (Figure 5.3). Some cells that were MHC negative exhibited reorganized nucleoli (Figure 5.4). Both fibrillarin and MHC are labeled in Texas Red secondary antibody because both antibodies were monoclonal antibodies and because the two proteins are in separate compartments of the cells, one secondary was used. Reorganized nucleoli were observed in cells which had not yet fused into multinucleated myotubes (Figure 5.4). Some spontaneously inducing cells also exhibited the reorganized phenotype (Theadore Hufford, Paula Bubulya, unpublished data). This data suggests that nucleolar reorganization occurs earlier in the differentiation time course than MHC expression and multinucleation.

Figure 5.3. Reorganization of nucleoli in differentiating myoblasts expressing myogenin. After induction of differentiation, myoblasts begin to show nuclear expression of muscle specific protein myogenin. By Day 2, all myoblasts positive for myogenin (Panels I-L, arrows, green signal indicates immunolabeling of myogenin with F5D anti-myogenin antibody) exhibit a change in nucleolar organization (Panels I-L, arrows, red signal indicates immunolabeling of nucleolar component fibrillarin with polyclonal anti-fibrillarin antibody) as compared to neighboring undifferentiated myoblasts (Panels I-L, arrowheads). DNA was stained with DAPI. Bar = 5μm.

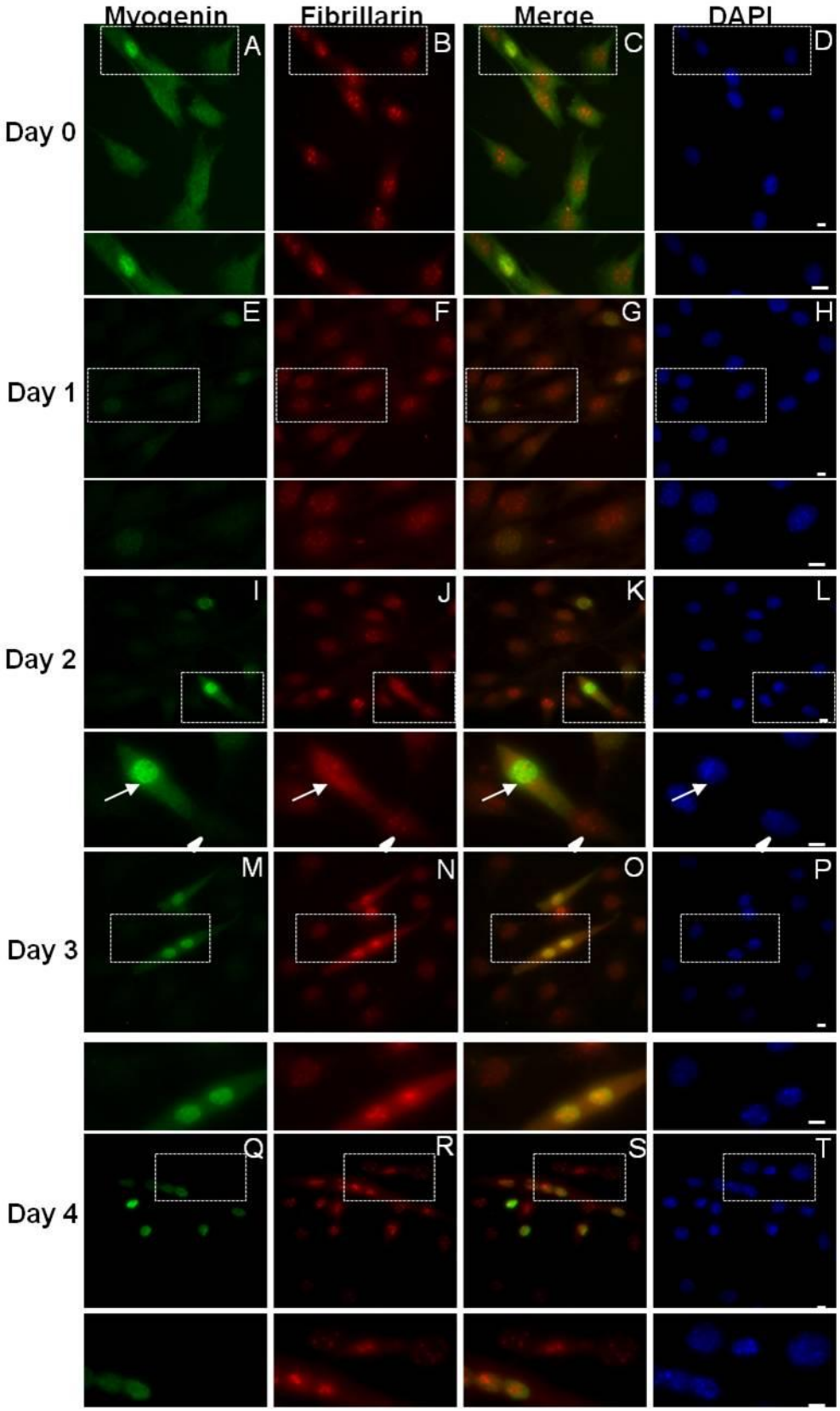
Myogenin
Fibrillarin
Merge
DAPI
Day 0
Day 1
Day 2
Day 3
Day 4
A
B
C
D
E
F
G
H
I
J
K
L
M
N
O
P
Q
R
S
T

Figure 5.4. Reorganization of nucleoli in differentiating myoblasts expressing MHC. Beginning on Day 1 of the differentiation time course nucleoli in differentiating myoblasts reorganize. By Day 1 of the differentiation time course, the cell indicated is negative for MHC expression (Panels D-F, arrows, red signal indicates immunolabeling of both MHC with MF20 anti-MHC antioby and fibrillarin with monoclonal anti-fibrillarin antibody) but still exhibits a reorganized nucleolar phenotype as compared to neighboring cells (Panels D-F, arrowheads). DNA was stained with DAPI. Bar = 5µm.

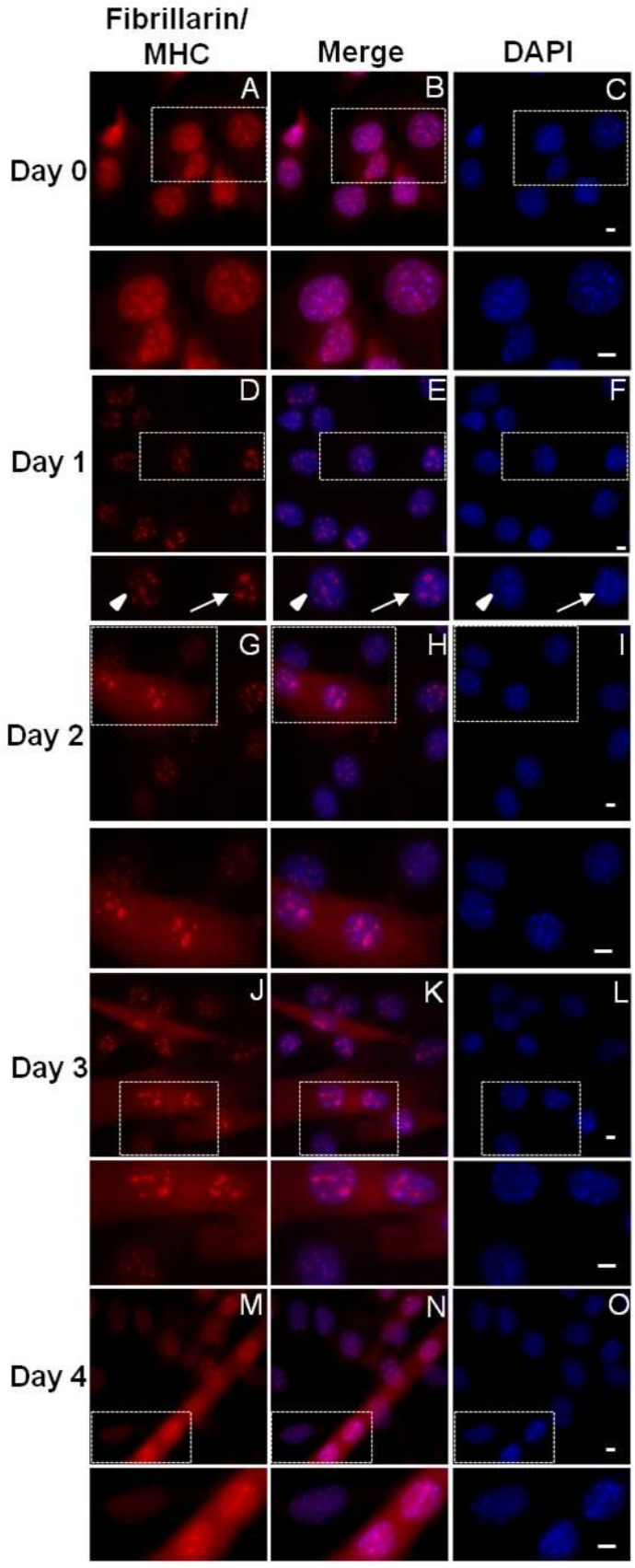
Fibrillarin/
MHC
Merge
DAPI
Day 0
Day 1
Day 2
Day 3
Day 4
A
B
C
D
E
F
G
H
I
J
K
L
M
N
O

5.3 Chromocenters reorganize during myogenesis in C2C12 cells

In addition to nuclear speckles and nucleoli, chromocenters in differentiating nuclei reorganized. Chromocenter reorganization and spatial clustering has been previously reported (Terranova et al., 2005). In undifferentiated C2C12 cells, chromocenters are evenly distributed throughout the nucleoplasm. However, as the myoblasts progress along the differentiation pathway chromocenters redistribute to the periphery of the nuclei. Throughout the various time course experiments performed, we observed in undifferentiated C2C12 cells the chromocenters were evenly distributed throughout the nucleoplasm. An example of this from one time experiment can be found in Figure 5.5, panel A. Once cells had differentiated, the chromocenters were distributed predominately on the periphery of the nuclei as previously reported.

5.4 Nuclear reorganization is not an artifact of serum starvation.

To assert that nuclear reorganization observed in differentiating C2C12 cells was not an artifact of serum starvation, I performed experiments using to test the effects of serum starvation on both HeLa and mouse embryonic fibroblast (MEF) cells. HeLa cells were chosen because they are a non-mouse cell line that does not undergo the differentiation process; furthermore, by using this cell line I could determine if serum starvation causes nuclear reorganization in a non-mouse cell line not undergoing differentiation. If nuclear reorganization occurred in serum-starved HeLa cells it would suggest that the nuclear reorganization I observed in differentiating C2C12 cells was a result of serum starvation rather than a specific differentiation event. MEF cells were chosen because they are a mouse cell line that does not undergo the differentiation process; furthermore, nuclear reorganization occurring in serum-starved MEF cells would suggest that nuclear reorganization in response to serum starvation was a mouse

Figure 5.5. Chromocenters reorganize during myoblast differentiation in C2C12 cells. At Day 0 of the differentiation time course chromocenters in undifferentiated cells are evenly distributed throughout the nucleoplasm (Panel A, white signal indicates DNA staining by DAPI). By Day 4 of the differentiation time course, chromocenters in differentiated cells have reorganized and are located predominately at the periphery of the nuclei (Panel B, white signal indicates DNA staining by DAPI). Bar = 5μm.

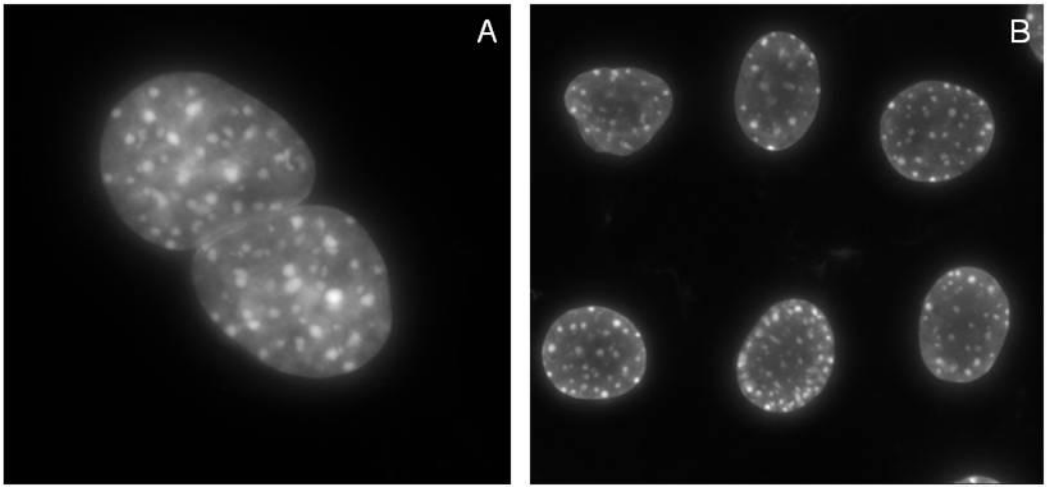
A
B

cell-specific phenomenon. HeLa and MEF cells were maintained in both “high serum” (DMEM + 10% FBS) and “low serum” (DMEM + 0.5% FBS) for four days. On each day, HeLa and MEF cells maintained in both serum conditions were processed for immunofluorescence labeling of both nuclear speckle protein Son and nucleolar protein fibrillarin to simultaneously monitor nuclear speckle and nucleolar organization. Because HeLa and MEF cells do not undergo differentiation, no proteins were used to mark cells undergoing differentiation. HeLa cells maintained in high serum conditions showed no reorganization of nuclear speckle morphology or nucleolar morphology between Day 1 and Day 4 (Figure 5.6). HeLa cells maintained low serum conditions exhibited no changes in nuclear speckle morphology or nucleolar morphology between Day 1 and Day 4 (Figure 5.7). MEF cells maintained in high serum conditions showed no reorganization of nuclear speckle or nucleolar morphology between Day 1 and Day 4 of the time course (Figure 5.8). MEF cells maintained in low serum conditions also showed no reorganization of nuclear speckle morphology or nucleolar morphology (Figure 5.9). Lack of nuclear speckle and nucleolar reorganization in either HeLa or MEF cells suggests that nuclear reorganization as observed in differentiating C2C12 cells was not an artifact of serum starvation. Because C2C12 cells undergoing differentiation show a decrease over time in the number of nucleoli per nucleus, I scored HeLa and MEF cells maintained in high and low serum conditions for number of nucleoli per nuclei for each day of the experiment. HeLa cells that were maintained in either high serum or low serum conditions showed no shift in the average number of nucleoli per nucleus between Day 1 and Day 4 indicating HeLa cell nucleoli do not reorganize as C2C12 cell nucleoli do during differentiation (Figure 5.10). MEF cells which were maintained in either high serum or low serum conditions showed no shift in average number of nucleoli per nucleus between Day 1 and Day 4 (5.11). Mitotic cells were scored for each experimental group for Day 1 through Day 4 to determine if cells maintained in either

Figure 5.6. Nuclear Organization in HeLa cells maintained in normal serum conditions. HeLa cells maintained in DMEM + 10% FBS showed no changes in organization of nuclear speckles (green signal indicates immunolabeling of nuclear speckle protein Son with polyclonal WU13 antibody) between Day 1 (Panels A, C and D, arrows) and Day 4 (Panels M, O, and P, arrows). Cells maintained in the same conditions also do not show changes in organization of nucleoli (red signal indicates immunolabeling of nucleolar component fibrillarin with monoclonal anti-fibrillarin antibody) between Day 1 (Panels B-D, arrowheads) and Day 4 (Panels N- P, arrowheads). DNA was stained with DAPI. Bar = 5μm.

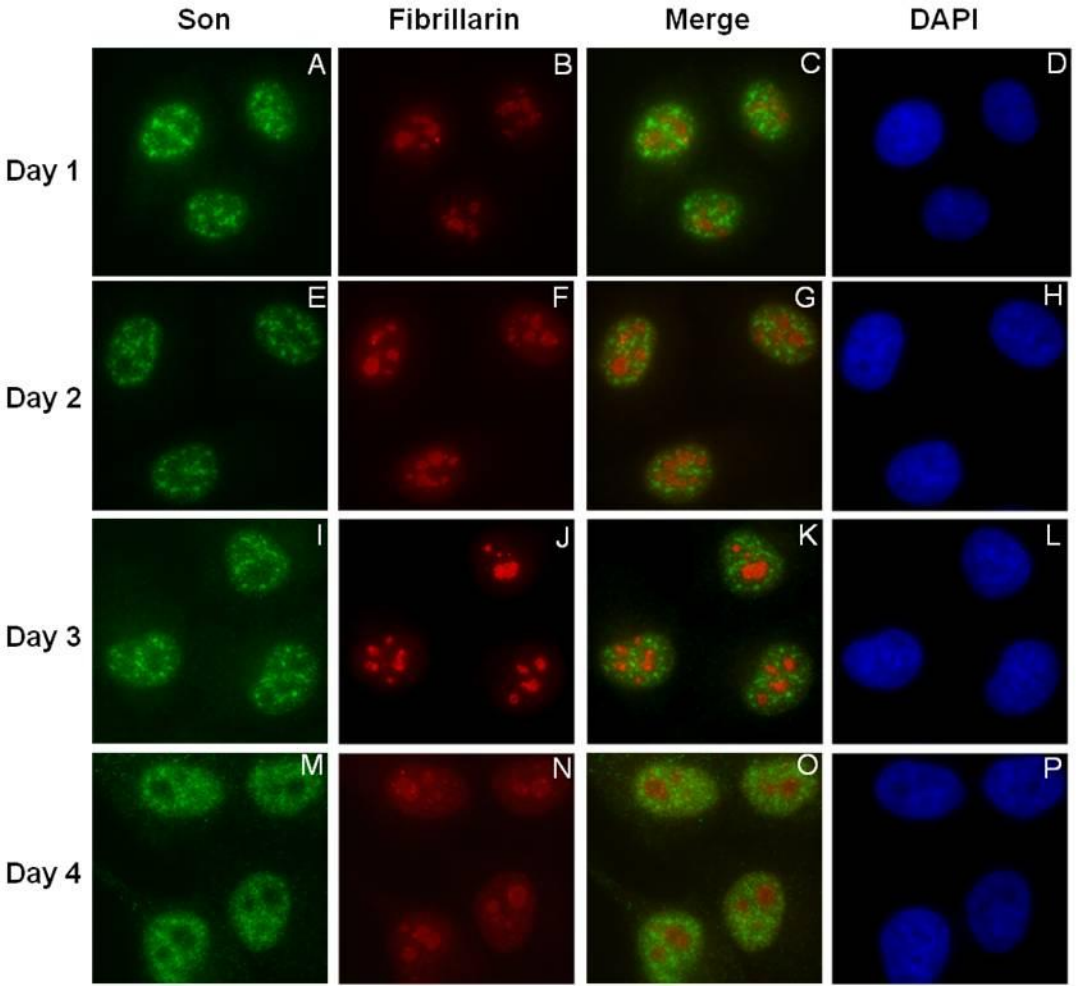
Son
Fibrillarin
Merge
DAPI
Day 1
Day 2
Day 3
Day 4
A
B
C
D
E
F
G
H
I
J
K
L
M
N
O
P

Figure 5.7. Serum starvation does not result in reorganization of HeLa nuclei. HeLa cells maintained in DMEM + 0.5% FBS (low serum conditions) showed unaltered organization of nuclear speckles (green signal indicates immunolabeling of nuclear speckle protein Son with polyclonal WU13 antibody) between Day 1 (Panels A, B, and D, arrows) and Day 4 (Panels M, O, and P, arrows). Cells maintained in the same conditions also exhibit unchanged organization of nucleoli (red signal indicates immunlabeling of nucleolar component fibrillarin with monoclonal anti-fibrillarin antibody) between Day 1 (Panels B-D, arrowheads) and Day 4 (Panels N-P, arrowheads). DNA was stained with DAPI. Bar = 5μm.

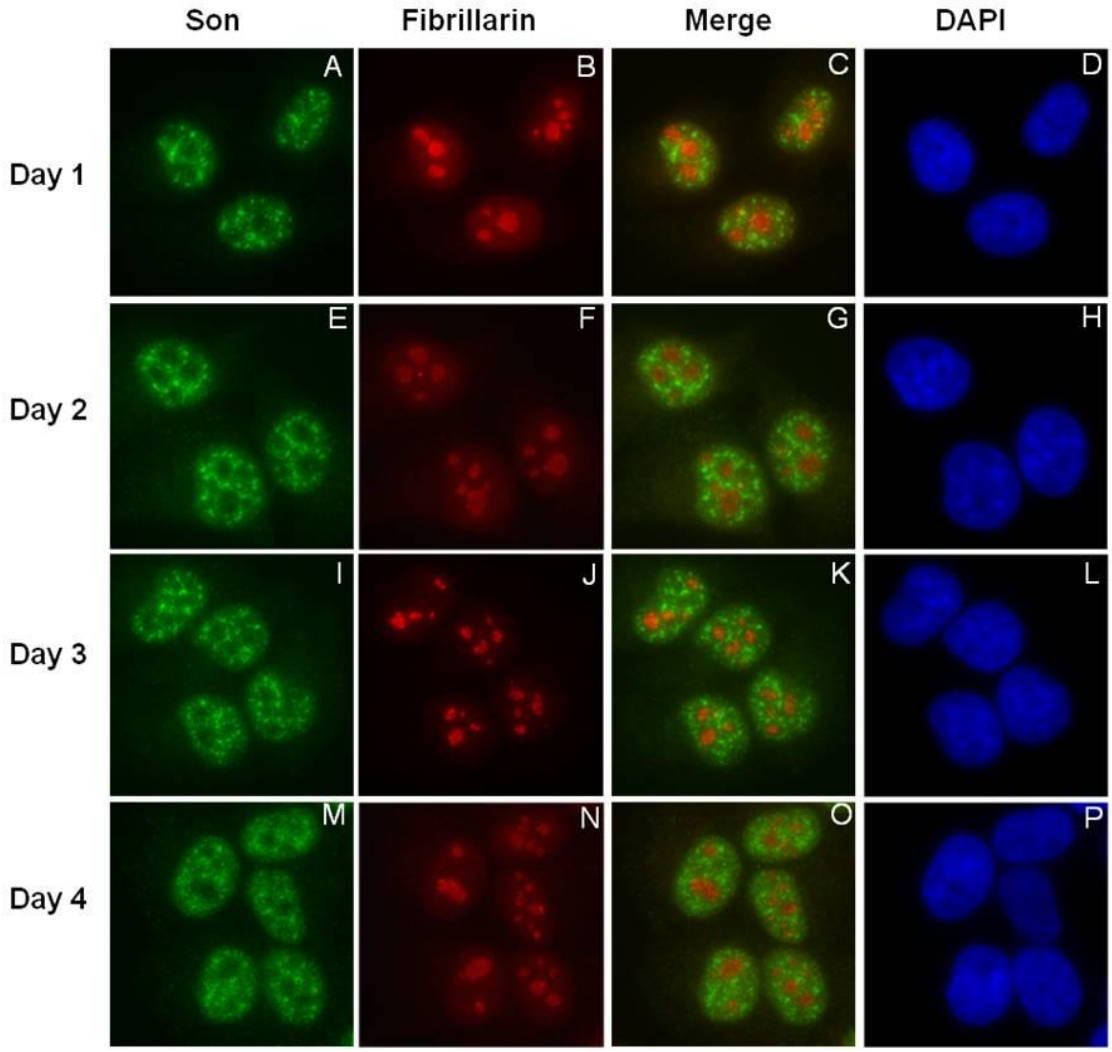
Son
Fibrillarin
Merge
DAPI
Day 1
Day 2
Day 3
Day 4
A
B
C
D
E
F
G
H
I
J
K
L
M
N
O
P

Figure 5.8. Nuclear organization of mouse embryonic fibroblasts (MEFs) maintained in normal serum conditions. MEFs maintained in DMEM + 10% FBS showed unaltered organization of nuclear speckles (green signal indicates immunolabeling of nuclear speckle protein Son with polyclonal WU13 antibody) between Day 1 (Panels A, C, and D, arrows) and Day 4 (Panels M, O, and P, arrows). Cells maintained in the same conditions also exhibit unchanged organization of nucleoli (red signal indicates immunolabeling of nucleolar component fibrillarin with monoclonal anti-fibrillarin antibody) between Day 1 (Panles B-D, arrowheads) and Day 4 (Panels N-P, arrowheads. DNA was stained with DAPI. Bar = 5μm.

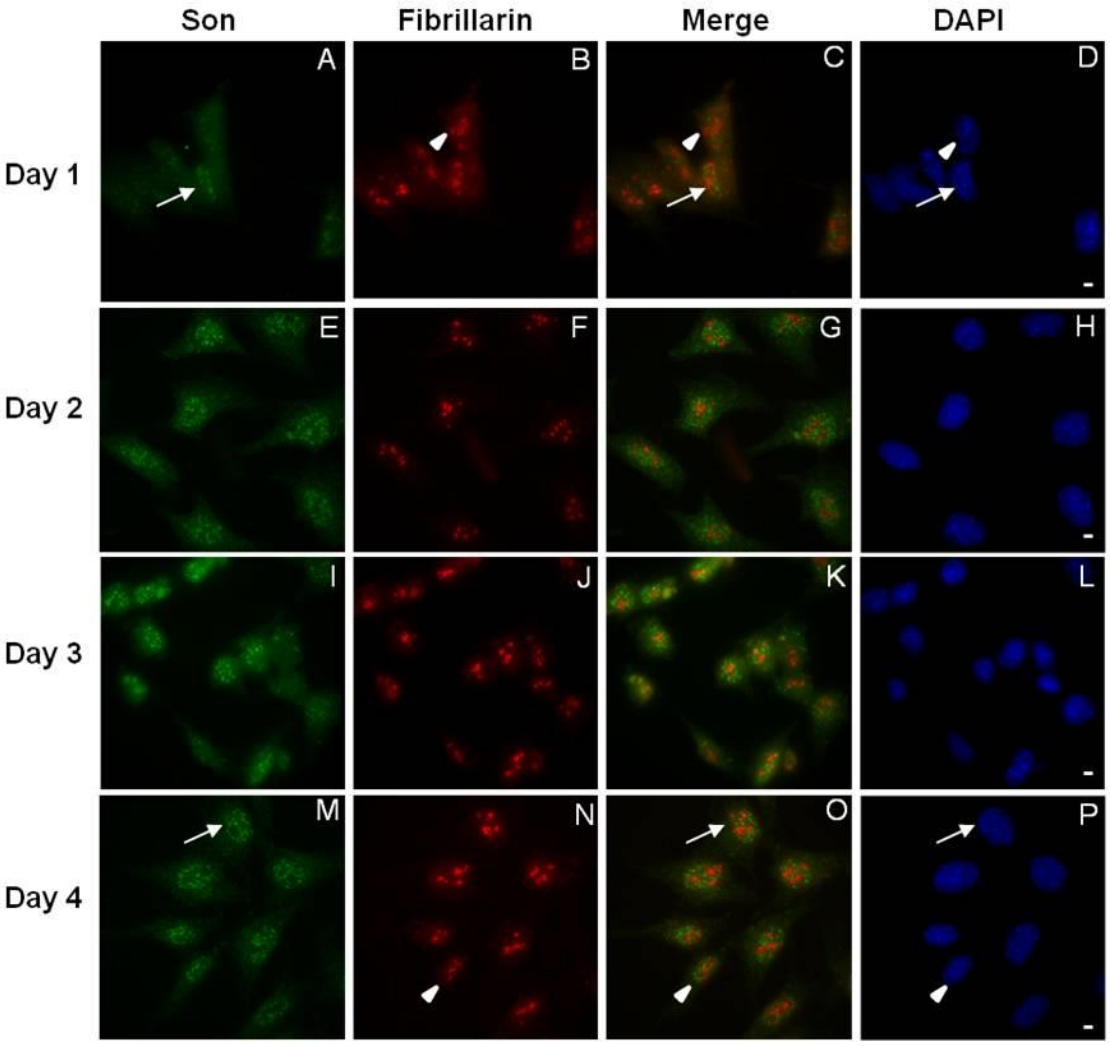
Son
Fibrillarin
Merge
DAPI
Day 1
Day 2
Day 3
Day 4
A
B
C
D
E
F
G
H
I
J
K
L
M
N
O
P

Figure 5.9. Serum starvation does not result in reorganization of MEF nuclei. MEFs maintained in DMEM + 0.5% FBS showed unaltered organization of nuclear speckles (green signal indicates immunolabeling of nuclear speckle protein Son with polyclonal WU13 antibody) between Day 1 (Panels A, C, and D, arrows) and Day 4 (Panels M, O, and P, arrows). Cells maintained in the same conditions also exhibit unchanged organization of nucleoli (red signal indicates immunlabeling of nucleolar component fibrillarin with monoclonal anti-fibrillarin antibody) between Day 1 (Panles B-D, arrowheads) and Day 4 (Panels N-P, arrowheads. DNA was stained with DAPI. Bar = 5μm.

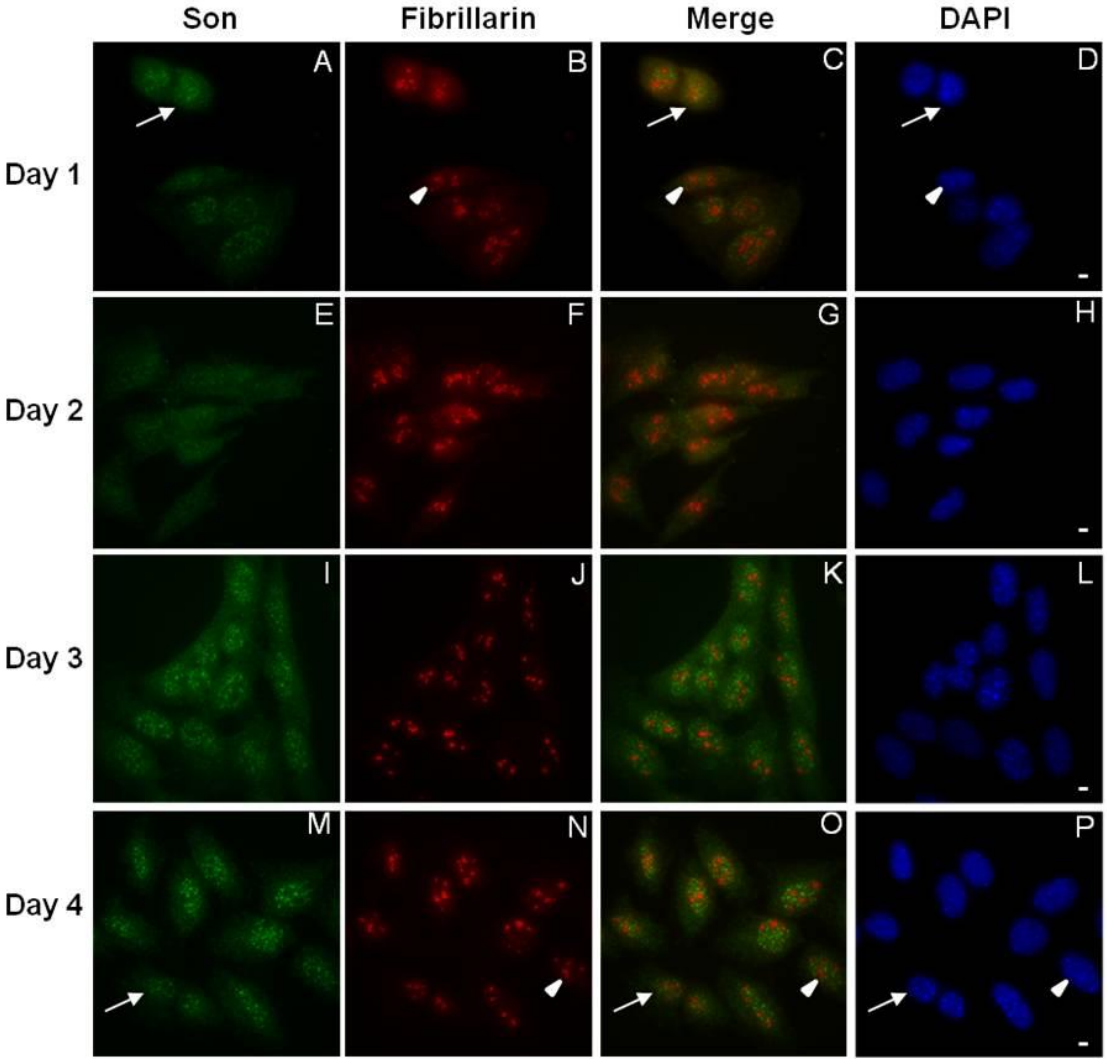
Son
Fibrillarin
Merge
DAPI
Day 1
Day 2
Day 3
Day 4
A
B
C
D
E
F
G
H
I
J
K
L
M
N
O
P

Figure 5.10. Number of Nucleoli per Nuclei Does Not Change For HeLa Cells In Response To Serum Starvation. HeLa cells maintained in either high serum concentrations (DMEM + 10% FBS, gray bars) or low serum concentrations (DMEM + 0.5% FBS, black bars) do not exhibit any difference in average number of nucleoli per nucleus between Day 1 (Panel A) through Day 4 (Panel D).

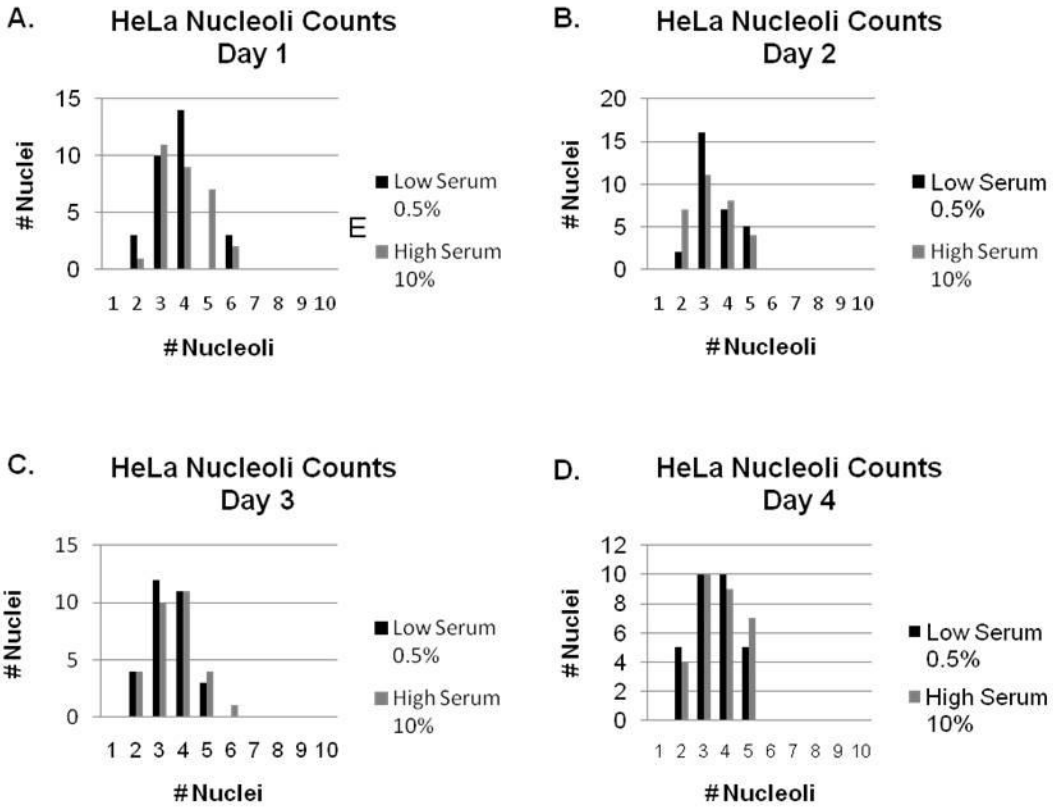
A.
HeLa Nucleoli Counts
Day 1
#Nuclei
#Nucleoli
Low Serum 0.5%
High Serum 10%
B.
HeLa Nucleoli Counts
Day 2
#Nuclei
#Nucleoli
Low Serum 0.5%
High Serum 10%
C.
HeLa Nucleoli Counts
Day 3
#Nuclei
#Nuclei
Low Serum 0.5%
High Serum 10%
D.
HeLa Nucleoli Counts
Day 4
#Nuclei
#Nucleoli
Low Serum 0.5%
High Serum 10%

Figure 5.11. Number of nucleoli per MEF nucleus does not change for MEF Cells after serum starvation. MEFs maintained in both high serum concentrations (DMEM + 10% FBS, gray bars) and low serum concentrations (DMEM + 0.5% FBS, black bars) do not exhibit a shift in average number of nucleoli per nuclei between Day 1 (Panel A) through Day 4 (Panel D).

A.

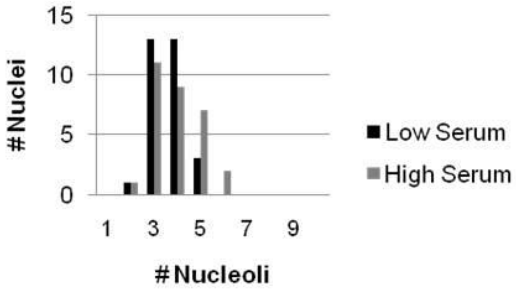
MEF Nucleoli Counts
Day 1
15
10
5
0
#Nuclei
1 3 5 7 9
#Nucleoli
Low Serum
High Serum

B.

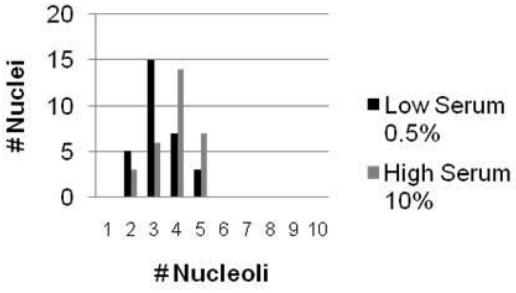
MEF Nucleoli Counts
Day 2
20
15
10
5
0
#Nuclei
1 2 3 4 5 6 7 8 9 10
#Nucleoli
Low Serum 0.5%
High Serum 10%

C.

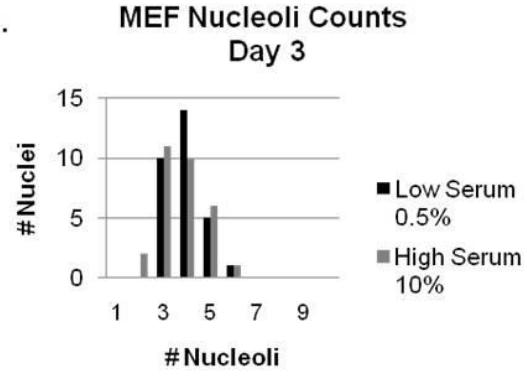
MEF Nucleoli Counts
Day 3
15
10
5
0
#Nuclei
1 3 5 7 9
#Nucleoli
Low Serum 0.5%
High Serum 10%

D.

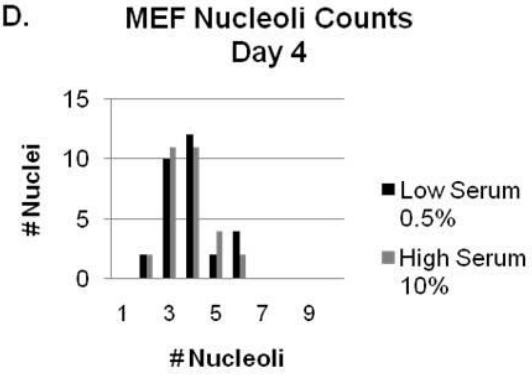
MEF Nucleoli Counts
Day 4
15
10
5
0
#Nuclei
1 3 5 7 9
#Nucleoli
Low Serum 0.5%
High Serum 10%

high or low serum conditions were actively cycling. Mitotic cells were scored for HeLa cells maintained in both high serum and low serum conditions for all four days of the time course. HeLa cells which were maintained in high serum conditions showed an overall increase in number of mitotic cells present within the population and HeLa cells maintained in low serum conditions shifted from 2% to 4% (Table 5.1). Mitotic cells were scored for MEF cells maintained in either high serum or low serum conditions for all four days of the time course. MEF cells maintained in high serum conditions showed an overall increase in number of mitotic cells present within the population and MEF cells maintained in low serum conditions showed a decrease of mitotic cells from 2% on Day 1 to 0% on Day 4 (Table 5.1). A lower percentage of mitotic cells in both HeLa and MEF cells maintained in low serum conditions as compared to HeLa and MEF cells maintained in high serum conditions was expected because serum starved cells stop proliferating.

5.5. Nuclear speckles and nucleoli reorganize in differenitiating myoblasts in the absence of serum starvation.

To further assert that nuclear reorganization was not an artifact of serum starvation in C2C12 cells, I performed a time course experiment in which C2C12 myoblasts were plated at a higher density to allow for increased cell-to cell contact. Cell-to cell contact among undifferentiated C2C12 cells leads to spontaneous differentiation in the absence of serum starvation. Additional C2C12 cells that were plated at the normal density and were induced to differentiate via serum starvation served as a control to which I could compare myoblasts undergoing self-induced differentiation. At Day 0 of the differentiation time course, no cells exhibited any nuclear reorganization as expected (Figure 5.12, panels A-D and Figure 5.13, panels A-C). By Day 4 of the time course, cells which were induced to differentiate via serum starvation exhibited reorganized

Table 5.1. Mitotic Counts for HeLa, MEF, and C2C12 Cells. Fifty cells were randomly selected for image capture and mitotic cells were counted for each cell line for all days of the serum test experiment. MEF cells maintained in high serum conditions exhibited an overall increase in the mitotic population from Day 1 (with 10% mitotic cells) through Day 4 (with 14% mitotic cells). MEF cells maintained in low serum conditions show an overall decrease in the mitotic population beginning with 2% mitotic cells on Day 1 and ending with 0% mitotic cells on Day 4. HeLa cells maintained in high serum concentrations also showed an overall increase in the mitotic population beginning with 6% on Day 1 and ending with 20% on Day 4. HeLa cells maintained in low serum concentrations showed an overall 2% increase in mitotic populations but still had a lower percentage in comparison to all cell lines maintained in high serum concentrations. Upon induction to differentiate via serum starvation, the mitotic population of C2C12 cells decreased from 14% on Day 0 to 0% by Day 4 and remained at 0% through Day 8 after addition of growth medium for four days.

	Day 0		Day 1		Day 2		Day 3		Day 4		Day 8	
Cell Line	#/50	%	#/50	%	#/50	%	#/50	%	#/50	%	#/50	%
MEF High Serum	N/A	N/A	5	10%	6	12%	5	10%	7	14%	N/A	N/A
MEF Low Serum	N/A	N/A	1	2%	2	4%	1	2%	0	0%	N/A	N/A
Hela High Serum	N/A	N/A	3	6%	6	12%	8	16%	10	20%	N/A	N/A
Hela Low Serum	N/A	N/A	1	2%	2	4%	0	0%	2	4%	N/A	N/A
C2C12	7	14%	4	8%	0	0%	1	2%	0	0%	0	0%

Figure 5.12. Nuclear speckles reorganize in differentiating C2C12 cells in the absence of serum starvation. On Day 0 of the differentiation time course, both cells which were induced to differentiate through either cell-to cell contact (self-induced) or serum starvation showed no reorganization of nuclear speckles (Panels A-D and I-L, green signal indicates immunolabeling of nuclear speckle protein with WU13 antibody and red signal indicates immunolabeling of muscle specific protein myogenin with anti-myogenin antibody). By Day 4 of the differentiation time course both self-induced and serum starved cells exhibited equivalent reorganization of nuclear speckles. DNA was stained with DAPI. Bar = 5μm.

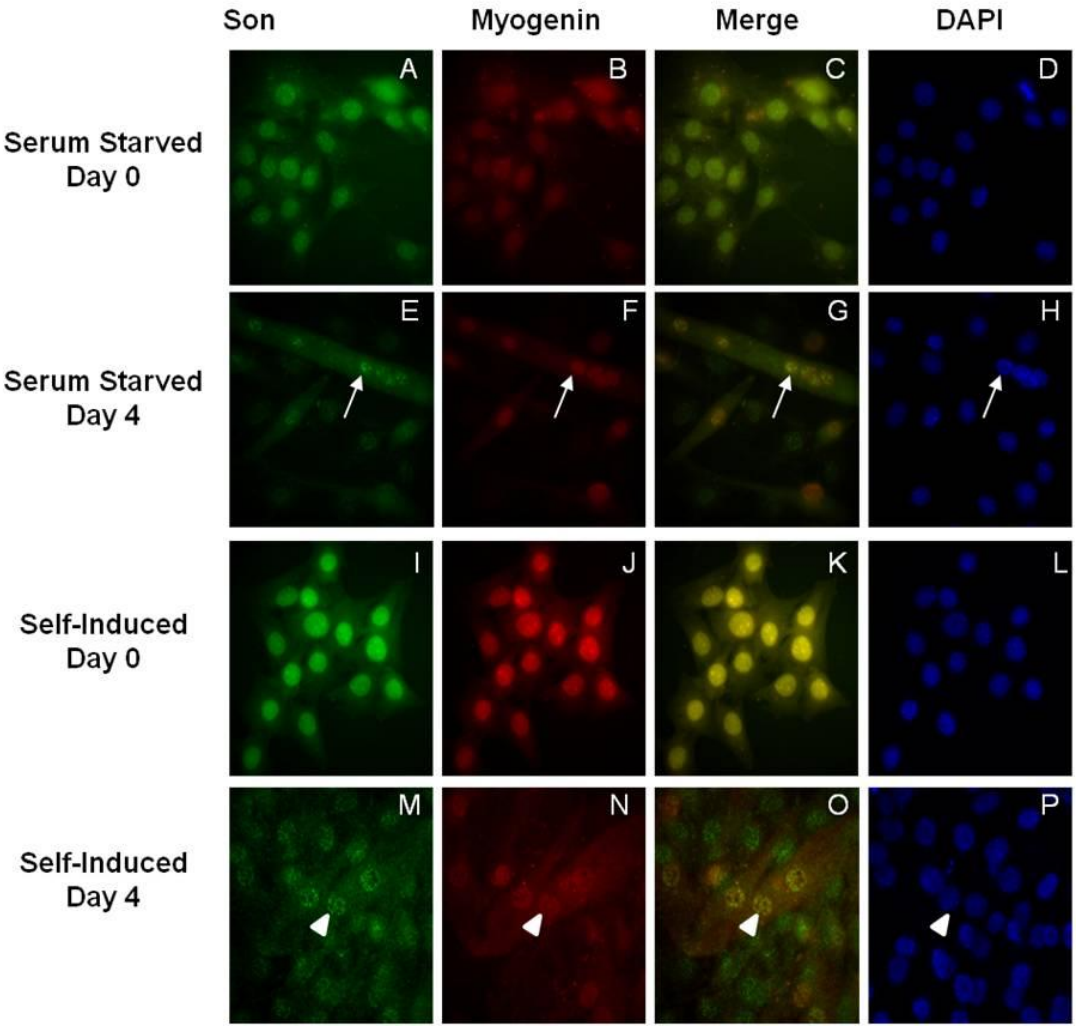
Son
Myogenin
Merge
DAPI
Serum Starved Day 0
Serum Starved Day 4
Self-Induced Day 0
Self-Induced Day 4
A
B
C
D
E
F
G
H
I
J
K
L
M
N
O
P

Figure 5.13. Nucleoli reorganize in differentiating C2C12 cells in the absence of serum starvation. On Day 0 of the differentiation time course, both cells which were induced to differentiate through either cell-to cell contact (self-induced) or serum starvation showed no reorganization of nucleoli (Panels A-D and I-L, red signal indicates immunolabeling of nucleolar component fibrillarin with monoclonal anti-fibrillarin antibody and MHC with MF20 anti-MHC antibody). By Day 4 of the differentiation time course both self-induced and serum starved cells exhibited equivalent reorganization of nucleoli (Panels E-H and M-P). DNA was stained with DAPI. Bar = 5μm.

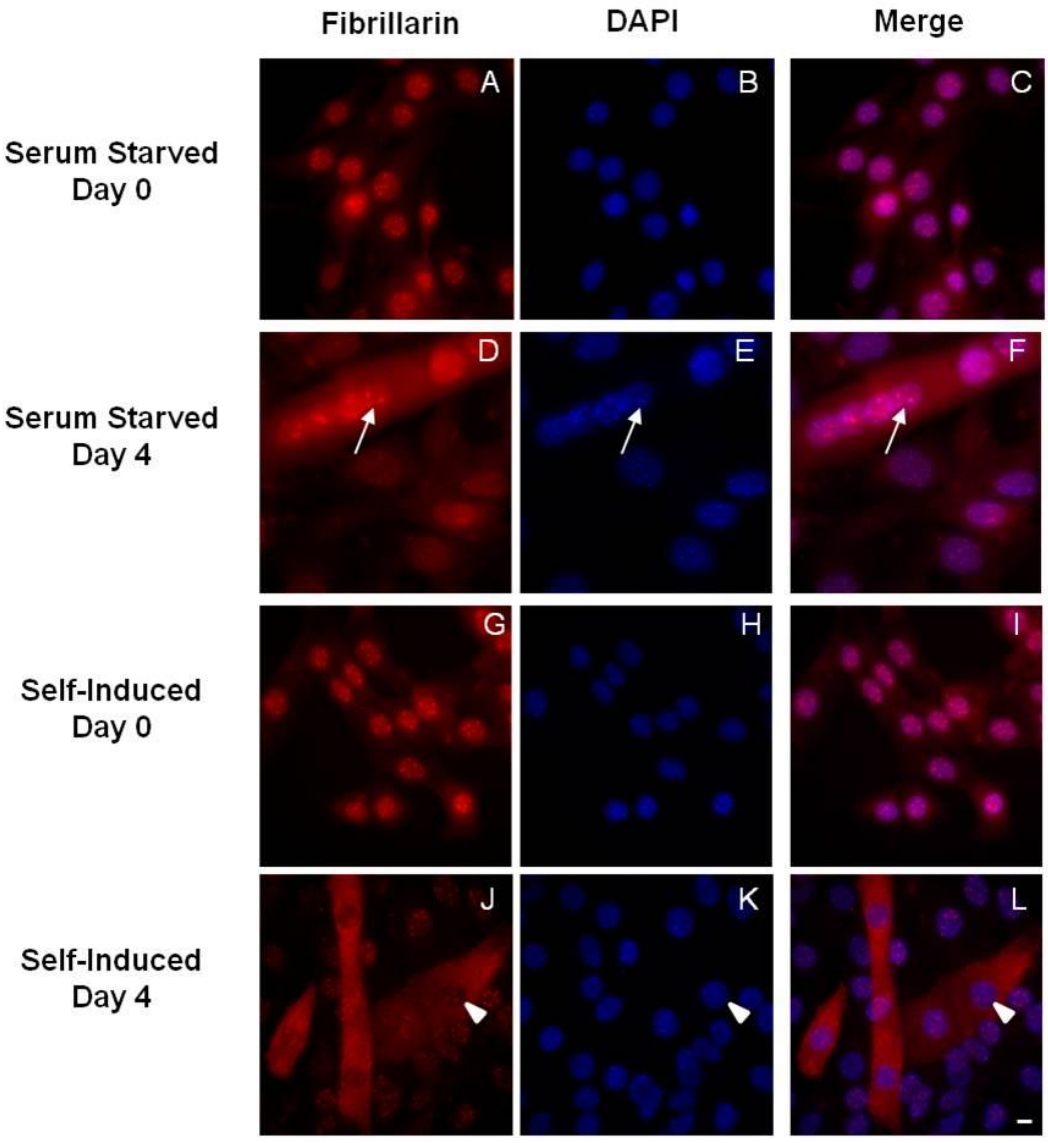
Fibrillarin
DAPI
Merge
Serum Starved
Day 0
Serum Starved
Day 4
Self-Induced
Day 0
Self-Induced
Day 4
A
B
C
D
E
F
G
H
I
J
K
L

nuclear speckles and nucleoli consistent with previous experiments (Figure 5.12, panels E-H and Figure 5.13, panels D-F). By Day 3 of the differentiation time course, the cells undergoing self-induced differentiation were processed as they had developed myotubes and were nearly 100% confluent as observed by phase contrast microscopy. At Day 3 of the differentiation time course, the self-induced cells showed reorganization of both nuclear speckles and nucleoli as observed in the serum starved cells (Figure 5.12, panels M-P and Figure 5.13, panels J-K). This data suggests that the nuclear reorganization observed in differentiating C2C12 cells is not a result of the metabolic changes that occur during serum starvation but rather a result of the differentiation process.

5.6. The number of nucleoli per nucleus decreases in an irreversible fashion during differentiation.

To determine if nuclear reorganization was reversible, I performed experiments in which GM was added back to C2C12 cells after Day 4 of the differentiation time course. C2C12 cells were scored for number of nucleoli per nuclei in both myoblasts (cells that were negative for muscle specific proteins myogenin or MHC) and myotubes (cells that were positive for muscle specific proteins myogenin or MHC) for Days 0-4 of the differentiation time course. Myotubes consistently had fewer nucleoli per nucleus in comparison to myoblasts for all four days of the differentiation time course (Figure 5.14). On Day 4 of one differentiation time course, GM was added back to the C2C12 cells for four additional days and the number of nucleoli per nucleus was again scored for both myoblasts and myotubes on Day 8. Myotubes again showed fewer nucleoli per nuclei (Figure 5.14). Failure of nucleoli to revert to the organization seen in undifferentiated C2C12 cells in the presence of GM suggests that nuclear reorganization is irreversible.

Figure 5.14. Differentiation causes irreversible nucleolar reorganization in C2C12 myoblasts. For each day of the differentiation time course, 30 myoblast (C2C12 cells negative for myogenin or MHC) and 30 myotube (C2C12 cells positive for myogenin or MHC) nuclei were counted and number of nucleoli per nuclei was recorded. This was repeated for three separate experiments (1 fibrillarin + myogenin, 2 fibrillarin + MHC) and the number of nucleoli per nuclei averaged. Myotubes consistently show a lower number of nucleoli, while myoblasts exhibit a higher number of nucleoli (Panels A-E). For one time course experiment, at Day 4 of differentiation, growth medium was added back to the cells and on Day 8 the cells were fixed and counted as previously stated to determine if nuclear reorganization would reverse when serum-rich medium was added back to the cells. Nucleoli counts on Day 8 indicate that nucleolar reorganization resulting from differentiation is similar to that on Day 4 (Panel F).

A.

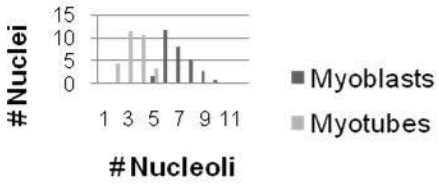
C2C12 Nucleoli Counts
Day 0
15
10
5
0
1 3 5 7 9 11
#Nuclei
#Nucleoli
Myoblasts
Myotubes

B.

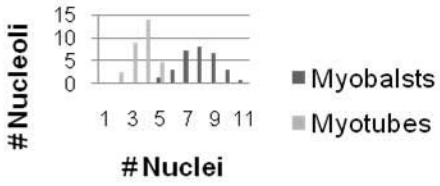
C2C12 Nucleoli Counts
Day 1
15
10
5
0
1 3 5 7 9 11
#Nucleoli
#Nuclei
Myobalsts
Myotubes

C.

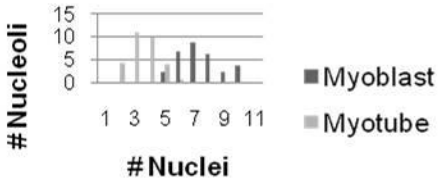
C2C12 Nucleoli Counts
Day 2
15
10
5
0
1 3 5 7 9 11
#Nucleoli
#Nuclei
Myoblast
Myotube

D.

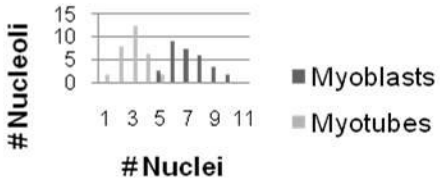
C2C12 Nucleoli Counts
Day 3
15
10
5
0
1 3 5 7 9 11
#Nucleoli
#Nuclei
Myoblasts
Myotubes

E.

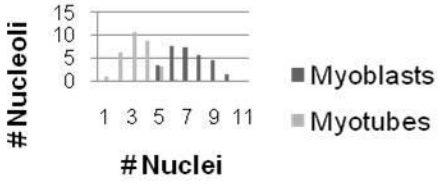
C2C12 Nucleoli Counts
Day 4
15
10
5
0
1 3 5 7 9 11
#Nucleoli
#Nuclei
Myoblasts
Myotubes

F.

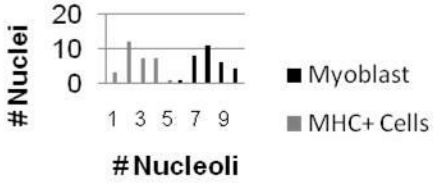
C2C12 Nucleoli Counts
Day 8
20
10
0
1 3 5 7 9
#Nuclei
#Nucleoli
Myoblast
MHC+ Cells

5.7. Live imaging of nuclear reorganization

Based on observations made of reorganization of nuclear speckles and nucleoli, we hypothesized two possible models for reorganization: nuclear domain fusion and/or nuclear domain recession and enlargement. In order to determine which model was correct, we designed experiments to image nucleolar reorganization via live cell microscopy. To our knowledge live imaging in C2C12 cells has not been previously done. As such, several parameters were optimized to increase the probability for successful imaging of nuclear proteins including transfection conditions and timing of transfection in the differentiation scheme. C2C12 cells were transfected with CFP-fibrillarin plasmid DNA for live imaging of exogenous protein. To optimize transfection conditions, C2C12 cells were first transfected with 40 µg of salmon sperm carrier DNA and increasing amounts of plasmid DNA ranging from 2 µg-10 µg. C2C12 cells transfected with 4 µg of CFP-fibrillarin DNA provided the greatest level of transfection efficiency (Figure 5.15). C2C12 cells transfected with 40 µg of salmon sperm carrier DNA and 4 µg of CFP-fibrillarin DNA exhibited high transfection efficiency but high levels of overexpression were also observed and seemed to alter nucleolar reorganization (data not shown). The goal of this optimization was to express enough CFP-fibrillarin for image detection without altering nuclear structure. To optimize salmon sperm carrier DNA concentrations in order decrease overexpression, C2C12 cells were then transfected with 20 µg, 40 µg, 60 µg and 80 µg of salmon sperm carrier DNA. 80 µg of salmon sperm carrier DNA provided the greatest transfection efficiency and lowest but detectable levels of overexpression (Figure 5.15). C2C12 cells were transfected with CFP-fibrillarin and induced to differentiate 48 hours later. To limit phototoxicity in live imaging, it is important to establish a minimal time frame for examining reorganization.

Figure 5.15. Optimization for transfection of CFP-fibrillarin plasmid DNA via electroporation. C2C12 cells were first transfected with varying amounts of CFP-fibrillarin plasmid DNA and 40 µg of salmon sperm carrier DNA. Following plasmid optimization, varying amounts of salmon sperm carrier DNA were used to transfect plasmid DNA. C2C12 cells transfected with 4 µg of plasmid DNA and 80 µg of salmon sperm carrier DNA exhibited the highest transfection efficiency and lowest levels of overexpression.

A. Plasmid DNA Optimization

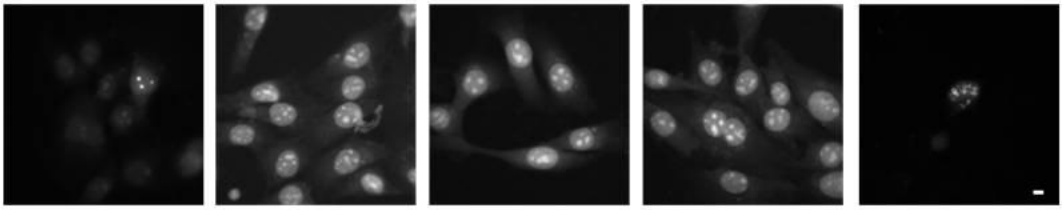

2µg Plasmid | 4µg Plasmid | 6µg Plasmid | 8µg Plasmid | 10µg Plasmid

B. Salmon Sperm DNA Optimization

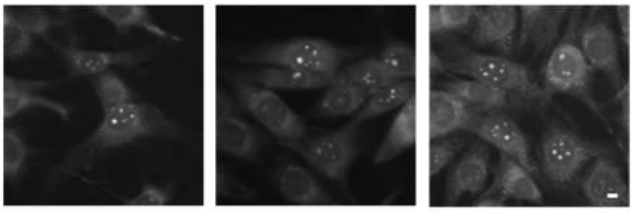

40µg Salmon Sperm DNA | 60µg Salmon Sperm DNA | 80µg Salmon Sperm DNA

Cells were fixed at the time of differentiation induction and every 8 hours after that to determine a window of time during which the nucleolar phenotype changed. The nucleolar phenotype reorganized approximately 32-40 hours after the cells were induced to differentiate (Figure 5.16). Untransfected C2C12 cells were fixed alongside transfected samples and immunolabeled for fibrillarin to determine if exogenous and endogenous fibrillarin protein showed similar reorganization behavior and timing throughout the differentiation time course. Endogenous fibrillarin also showed that nuclear reorganization occurred between approximately 32-40 hours after the cells were induced to differentiate indicating that exogenous and endogenous protein exhibits similar timing throughout the differentiation time course (Figure 5.16). Because our approach involved transient transfection, and because live imaging was not started until 30 hours after differentiation was induced (as established by Figure 5.16), we wanted to know how soon after transfection CFP-fibrillarin was detectable in C2C12 cells to avoid possible loss of detectable CFP-fibrillarin expression during live imaging. C2C12 cells were then transfected by using the optimized conditions (Figure 5.15) and were fixed at 12 hours, 24 hours, 36 hours and 48 hours after transfection. Expression of CFP-fibrillarin was detectable at the earliest monitored time point of 12 hours post-transfection (Figure 5.17). This experiment showed that it is not necessary to wait 48 hours after transfection for inducing differentiation, as the optimal timing for imaging begins at 12 hours after transfection. To image nucleolar reorganization in C2C12 cells, C2C12 cells were transfected with 4 µg of CFP-fibrillarin DNA and 80 µg of salmon sperm carrier DNA. Differentiation was induced 12 hours after transfection and live imaging was started 30 hours after induction and continued through 40 hours after induction. In order to image nuclear speckles and Cajal bodies, optimization experiments similar to those done with CFP-fibrillarin were performed for transfection of YFP-SF2/ASF and GFP-

Figure 5.16. Time track of nucleolar reorganization phenotype. C2C12 cells were transfected with CFP-fibrillarin and induced to differentiate 48 hours after transfection. Upon induction to differentiate, cells were fixed in 2% formaldehyde at 24 hours (Panel A, a), 32 hours (Panel B, b), and 40 hours (Figure 5.16A, panel c). At approximately 32 hours after induction of differentiation nucleoli start to exhibit a change in nucleolar organization. Untransfected cells were processed alongside samples electroporated with CFP-fibrillarin for comparison of endogenous and exogenous fibrillarin protein localization patterns as well as the timing for nucleolar reorganization. Untransfected samples were immunolabeled for fibrillarin (green signal indicates immunolabeling of fibrillarin). 32 hours after induction of differentiation, some myoblasts begin to exhibit a reorganized phenotype (Figure 5.16B, panels g-i, arrows) while other myoblasts still exhibit the undifferentiated phenotype (Figure 5.16B, panels g-I, arrowheads). By 40 hours after induction, the majority of the myoblasts exhibit the reorganized phenotype (Figure 5.16B, panels j-I, arrows). DNA was stained with DAPI. Bar = 5μm.

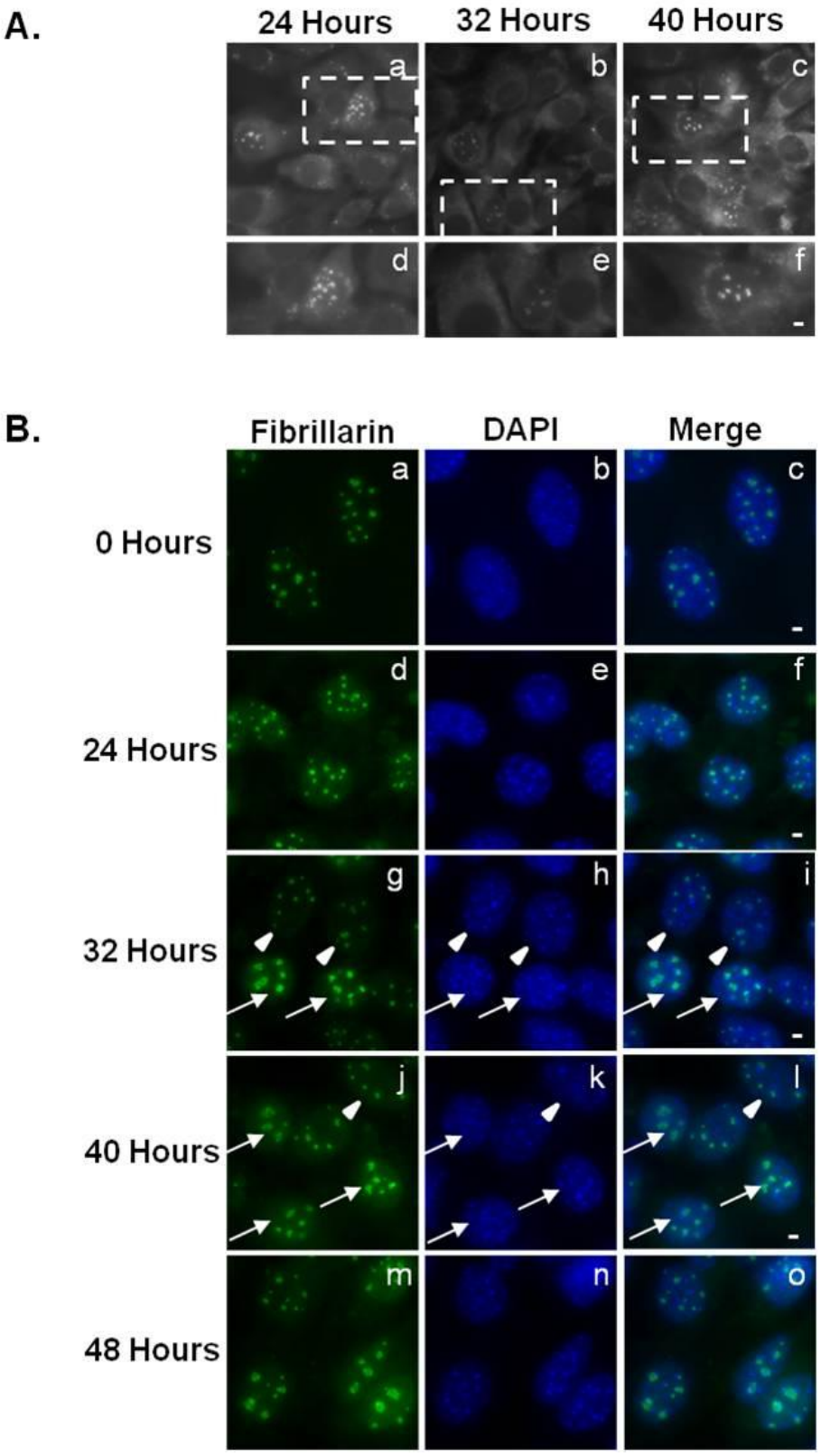
A.
24 Hours
32 Hours
40 Hours
a
b
c
d
e
f
B.
Fibrillarin
DAPI
Merge
0 Hours
24 Hours
32 Hours
40 Hours
48 Hours
a
b
c
d
e
f
g
h
i
j
k
l
m
n
o

Figure 5.17. Determining how long after transfection expression of CFP-fibrillarin persists. C2C12 cells were transfected with CFP-fibrillarin and fixed at 12 hours (A), 24 hours (B), 36 hours (C), and 48 hours after transfection. Expression of CFP-fibrillarin was detectible at 12 hours after transfection in some myoblasts (Panel A) and increased through 48 hours (Panel D). DAPI was not used due to bleed through between the CFP and DAPI channels on the microscope. Bar = 5μm.

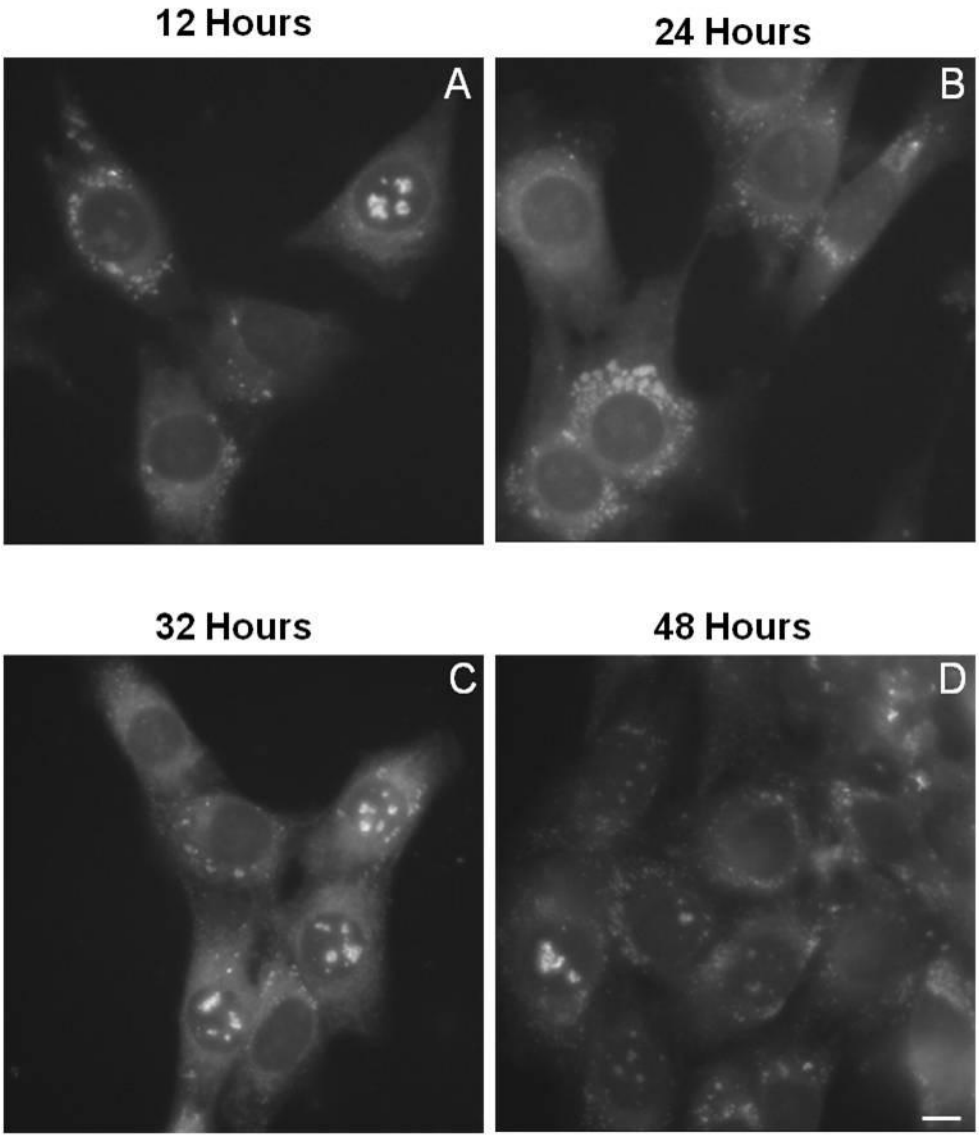
12 Hours
A
24 Hours
B
32 Hours
C
48 Hours
D

coilin in C2C12 cells. Optimization of YFP-SF2/ASF revealed that transfection of 4µg of YFP-SF2/ASF plasmid DNA and 60 µg of salmon sperm carrier DNA yielded the highest transfection efficiency with the lowest levels of exogenous expression Figure 5.18). Significant overexpression of exogenous fusion proteins was avoided to ensure that any observed changes in nuclear organization would not be attributed to elevated levels of fusion proteins. Optimization experiments with GFP-coilin showed that GFP-coilin does not localize conclusively to Cajal bodies in C2C12 cells (Figure 5.19).

Figure 5.18. Optimization of transfection of YFP-SF2/ASF plasmid DNA via electroporation. C2C12 cells were transfected with 60 µg of Salmon Sperm carrier DNA and 4 µg (Panel Aa-Ac), 6 µg (Panels Ad-Af), and 8 µg (Panels Ah-Ai) YFP-SF2/ASF DNA. C2C12 cells were also transfected with 80 µg of Salmon Sperm carrier DNA and C2C12 cells transfected with 60 µg of salmon sperm carrier DNA and 4 µg (Panel Ba-Bc), 6 µg (Panels Bd-Bf), and 8 µg (Panels Bg-Bi). Bar = 5µm.

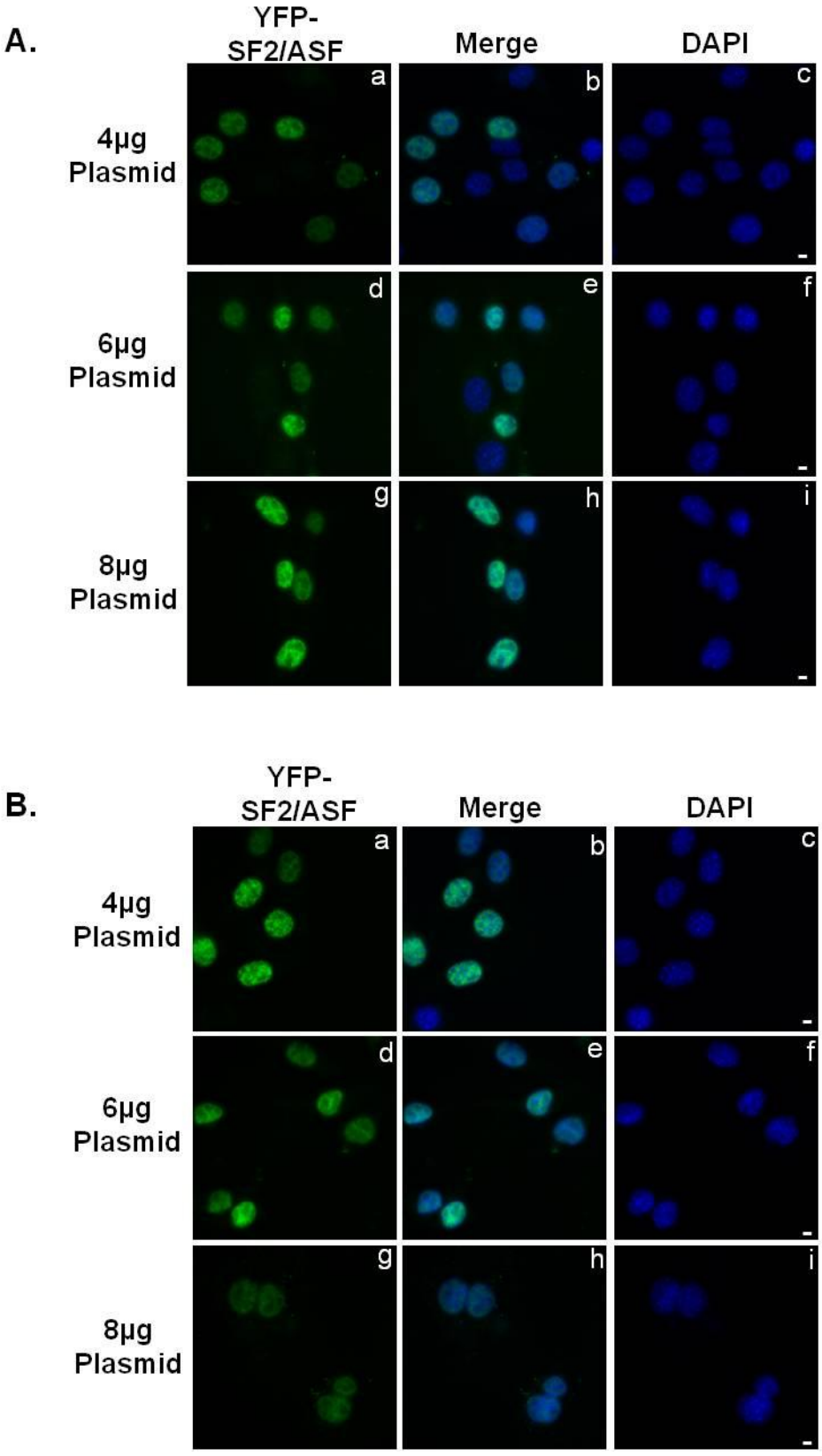
A.
YFP-SF2/ASF
Merge
DAPI
4µg Plasmid
6µg Plasmid
8µg Plasmid
a
b
c
d
e
f
g
h
i
B.
YFP-SF2/ASF
Merge
DAPI
4µg Plasmid
6µg Plasmid
8µg Plasmid
a
b
c
d
e
f
g
h
i

Figure 5.19. GFP-coilin does not localize correctly in C2C12 cells. C2C12 cells were transfected with 60µg of salmon sperm carrier DNA and varrying amounts of GFP-Coilin plasmid DNA (A) as well as 80µg of salmon sperm carrier DNA and varying amounts of GFP-Colin plasmid DNA (B). In all cells transfected, GFP-coilin failed to localize to Cajal bodies. DNA was stained with DAPI. Bar = 5µm.

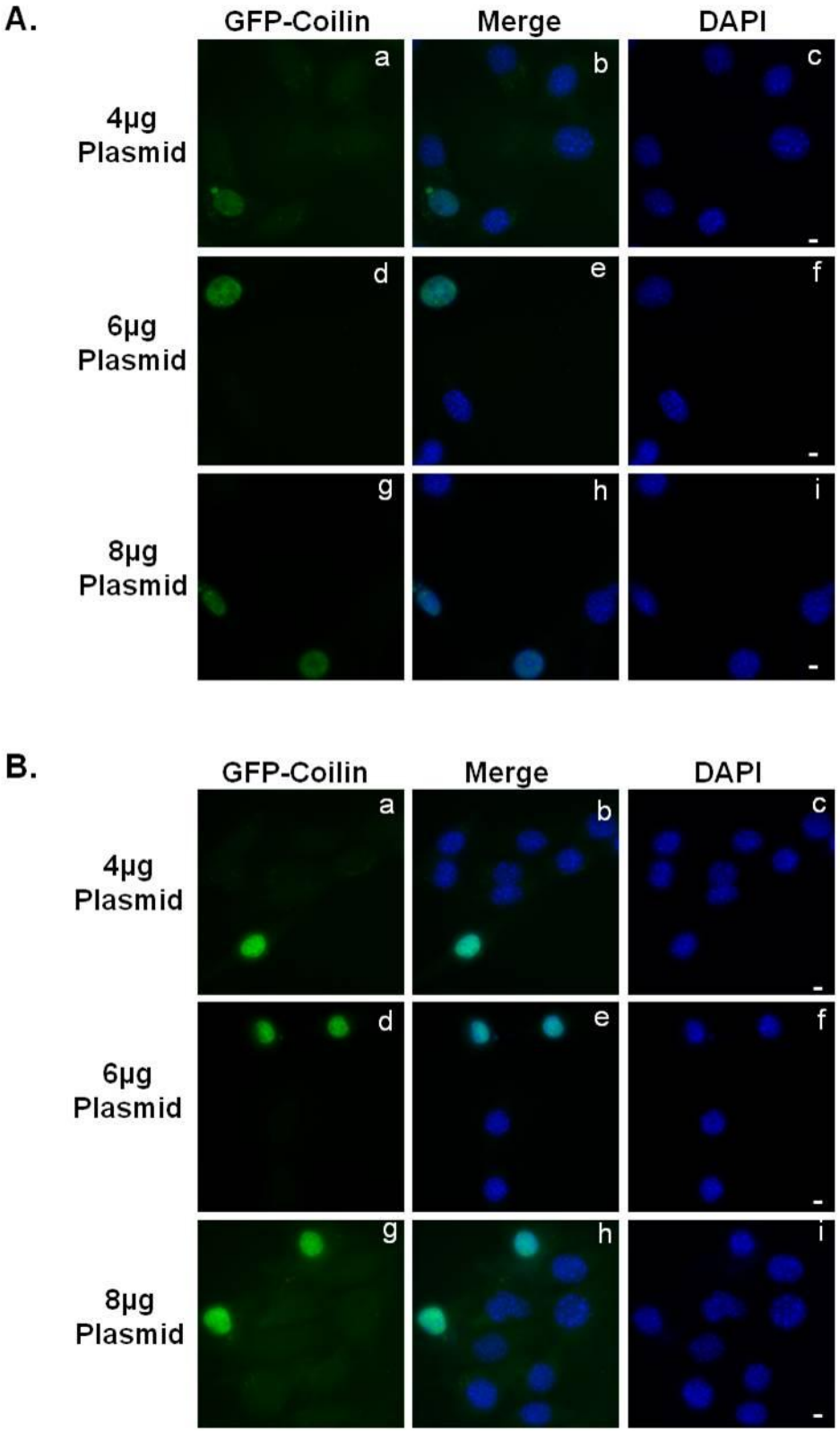
A.
GFP-Coilin
Merge
DAPI
4µg Plasmid
6µg Plasmid
8µg Plasmid
a
b
c
d
e
f
g
h
i
B.
GFP-Coilin
Merge
DAPI
4µg Plasmid
6µg Plasmid
8µg Plasmid
a
b
c
d
e
f
g
h
i

Chapter Six: Discussion

Emery-Dreifuss is one of three major forms of muscular dystrophy and is an X-linked disorder that arises from defects in nuclear-associated proteins, most notably emerin (Fairley et al., 1999). A subset of EMDM patients exhibit mutation in emerin, and they demonstrate normal expression levels and subcellular localization of emerin at the inner nuclear membrane. This is in contrast to the majority of EMDM patients whom produce no detectable emerin as observed by immunoblotting and immunohistochemistry (Haraguchi et al., 2004). This set of mutations includes a serine to phenylalanine substitution at residue 54 (S54F), a proline to histidine substitution at residue 183, a deletion of residues 95-99 (Δ95-99), and a proline to threonine substitution at residue 183 (Haraguchi et al., 2004). Two of these mutations, S54F and Δ95-99 have been mapped to regions of emerin that associate with Btf fragments by yeast-two-hybrid assay (Haraguchi et al., 2004). Given Btf's possible role in EDMD, I set out to investigate a possible role for Btf in muscle cells. Initial experiments revealed that Btf is upregulated during muscle cell differentiation; furthermore, surprising changes in nuclear organization during differentiation were discovered (Theadore Hufford and Paula Bubulya, unpublished data).

In order to elucidate a possible role for Btf in muscle cells, I performed differentiation time courses throughout which I immunolabeled Btf and muscle specific proteins myogenin and MHC. Myogenin expression in the nucleus increases early in the differentiation time course with expression increasing at approximately Day 1 of the time course. MHC expression in the cytoplasm increases later in the differentiation time

course at approximately Day 3; however, MHC expression has been observed at Day 2 in a limited number of myoblasts. Using these two muscle markers allowed us to classify increased expression of Btf as an early or late event the differentiation time course. Throughout the differentiation time course all cells which were positive for either myogenin or MHC showed increased expression levels of Btf. Increased expression levels of Btf was determined to be an early event in the differentiation time course. Upon first observation, it appeared that all myogenin positive myoblasts were also positive for increased expression levels of Btf. However, many MHC positive myoblasts were not positive for increased levels of expression. To quantify this, 100 myogenin positive cells were scored for the presence or absence of increased expression levels of Btf and all 100 myogenin positive myoblasts were also positive for increased expression levels of Btf. In addition, I could not locate any myogenin negative myoblasts which were positive for increased expression levels of Btf. No parallel counts were done for myoblasts immunolabeled for MHC and Btf because it can be assumed based on the differentiation time line that if MHC is present, myogenin must also be present as it precedes MHC in the differentiation time course and increased expression of Btf is always present when myogenin is present. However, numerous MHC negative cells were observed to be positive for increased expression levels of Btf. This data together indicates that increased expression of Btf occurs either simultaneously with increased myogenin expression or very soon after increased myogenin expression and before increased MHC expression. Given that increased expression levels of Btf is an early event in the differentiation time course, we wanted to determine if overexpression of Btf could alone lead to the increased expression of muscle markers myogenin and MHC and drive the differentiation pathway.

To determine if overexpression of Btf was capable of inducing differentiation in the absence of serum deprivation, Btf was overexpressed in C2C12 cells and maintained in GM. C2C12 cells were also transfected with YFP plasmid DNA to rule out transfection alone as the cause of any alterations observed in C2C12 cells transfected with YFP-Btf plasmid DNA. C2C12 cells were also transfected with YFP-Btf and induced to differentiate via serum deprivation to confirm that cells overexpressing Btf were capable of differentiating and that overexpression of Btf did not speed up or slow down the differentiation time course. Untransfected C2C12 cells were maintained in growth medium to ensure that any observations made in transfected samples which were not induced to differentiate would not occur normally in C2C12 cells without serum starvation. Another group of untransfected C2C12 cells were induced to diffentiate to serve as a direct comparison to a normal differentiation time course.

According to immunfluorescence data, cells which were transfected with YFP plasmid DNA, YFP-Btf DNA and not induced to differentiate, and untransfected cells which were not induced to differentiate showed very slight differentiation by Day 4 indicating that overexpression of Btf alone was not enough to induce differentiation. Furthermore, by Day 4 of the time course we observe transfected myoblasts incorporated into myotubes with other non-transfected myoblasts indicating that they are still competent to differentiate and are indistinguishable to other non-transfected myobasts (Figure 4.19). Given that both transfected and untransfected samples which were not induced to differentiate showed similar levels of differentiation indicates that transfection did not hinder the cells' ability to differentiate. C2C12 cells which were transfected with YFP-Btf and induced to differentiate and untransfected cells which were induced to differentiate exhibited similar levels of differentiation at Day 0, Day 2, and Day 4 indicating that overexpression of Btf neither slowed down or expedited differentiation.

In addition to immunolabeling for muscle specific proteins, future repetitions of this experiment could be repeated including duplicates of each sample that are immunolabeled for both nuclear speckle protein Son and nucleolar component fibrillarin to observe for nuclear reorganization as another dimension of differentiation.

Immunoblot data in this experiment seems to correlate with the immunofluorescence data in that cells which were transfected with YFP-Btf and not induced to differentiate show equivalent Btf expression with untransfected and uninduced samples. This data indicates that in the absence of serum starvation cells overexpressing Btf progress along the differentiation pathway at the same rate as the uninduced differentiation time course. In order to confirm YFP-Btf was truly overexpressed, the blot was re-probed to detect the YFP signal. Repeated attempts failed to show an YFP signal on the blot; however, using immunofluorescence data, 100 myoblasts that were transfected with YFP-Btf and not induced to differentiate and 100 myoblasts that were transfected with YFP-Btf and induced to differentiate were scored on Day 0 of the differentiation time course. Day 0 was chosen because the transfection was transient so Day 0 was the time point at which successfully transfected cells would be present at the highest levels. In cells that were transfected with YFP-Btf and not induced to differentiate 42/100 myoblasts were positive for YFP-Btf. In cells that were transfected with YFP-Btf and induced to differentiate 39/100 myoblasts were positive for YFP-Btf. Once a myoblast has started the differentiation program, that myoblast will signal any other myoblast it comes into cell-to cell contact with to differentiate as well. Therefore, given the rate of transfection and that the cells were approximately 50-60% confluent at Day 0 it is reasonable to conclude that enough transfected cells were present and were in close enough proximity to untransfected cells to cause a observable change in the differentiation time course if overexpression of Btf did indeed alter the

differentiation time course. In addition to probing for endogenous Btf, this immunoblot could be probed for muscle specific proteins myogenin and MHC to further confirm or refute that the differentiation time course is not expedited or hindered by overexpression of YFP-Btf. When examining the immunoblot data there is one discrepancy between the immunoblot and immunofluorescence data. At Day 0 in the immunofluorescence data there appears to be a slight signal for endogenous Btf; however, in the immunoblot there is no baseline signal for Btf at Day 0 in any of the samples. This discrepancy could have resulted from the fact that the WU10 anti-Btf antibody is more sensitive or effective at detecting Btf protein in the immunofluorescence method versus the immunoblot method. Many antibodies are known to work more effectively or exclusively for one method or the other. Another irregularity found within the blot is the absence of a second Btf band. Give that the YFP-tag adds molecular weight to the protein another band indicating exogenous Btf should be found slightly above the endogenous Btf band; however, no band was present. One final unexpected piece of data found within the immunoblot corresponds to the Btf signal for cells which were not transfected and not induced to differentiate at Day 4. This sample shows a much more intense signal for endogenous Btf. If this signal truly correlates to a higher expression level of Btf in these cells, it would be worthwhile in future experiments to see if myoblasts which were not induced to differentiate consistently show higher expression levels of Btf in comparison to other myoblasts that were induced to differentiate by Day 4 of the differentiation time course. If this were the case, it would be valuble to investigate a possible role for Btf in promoting cycling in cells. In order to test this theory, one could overexpress YFP-Btf in a number of cells lines that do not differentiate and compare mitotic indices of the cells overexpressing YFP-Btf to each cell line's baseline mitotic index.

Together, the immunofluorescence and immunobot data indicates that increased expression levels of Btf do not alter the differentiation time course. It must be considered that the YFP- tag on the Btf protein might interfere with the function of Btf in this instance. However, immunoprecipitation experiments performed by other students in our lab showed that YFP-Btf formed complexes with nuclear membrane protein emerin just as endogenous Btf does (Lauren Ford, Kelly Conti and Paula Bubulya, unpublished data). Furthermore, this experiment showed that myoblasts overexpressing Btf were still competent to differentiate and form myotubes along with myoblasts expressing endogenous Btf. Together this data indicates to us that the function of Btf is most likely not hindered by the YFP tag. However, given that no information regarding Btf's tertiary structure is available, it must remain a possibility that the placement of the YFP tag may interfere with some unknown functions of Btf *in vivo*.

Protein depletion is one of the most basic molecular approaches to elucidating a protein's function. In order to determine a possible role or function for Btf in myogenesis, we designed experiments to deplete Btf mRNA (and thereby Btf protein) using a lipofectamine-mediated transfection. In order to ensure that these experiments were effective, I first performed siRNA depletion of Btf in HeLa cells using a previously established protocol from our lab. These experiments were successful and showed that in my hands I could produce a successful depletion of Btf. To begin optimizing the protocol for mouse cells, I first performed experiments in which I depleted Btf in mouse embryonic fibroblasts (MEFs). MEFs were used because undifferentiated C2C12 cells have nearly undetectable baseline levels of Btf; however, baseline levels of Btf in MEFs are much higher. This eliminated the complication of optimizing depletion of Btf in C2C12 cells while attempting to differentiate which would be nearly impossible. While optimizing the protocol in MEFs, four different siRNA oligos targeted against mouse Btf

were tested as well as one siRNA oligo targeted against human Btf which was identical in sequence to a portion of the mouse Btf sequence. These experiments revealed that the siRNA oligo targeted against human Btf (hsi-2) produced complete knockdown of Btf in MEFs as detected by immunoblot. After numerous attempts using the optimized conditions, siRNA transfection failed to produce effective knockdown of Btf in C2C12 cells as observed by both immunofluorescence and immunoblot. The inability to produce an effective knockdown of Btf in C2C12 cells is not surprising because C2C12 cells are notoriously hard to transfect and special products are often needed to increase the efficiency of lipofectamine-mediated transfection. In the future, it might be more useful to use electroporation as the method of transfection because a successful electroporation protocol for C2C12 cells has been established. Depletion of Btf in HeLa and MEF cells takes approximately 72 hours; therefore, even if successful depletion of Btf was achieved in C2C12 cells, by the time Btf was depleted the cells would most likely become too confluent and spontaneous differentiation could occur. If the experimental conditions can't be controlled, such as induction of differentiation, then the experiment will not produce reliable results and that data would be rendered useless. In addition to immunoblot data, incorporating RT-PCR data to examine RNA levels of Btf following siRNA transfection would be helpful. If the RT-PCR results revealed that Btf was depleted at the RNA level it might be interesting to investigate the turnover rate and half-life of the Btf protein through fluorescence recovery after photobleaching (FRAP) and cyclohexamide studies. Although the siRNA transfection did not effectively deplete Btf, this was an important experiment to attempt given that expression levels of Btf increase early in muscle cell differentiation and therefore may have a vital function in myogenesis. If depletion of Btf had been successful and sequential experiments showed that in the absence of Btf C2C12 cells failed to differentiate in response to serum starvation this would have indicated that Btf does play an essential role in myogenesis. If previously

proposed experiments in which YFP-Btf was overexpressed in various cell lines revealed Btf positively regulated cell proliferation, it would be interesting to see if successful depletion of Btf could result in C2C12 differentiation in the absence of serum starvation.

In order to study nuclear reorganization in differentiating C2C12 myoblasts, I focused on tracking nuclear speckles and nucleoli throughout differentiation. Throughout differentiation of C2C12 myoblasts, nuclear speckles reorganized from a diffuse pattern to a more defined, large, and bright pattern as observed by immunofluorescence microscopy (Figures 4.1 and 4.2). Myogenin is upregulated earlier in the differentiation time course, by Day 1 (Figure 2.1) and MHC is upregulated later at Day 2 of the differentiation time course. Using these two muscle specific proteins to label differentiating myoblasts, I was able to conclude that nuclear speckle reorganization occurs at least as early as myogenin upregulation (Day 1) and before MHC upregulation (Day 2) as all myogenin positive cells exhibited reorganized nuclear speckles as well as some MHC negative myoblasts (Figure 4.1 and Figure 4.2). Nuclear speckle reorganization also occurs independently of multinucleation (Figure 4.1 and Figure 4.2). Nuclear speckle reorganization is slightly less distinct than nucleolar reorganization. Furthermore, given that the brightness of the immunofluorescence signal is one characteristic used to identify reorganized nuclei, it is important to find some way of standardizing and quantifying this reorganization. One way to do this would be to measure multiple nuclear speckles in both myoblasts and myobubes and set a threshold measurement to distinguish the reorganized nuclear speckle pattern from the nuclear speckle pattern in undifferentiated nuclei.

Nucleoli also underwent reorganization during differentiation of C2C12 myoblasts. It was observed that myoblasts consistently possessed approximately 5-10 nucleoli per nuclei and myotubes possessed approximately 1-5 nucleoli per nuclei, a

trend that when graphed created a characteristic shift in peaks between myoblasts and myotubes (Figure 4.11). GM was added back to differentiated myoblasts at Day 4 and nucleoli counts were repeated at Day 8 and the shift in peaks was still present indicating that nucleolar reorganization is not irreversible. Nucleoli reorganized between approximately Day 1 and Day 2 (Figure 4.3 and Figure 4.4). At Day 0, spontaneously differentiating myoblasts which were positive for myogenin did not exhibit the reorganized nucleolar phenotype (Figure 4.3, Panels A-D) but all MHC positive myoblasts did (Figure 4.4) indicating that nucleolar phenotype may take place soon after myogenin upregulation but before MHC expression. To further examine nucleolar reorganization, I optimized conditions for live cell imaging of differentiating C2C12 cells. To our knowledge live cell imaging of C2C12 cells had never been published. In order to film nucleolar reorganization in differentiating C2C12 cells I had to first optimize transfection of CFP-fibrillarin. Once I had optimized transfection of CFP-fibrillarin, I then performed time course experiments in which I fixed transfected cells every eight hours in order to determine a optimal window of time during which nucleoli reorganize. Untransfected cells were fixed congruently with the transfected cells and labeled for endogenouse fibrillarin to confirm that endogenous and exogenous fibrillarin localized and reorganized in the same manner. Finally, because the transfection of CFP-fibrillarin was transient, I performed experiment to determine the earliest point at which the CFP-fibrillarin was detectable so that I could begin the differentiation time course as soon as possible. After numerous attempts, I obtained a video which suggests that nucleolar fusion is the method of reorganization for nucleoli. Many more data sets must be obtained and quantified before we can confidently conclude that nucleolar fusion is the method of nucleolar reorganization.

In order to assert that the observed nuclear reorganization was not an artifact of experimental manipulation performed to induce differentiation, specifically, serum starvation, I performed a serum starvation test on additional cells lines which do not undergo differentiation. MEF cells were chosen because they do not undergo differentiation and MEFs are a mouse cell line. HeLa cells were also used for the serum starvation test. By using MEF and HeLa cells, I was able to rule out that nuclear reorganization was simply an artifact of serum starvation and that the nuclear reorganization observed was a mouse-specific phenomenon. For each day to the serum starvation test, MEF and HeLa cells maintained in high serum conditions (DMEM + 10% FBS) as well as low serum conditions (DMEM + 0.05% FBS) were fixed in formaldehyde and immunolabled for nuclear speckle protein Son and nucleolar protein fibrillarin (Figures 4.5, 4.6, 4.8, and 4.9). The number of nucleoli per nuclei of both HeLa (Figure 4.7) and MEF (Figure 4.10) cells were scored to see if the number of nucleoli per nuclei would change as observed in C2C12 nucleoli counts of myoblasts and myotubes (Figure 4.11). A change in the average number of nucleoli per nuclei between high serum and low serum was not observed for either HeLa or MEF cells which again indicated that nuclear reorganization is neither mouse specific or a result of serum starvation. On Day 2, MEF cells exhibited a slight change in the average number of nucleoli per nuclei, MEF cells maintained in low showed an average of three nucleoli per nuclei and MEF cells maintained in high concentrations showed an average of four nucleoli per nuclei (Figure 4.10). However, the shift in average number of nucleoli per nuclei was very slight in comparison to the shift of peaks which were observed in C212 counts in which myoblasts (cells negative for muscle specific proteins myogenin and MHC) showed an average of six to nine nucleoli per nuclei and myotubes (cells positive for muscle specific proteins myogenin or MHC) showed an average of three nucleoli per nuclei. Mitotic cells were also scored for HeLa, MEF, and C2C12 cells to assert that the HeLa and MEF cells

were reacting to serum starvation as expected. Both MEF cells maintained in low serum conditions and C2C12 cells showed a significant decrease in mtitoc cells between Day 1 and Day 4 of the time course, which was expected. HeLa cells maintained in low serum conditions actually showed an overall 2% increase in mitotic cells and ended with a 4% mitotic population on Day 4; however, in comparison to all cells maintained in high serum conditions the HeLa cells maintained in low serum conditions still had a much lower proportion of mitotic cells within the population (Table 4.1).

In addition to experiments using HeLa and MEF cell lines, an experiment was done with C2C12 cells in which differentiation was induced without serum starvation. In this experiment the C2C12 cells were plated at a higher density than normal to allow for increased cell-to cell contact resulting in spontaneous differentiation. Throughout this differentiation time course the growth medium (GM) was replenished every 48 hours to ensure the absence of serum starvation. The cells that were induced to differentiate through cell-to cell contact in the absence of serum starvation exhibited reorganization of both nuclear speckles and nucleoli identical to the nuclear reorganization observed in a normal time course. This data, together with the HeLa and MEF serum starvation experiments, suggests that the nuclear reorganization observed in differentiating C2C12 cells is not mouse specific nor a result of serum starvation but a result of the differentiation process. This experiment could have also been done by plating the cells at the normal density and inducing differentiation chemically with paraquat, which has been previously shown to induce differentiation in C2C12 cells (Okabe et al., 2009). Overexpressing the inhibitor of differentiation (Id) protein in order to prevent differentiation in the presence of serum starvation in C2C12 cells would also assert whether or not the observed nuclear reorganization is a result of serum starvation.

Finally, depleting MyoD and serum starving C2C12 cells could also be used to assert or deny that nuclear reorganization is a result of nuclear reoganziation.

Given that nuclear speckles posses numerous pre-mRNA processing factors and gene expression is greatly altered in order in order to induce differentiation, I believe that reorganization of nuclear speckles is a result of shifts in gene expression which occur during differentiation and nucleoli appear larger and more prominent in differentiated cells. The number of nucleoli present in C2C12 nuclei is reduced during differentiation. Studies have shown that proliferating cells have a much higher number of nucleoli in comparison to primary cells which are not in a proliferative state (Terekov, et al., 1984). In order to differentiate, myoblasts must first stop dividing and exit the cell cycle; therefore, the decrease in number of nucleoli per nuclei observed in differentiating myoblasts may be a result of the shift away from a proliferative state which occurs during differentiation.

Bibilography

Andrade, L.E., Chan, E., Raska, I., et al. 1991. Human autoantibody to a novel protein of the nuclear coiled body: immunological characterization and cDNA cloning of p80-coilin. *J Exp Med*. 173:1407-1419.

Andrade, L.E., Eng, M., Chan, E. 1993. Immunocytochemical analysis of the coiled body in the cell cycle and during cell proliferation. *Proc. Natl. Acad. Sci.* 90:1947-1951.

Amthor, H., Nicholas, G., McKinnell, I., Kemp, C.F., Sharma, M. et al. 2004. Follistatin complexes myostatin and antagonizes myostatin-mediated inhibition of myogenesis. *Dev. Biol.* 270:19-30.

Baus, M., Kadesch, T. 2010. Regulation of skeletal myogenesis by Notch. *Exp. Cell Res.* 316:3028-3033.

Beck, J.S. 1961. Variations in morphological patterns of “autoimmune” nuclear fluorescence. *Lancet*. 1:1203-1205.

Benezar, R., Davis, R.L., Lockshon, D., Turner, D.L., Weintraub, H. 1990. The protein Id: a negative regulator of helix-loop-helix DNA binding proteins. *Cell.* 61:49-59.

Berkes, C.A., Tapscott, S.J. 2005. MyoD and the transcriptional control of myogenesis. *Semin. Cell Dev. Biol.* 16:585-595.

Brero, A., Easwaran, H., Nowak, D., Grunewald, I., Cremer, T., Leonhardt, H., Cardoso, M. 2005. Methyl CpG-binding proteins induce large-scale chromatin reorganization during terminal differentiation. *The Journal of Cell Biology*. 5: 733-743.

Broers, J.L., Peeters, E.A., Kuipers, J.J., Endert, J., Bouten, C.V., Oomens, C.W., Baaijens, F.P., Ramaekers, F.C. 2004. Decreased mechanical stiffness in LMNA -/- cells is caused by defective nucleo-cytoskeletal integrity: implications for the developments of laminopathies. *Human Mol. Genet.* 13:2567-2580.

Buffinger, N., Stockdale, F.E. 1995. Myogenic specification of somites is mediated by diffusible factors. *Dev. Biol.* 169:96-108.

Cairns, B.R. 2009. The logic of chromatin architecture and remodeling at promoters. *Nature.* 461:193-198.

Chaudhary, J., Skinner, M. 1999. Basic helix-loop-helix proteins can act at the E Box within the serum response element of the c-fos promoter to influence hormone induced promoter activation in sertoli cells. *Molecular Endocrinology.* 12:774-786.

Choi, J., Costa, M.L., Mermelstein, C.S., Holtzer, H. 1990. MyoD converts primary dermal fibroblasts, chondroblasts, smooth muscle, and retinal pigmented epitheilial cells into striated mononucleated myobalsts and multinucleated myotubes. *Proc. Natl. Acad. Sci USA.* 87:7988-7892.

Christ, B., Ordahl, C.P. 1995. Early stages of chick somite development. *Anat. Embryol.* 191:381-396.

Constantin, B., Imbert, N., Besse, C., Congard, C., Raymond, G. 1995.Cultured skeletal rat muscle cells treated with cytochalsin exhibit normal dystrophin expression and intracellular free calcium control. *Biol. Cell*. 85:125-135.

Coue, M., Brenner, S.L., Spector, I., Korn, E.D. 1987. Inhibition of actin polymerization by latrunculin A. *FEBS Lett.* 213:316-318.

Cremer,T., Kurz, A., Zirbel, R., Dietzel, S, et al. 1993. Role of chromosome territories inThe functional compartmentalization of the cell nucleus. *Cold Spring Harbor Symp. Quant. Biol.* 58:777-792.

Crisp, M., Liu, Q, Roux, K, Rattner, J.B., Shanahan, C., Burke, B., Stahl, P.D., Hodzic, D. 2006. Coupling of the nucleus and cytoplasm: the role of LINC complexes. *J. Cell Biol.* 172:41-43.

Davis, R.L., Weintraub, H., Lassar, A.B. 1987. Expression of a single transfected cDNA converts fibroblasts to myoblasts. *Cell.* 51:987-1000.

de la Serna, I.L., Calrson, A.N. 2001.SWI/SNF complexes promote MyoD-mediated muscle differentiation. *Nat Genet.* 27:187-190.

de la Serna, I.L., Ohkawa, Y., Imbalzano, A.N. 2006. Chromatin remodeling in mammalian differentiation: lessons from ATP-dependent remodelers. *Nat. Rev. Genet.* 7:461-473.

Dhawan, J., Helfman, D.M. 2004. Modulation of actin-myosin contractility in skeletal muscle myoblasts uncouples growth arrest from differentiation. *J. Cell Sci.* 117:3735-3748.

Elis, R., Bertin, E., Schrock, E., Speicher, M.R., Ried, T., et al. 1996. Three dimensional reconstruction of painted human interphase chromosomes: active and inactive x chromosome territories have similar volumes but differ in shape and surface structure. *J. Cell Biol.* 135:1427-1440.

Emerson, C.P. 1990. Myogenesis and developmental gene controls. *Curr. Opin. Cell Biol.* 2:1065-1075.

Fairley, E., Kendrich-Jones, J., Ellis, J. 1999. The Emry-Dreifuss muscular dystrophy phenotype can arise from aberrant targeting and binding of emerin at the inner nuclear membrane. *J. Cell Sci.* 112:2571-2582.

Ferguson, M., Ward, D.C. 1992. Cell cycle dependent chromosomal movement in pre-mitotoc T-lymphocyte nuclei. *Chromosoma.* 10:55-565.

Ferreira, J.A., Carmo-Fonseca, M., Lamond, A. 1994. Differential interaction of splicing snRNPs with coilied bodies in interchromatin granules during mitosis and assembly of daughter cell nuclei. *J. Cell Biol.* 136:11-23.

Freeman, J.W., Busch, R.K., Gyorky, P., ross, B.E., Busch, H. 1988. Identification and characterization of a human proliferation-associated nucleolar antigen with a molecular weight of 120,000 expressed early in G_1 phase. *Cancer Res.*48: 1244.

Fu, S.D. 1995. The superfamily of arginine/serine rich splicing factors. *RNA*. 1:663-680.

Galbaiti, F., Volante, D., Engleman, J.A., Scherer, P.E., Lisanti, M.P. 199. Tergeted down-regulation of caveolin-3 is sufficient to inhibit myotube formation in

differentiating C2C12 myoblasts. Transient activation of p38 mitogen-activated protein kinase is required for induction of caveolin-3 expression and subsequent myotube formation. *J. Biol. Chem*. 274:30315-30321.

Gautier, T., Rober-Nicoud, M., Gully, M., Hernandez-Verdun, D. 1992. Relocation of nucleolar proteinsaround chromosomes at mitosis. A study by confocal laser scanning microscopy. *J Cell Sci.* 102:729-373.

Gustafson, W.C., Taylor, C.W., Valdez, B.C., Henning, D., et al. 1998. Nucleolar protein p120 contains an arginine-rich domain that binds to rRNA. *Biochem J.* 381:387-393.

Guttridge, D.C. 2004. Signaling pathways weigh in on decision to make or break skeletal muscle. *Curr Opin. Clin. Nutr. Metab. Care*. 7:443-450.

Haraguchi, T., Holaska, J., Yamane, M., Jouhin, T., Hasiguchi, N., Mori, C. Wilson, K., Hiraoka, Y. 2004. Emerin binding to Btf, a death promoting transcriptional repressor, is disrupted by a missense mutation that causes Emry-Dreifuss muscular dystrophy. *Euro. J. Biochem*. 271:1035-1045.

Huang, S., Spector, D.L. 1997. Pre-mRNA splicing: nuclear organization of factors and substrates. *Eukaryotic Messenger RNA Processing: Frontiers in Molecular Biology.* 37-36.

Hutchinson, C.J. 2002. Lamins: building blocks or regulators of gene expression? *Nature Rev. Mol. Biol.* 3:848-858.

Kasof, G.M., Goyal, L., White, E. 1999. Btf, a novel death-promoting transcriptional repressor that interacts with Bcl-2 related proteins. *Mol. Biol. Cell.* 19:4390-4404.

Kim, C.H., Neiswender, H., Baik, E.J., Xiong, W.C., Mei, L. 2008. B-catenin interacts with MyoD and regulates is transcriptional activity. *Mol. Cell Biol.* 29:2941-2951.

Knudsen, K.A. 1990. Cell adhesion molecules in myogenesis. *Med. J.* 153:902-906.

Konigsberg, I.R. 1963. Clonal analysis of myogenesis. *Science*. 140:1272-1284.

Kopan, R., Nye, J.S., Weintraub, H. 1994. The intracellular domain of mouse Notch: a constitutively activated repression of myogenesis directed at the basic helix-loop=helix region of MyoD. *Development*. 120:2385-2396.

Kurz, A, et al. 1996. Active and inactive genes localize preferentially in the periphery of chromosome territories. *J. Cell Biol.* 135:1195.

Lamond, A. and Earnshaw, W.C. 1998. Structure and function in the nucleus. *Science*, 280;547-553.

Lamond, A., Spector, D.L. 2003. Nuclear Speckles: a model for nuclear organelles. *Nature Reviews*. 4: 605-612.

Lassar, A.B., Davis, R.L., Wright, W.E., Kadesch, T., Murre, C., et al. 1991. Functional activity if myogenic HLH proteins requires heter-oligomerization with E12/E47-like protein *in vivo*. *Cell.* 66:305-315.

Leung, A., Gevlich, D., Miller, G., Lyon, C., et al. 2004. Quantitative kinetic analysis of nucleolar breakdown and reassembly during mitosis in live human cell. *JCB*. 166:787-800.

Lesser, G.P., Fakan, S., Martin, T.E. 1989. Ultrastructural distribution of ribonucleoprotein complexes during mitosis, snRNP antigens are contained in mitotic granule clusters. *Eur. J. Cell Biol.* 50:376-389.

Luguo, S., Kewei, M., Haixia, W., Fang, X., Gao, Y., et al. 2007. JAK1-STAT1-STAT3, a key pathway promoting and preventing premature differentiation of myoblasts. *J Cell Biol.* 179:139-138.

McGill, M., Dho, S., Weinmaster, G., McGlade, J. 2009. Numb regulates post-endocytic trafficking and degradation of Notch1. *The Journal of Biological Chemistry*. 39: 26427-26438.

McPherron, A.C., Lawler, A.M., Lee, S.J. 1997. Regulation of skeletal muscle mass in mice by a new TGF-β superfamily member. *Nature*. 387: 83-90.

Maroto, M., Reshef, R., Munsterberger, A.E., Koester, S., Goulding, M., Lassar, A.B. 1997. Ectopic Pax3 activates MyoD and Myf-5 expression in embryonic mesoderm and neural tissue. *Cell.* 89:139-148.

Menko, Boettiger. 1987. Occupation of the extracellular matrix receptor, integrin, is a control point for myogenic differentiation. *Cell*. 51:51-57.

Mintz, B., Baker, W.W. 1967. Normal mammalian muscle differentiation and gene control of isocitrate dehydrogenase synthesis. *Proc. Natl. Acad. Sci. USA.* 58:592-598.

Mintz, P., Patterson, S., Sphar, C., Neuwald, Spector, D.L. 1999. Purification and characterization of interchromatin granule clusters. *EMBO Journal*. 19:4308-4320.

Misteli, T., Spector, D.L. 1996. Serine/threonine phosphotase 1 modulates the subnuclear distribution of pre-mRNA splicing factors. *Mol. Biol. Cell*. 7:1159-1572.

Misteli, T., Caceres, J., Spector, D.L. 1997. The dynamics of pre-mRNA splicing factors in living cells. *Nature.* 387:527-537.

Molkentin, J.D., Black, B.L., Marin, J.F., Olson, E.N. 1995. Cooperative activation of muscle gene expression by MEF2 and myogenic bHLH proteins. *Cell*. 83:1125-1136.

Munsterberger, A.E., Lassar, A.B. 1995. Cominational signal from neural tube, floor plate, and notochord induce myogenic bHLH gene expression in the somite. *Development.* 121:651-660.

Muratani, M., Gerlich, D., Janicki, S., Gebhard, M., et al. 2001. Metabolic-energy-dependent movement of PML bodies within the mammalian cell nucleus. *Nature Cell Biology*. 4:106-110.

Nagase, T., Seki, N., Ishikawa, K., Tanaka, A., Nomura, N. 1996. Prediction of the coding sequences of unidentified human genes. V. The coding sequences of 40 new genes (KIAA0161-KIAA)200) deduced by analysis of cDNA clones from human cell line KG-1.*DNA Res.* 3: 17-24.

Nicholas, G., Thomas, M., Langely, B., Somers, W., Patel, K., Cemp, C.F., et al. 2002. Titin cap associates with, and regulates secretion of, myostatin. *J. Cell Physiol.* 193: 120-131.

Nowak, J., Nahirney, P.C., Hadjantonakis, A.K., Baylies, M.K. 2009. Nap-1 mediated actin remodelingis essential for mammalian myoblast fusion. *J. Cell Sci.* 122:3282-3293.

Oakes, M., Aris, J.P., Brockenbrough, J.S., Wai, H., et al. 1998. Mutational analysis of the structure and localization of the nucleolus in yeast *Saccharomyces cerevisiae*. *J. Cell*. 143:23-34.

Okabe, M., Akiyama, K., Nishimoto, S., Sugahara, T., et al. 2009. Paraquat modulates the differentiation of C2C12 cells to myotube. *Interdisciplinary Studies on Environmental Chemistry — Environmental Research in Asia.* 219-225.

Ostlund,C., Ellenburg, J., Hallberg, E., Lippincott-Schwartz, J., Worman, H.J. 1999. Intracellular trafficking of emerin, the Emry-Dreifuss muscular dystrophy protein. *J. Cell Sci.* 11:1709-1719.

O'Keefe, R.T., Mayeda, A., Sadowski, C.L., Krainer, A.R., Spector, D.L. 1994. Disruption of pre-mRNA splicing *in vivo* results in reorganization of splicing factors. *J. Cell Biol.* 124:249-260.

Pazin, M.J., Kadonaga, J.T. 1997. SW1/SNF2 and related proteins: ATP-driven motors that disrupt protein-DNA interaction? *Cell.* 88:737-740.

Prasanth, K.V., Sacco-Bubulya, P.A., Prasanth, S.G., Sepctor, D.L. 2003. Sequential entry of components of the gene expression machinery into daughter nuclei. *Mol. Biol. Cell*. 14:1043-1057.

Rhodes, S.J., Konieczny, S.F. 1989. Identification of MRF4: a new memberof the muscle regulator factor gene family. *Genes Dev.* 3:2050-2061.

Rochlin, K., Yu, S., Roy, S., Baylies, M. 2010. Myoblast fusion: when it takes more to make one. *Dev. Biol.* 341:66-83.

Rosen, G.D., Sanes, J.R., LaChance, R., Cunningham, J.M., Roman, J., et al. 1992. Roles for the integrin VLA-4 and its counter receptor VCAM-1 in myogenesis. *Cell*. 69:1107-1119.

Saitoh, N., Spahr, C. Patterson, S. Bubulya, P., Neuwald, A., Spector, D.L. 2004. Proteomic analysis of interchromatin granule clusters. *Mol. Biol. Cell.* 15:3876-3890.

Salpingidou, G., Smertenko, A., Hausmanowa-Petrucewicz, I., Hussey, P., Hutchinson, C. 2007. A novel role for the nuclear membrane protein emerin in association of the centrosome to the outer nuclear membrane. *J. Cell Biol.* 178:897-904.

Sanger, J.W., Holtzer, H. 1972. Cytochalasin B: effects on all morphology, cell adhesion, and mycopolysaccharide synthesis. *Proc. Natl. Acad. Sci. USA.* 69:253-257.

Savino, T.M., Gebrane-Younes, J., DeMay, J., Sibanta, J., Hernandez-Verdun, D. 2001. Nucleolar assembly of the rRNA processing machinery in living cells. *J. Cell Biol.* 153:1097-1110.

Schardin, M., Cremer, T., Hager, H.D., Lang, M. 1985. Specific staining of human chromosomes in Chinese x man hybrid cell lines demonstrates interphase chromosome territories. *Human Genetics*. 71:281.

Schwander, M., Leu, M., Stumm, M., Dorchies, O.M., et al. 2003. Beta-1 integrins regulate myoblast fusion and sacromere assembly. *Dev. Cell*. 4:673-685.

Sharma, A., Takata, H., Shibahara, K., Bubulya, P., Bubulya, PA. 2010. Son is essential for nuclear speckle organization and cell cycle progression. *Molecular Biology of the Cell.* 14:650-663.

Simone, C., Forcales, S.V., Hill, D.A., Imbalzano, A.N. 2004. P38 pathway suggests SWI-SNF chromatin-remodeling complex to muscle specific loci. *Nat Genet.* 36:738-743.

Sirri, V., Urduqui-Inchimas, S., Roussel, P., Hernandez-Verdun, D. 2008. Nucleolus: the fascinating nuclear body. *Histochem. Cell Biol.* 129:13-31.

Skapek, S.X., Rhee, J., Spicer, D.B., Lassar, A.B. 1995. Inhibition of myogenic differentiation in proliferating myoblast by cyclin D1-dependent kinase. *Science*. 267: 1022-1024.

Spector, D.L., Schrier, W.H., Busch, H. 1983. Immunoelectron microscopic localization of snRNPs. *Biol. Cell*. 49:1-10.

Spector, D.L., Smith, H.C. 1986. Redistribution of U-snRNPs antigens during mitosis. *Exp. Cell Res.* 163:87-94.

Spector, D.L. 2001. Nuclear Domains. *J Cell. Sci.* 114:2891-2893.

Sunwoo, H., Dinger, ME., Wilusz, JE., Amaral, PP., et al. 2008. MEN epsilon/beta nuclear-retained non-coding RNAs are up-regulated upon muscle differentiation and are essential components of paraspeckles. *Genome Res.* 3:347-359.

Swift, H. 1959. Studies on fine nuclear structure. *Brookhaven Sypm. Biol.* 12:134-152.

Taddei, A., Hediger, F., Neumann, F., Gasser, S. 2004. The function of nuclear architecture: a genetic approach. *Annu. Rev. Genet.* 38:305-345.

Tajbakhsh, S, Rocancourt, D., Cossu, G., Buckingham, M. 1997. Redefining the genetic hierarchies controlling skeletal myogenesis: Pax3 and My-f5 act upstream of MyoD. *Cell.* 89:1127-138

Terekhov, S.M., Sozanski, A., Getsadze, K.A. 1984. The number of nucleoli as an indicator of proliferative activity of cells *in vitro*. *UDC*. 97:727-729.

Terranova, R., Sauer, S., Merkensehlager, M., Fisher, A. 2005. The reorganization of constitutive heterochromatin in differentiating muscle requires HDAC activity. *Exp. Cell Res.* 310:344-356.

Thayer, M.J., Tapscott, S.J., Davis, R.L., Wright, W.E., Lassar, A.B., Weintraub, H. 1989. Positive autoregulation of the myogenic determiniation gene MyoD. *Cell*. 58:241-248.

Thiry, M. 1995. Behavior of interchromatin granules during the cell cycle. *Eur. J. Cell Biol.* 68:14-24.

Trumtel, S., Lager-Silvestre, I., Gleizes, P.E., et al. 2000. Assembly and functional organization of the nucleolus: ultrastructural analysis of *Saccharomyces cervisiea* mutants. *Mol. Biol. Cell*. 11:2175-2189.

Vourch'h, C., Taruscio, d., Boyle, a.L., Ward, D.C. 1993. Cell cycle-dependent distribution of telomeres, centromeres, and chromosome-specific sub satellite domains in the interphase nucleus of mouse lymphocytes. *Exp. Cell Res.* 205:142-151.

Wei, X., Somanathan, S., Samarabandu, J., Berenzey, R. 1999. Three-dimensional visualization of transcription sites and their association with splicing-factor rich nuclear speckles. *J. Cell Biol.* 146:543-558.

Weintraub, H., Dwarki, V.J., Verma, I., Davis, R., Hollenberg, S., Snider, L., Lassar, A., Tapscott, S.J. 1991. Muscle specific transcriptional activation of MyoD. *Genes Dev.* 5:1377-1386.

Whitehouse, I., Faus, A., Cairns, B.R., White, M.F., Workman, J.L., Owen-Hughs, T. 1999. Nucleosome mobilization catalysed by the yeast SWI-SNF complex. *Nature.* 400:784-787.

Wright, W.E., Sassoon, D.A., Lin, V.K. 1989. Myogenin, a factor regulating myogenesis, has a domain homologous to MyoD. *Cell.* 56:607-617..

Wu, J.I., Lessard, J., Crabtree, G.R. 2009. Understanding the words of chromatin regulation. *Cell.* 136:200-206.

Yaffe, D., Saxel, O. 1977. Serial passeging and differentiation of myogenic cells isolated from dystrophic mouse muscle. *Nature*. 270:725-727.

Yamaguchi, Y., Oohinata, R., Naiki, T. Irie, K. 2008. Stau1 negatively regulates myogenic differentiation in C2C12 cells. *Genes to Cells*. 13:583-592.